Article

Bicyclic #-iminophosphonates as highly affinity imidazoline I2 receptor ligands for Alzheimer's Disease

Carmen Escolano, Sònia Abás, Sergio Rodríguez-Arévalo, Andrea Bagán, Christian Griñán-Ferré, Foteini Vasilopoulou, Iria Brocos-Mosquera, CAROLINA MUGURUZA, Belén Pérez, Elies Molins, F. Javier Luque, Pilar Pérez-Lozano, Steven De Jonghe, Dirk Daelemans, Lieve Naesens, José M. Brea, María Isabel Loza, Elena Hernández-Hernández, Jesús A. García-Sevilla, M. Julia Dr García-Fuster, Milica Radan, Teodora Djikic, Katarina Nikolic, Mercè Pallàs, and Luis F. Callado

Just Accepted

1
2
3
4
5
6
7
8
9
10
11
12
13
14
15
16
17
18
19
20
21
22
23
24
25
26
27
28
29
30
31
32
33
34
35
36
37
38
39
40
41
42
43
44
45
46
47
48
49
50
51
52
53
54
55
56
57
58
59
60

	Pharmacology

SCHOLARONE™
Manuscripts

Bicyclic α-iminophosphonates as highly affinity imidazoline I₂ receptor ligands for Alzheimer's Disease

Sònia Abás,[†,∇] Sergio Rodríguez-Arévalo,[†,∇] Andrea Bagán,[†] Christian Griñán-Ferré,[‡]

Foteini Vasilopoulou,[‡] Iria Brocos-Mosquera,[§] Carolina Muguruza,[§] Belén Pérez,[∥] Elies

Molins,[⊥] F. Javier Luque,[#] Pilar Pérez-Lozano,[○] Steven de Jonghe,[Δ] Dirk Daelemans,[Δ]

Lieve Naesens,[Δ] José Brea,[♦] M. Isabel Loza,[♦] Elena Hernández-Hernández,[‡] Jesús A.

García-Sevilla,[‡] M. Julia García-Fuster,[‡] Milica Radan,[#] Teodora Djikic,[#] Katarina

Nikolic,[#] Mercè Pallàs,[‡] Luis F. Callado,[§] Carmen Escolano[†,*]

[†] Laboratory of Medicinal Chemistry (Associated Unit to CSIC), Department of Pharmacology,

Toxicology and Medicinal Chemistry, Faculty of Pharmacy and Food Sciences, and Institute of

Biomedicine (IBUB), University of Barcelona, Av. Joan XXIII, 27-31, E-08028 Barcelona,

Spain.

‡ Pharmacology Section, Toxicology and Medicinal Chemistry, Faculty of Pharmacy and Food Sciences, and Institut de Neurociències, University of Barcelona, Av. Joan XXIII, 27-31, E-08028 Barcelona, Spain.

§ Department of Pharmacology, University of the Basque Country, UPV/EHU, E-48940 Leioa, Bizkaia, and Centro de Investigación Biomédica en Red de Salud Mental, CIBERSAM, Spain.

‖ Department of Pharmacology, Therapeutic and Toxicology. Autonomous University of Barcelona, E-08193 Barcelona, Spain.

⊥ Institut de Ciència de Materials de Barcelona (CSIC), Campus UAB, E-08193 Cerdanyola, Spain.

Department of Nutrition, Food Sciences and Gastronomy, School of Pharmacy and Food Sciences, Institute of Biomedicine (IBUB), and Institute of Theoretical and Computational Chemistry (IQTCUB), University of Barcelona, E-08921, Santa Coloma de Gramanet, Spain.

° Unit of Pharmaceutical Technology, Pharmacy and Pharmaceutical Technology, and Physical Chemistry Department, Faculty of Pharmacy and Food Sciences, University of Barcelona, Av. Joan XXIII, 27-31, E-08028 Barcelona, Spain.

△ Rega Institute for Medical Research, Katholieke Universiteit Leuven, 3000 Leuven, Belgium.

♦ Innopharma screening platform. BioFarma research group. Centro de Investigación en Medicina Molecular y Enfermedades Crónicas (CIMUS). Universidad de Santiago de Compostela, Santiago de Compostela, Spain.

Department of Pharmaceutical Chemistry, Faculty of Pharmacy, University of Belgrade, Vojvode Stepe 450, 11000 Belgrade, Serbia.

‡ IUNICS University of the Balearic Islands (UIB), and IdISBa, Cra. Valldemossa km 7.5, E-07122 Palma de Mallorca, Spain.

KEYWORDS. Alzheimer's disease, bicyclic α-iminophosphonates, imidazoline I_2 receptors, imidazoline I_2 ligands, neuroprotection, 3D-QSAR, 5xFAD.

ABSTRACT.

Imidazoline I_2 receptors (I_2-IR), widely distributed in the CNS and altered in patients that suffered from neurodegenerative disorders, are orphan from the structural point of view and new I_2-IR ligands are urgently required for improving their pharmacological characterization. We report the synthesis and 3D-QSAR studies of a new family of bicyclic α-iminophosphonates endowed with relevant affinities for human brain I_2-IR. Acute treatment in mice with a selected compound significantly decreased the FADD protein in the hippocampus, a key marker in neuroprotective actions. Additionally, *in vivo* studies in the familial Alzheimer's disease 5xFAD murine model revealed beneficial effects in behavior and cognition. These results are supported by changes in molecular pathways related to cognitive decline and Alzheimer's disease. Therefore bicyclic α-iminophosphonates are tools that may open new therapeutic avenues for I_2-IR, particularly for unmet neurodegenerative conditions.

4

INTRODUCTION

The imidazoline receptors (IR) (non-adrenergic receptors for imidazolines)[1] have attracted the attention of the scientific community during decades building a body of knowledge that place them as relevant biological targets.[2,3] IR are classified in I_1, I_2 and I_3-types depending on the specific radio-labelled ligands that recognize their binding sites. These receptors are situated in different locations and are involved in different physiological functions.[4] I_1, I_2 and I_3-IR have been unequally studied. Pharmacologically, I_1-IR are well characterized and understood, leading to the clinically approved antihypertensive drugs moxonodine[5] and rilmenidine.[6] The most-unknown are I_3-IR, identified in pancreatic β-cells and involved in insulin secretion.[7] Regarding I_2-IR, although structurally undescribed, a considerable understanding has been achieved on these heterogeneous receptors by using well-characterized I_2-IR ligands.[8] I_2-IR are widely distributed in the brain and, at the molecular level, are located in the outer membrane of mitochondria. Selective I_2-IR ligands have proven that I_2-IR are involved in analgesia,[9] inflammation,[10] and a plethora of human brain disorders.[11] Dysregulations in

the levels of I_2-IR are a hallmark in illnesses such as glial tumors,[12,13] Huntington's

disease,[14] Parkinson's disease,[15] and depression[16,17] amongst others. In particular, I_2-IR

are reported to be increased in the brain of patients that suffered from Alzheimer's

Disease (AD).[18,19] Recently, two I_2-IR ligands, CR4056 **1** and [^{13}C]BU99008 **2**, have

been progressed to clinical trials. CR4056 **1**,[20,21] described as the first-in-class I_2-IR

ligand embodying analgesic properties, is in clinical phase II studies for osteoarthritis

and postoperative dental pain, and [^{13}C]BU99008 **2**[22,23] is in early clinical phase I for

PET diagnosis for patients that suffer from AD.

The implication of I_2-IR in many physiological and pathological processes emphasizes

their pharmacological relevance and deserves in-depth studies. Since the structural

data for I_2-IR remains unknown, the discovery of better and more selective I_2-IR ligands

is crucial to build a comprehensive understanding of the pharmacological implications of

I_2-IR.

Although there are a few exceptions, LSL60101 **3** and most notably the clinical

candidate CR4056 **1**, the vast majority of known I_2-IR ligands (idazoxan, **4**; tracizoline **5**,

6

and 2-BFI, **6**) are 2-substituted-2-imidazolines without further decoration in the 1-, 4- and 5-positions (Figure 1).[24]
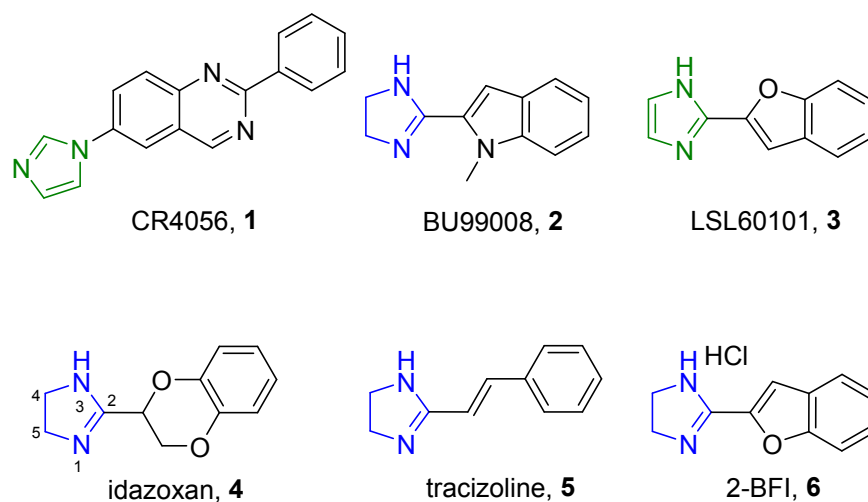
Figure 1. Representative I_2-IR ligands.

In order to explore new imidazoline-based I_2-IR ligands moving out of the comfort zone offered by the rather structurally homogeneous I_2-IR ligands reported so far (Figure 1), we have recently disclosed a family of (2-imidazolin-4-yl)phosphonates.[25,26] The putative therapeutic relevance of a member of this new family of I_2-IR ligands, MCR5 **7**, was validated in a murine model of neurodegeneration, the senescence accelerated mouse-prone 8 (SAMP8).[27] An improvement in the cognitive decline and related biomarkers was found when MCR5 **7** was orally administered to the animals. This study

was the first *in vivo* evidence that reinforced I_2-IR as a promising target for the treatment

of cognitive impairment, associated to multiple neurodegenerative diseases.[27]

Separately, we had reported that the diastereoselective [3+2] cycloaddition of diethyl

isocyanomethylphosphonate with ten diversely substituted maleimides in acetonitrile under

AgOAc catalysis furnished a series of bicycles of general structure **Ia** (Scheme 1a).[28] The

presence, within this series of compounds of an α-iminophosphonate unit, also featured in the

abovementioned (2-imidazolin-4-yl)phosphonates, prompted us to evaluate whether these

bicycloderivatives would also behave as I_2-IR ligands. We indeed found that two of these

ten already reported compounds, **8a** and **8c** (Scheme 1b), displayed an affinity for the I_2-IR

similar to that of idazoxan **4** (see below). These promising results encouraged us to resume our

research with this family of bicyclic α-iminophosphonates with the two-fold aim of further

exploring the scope of the aforementioned [3+2] cycloaddition reaction and of establishing their

structure-activity relationships (SAR) as I_2-IR ligands.

Scheme 1. a) General structure of bicyclic α-iminophosphonates Ia (previously reported) and Ib (reported herein) and reaction conditions;ᵃ b) Chemical structures of 8a and 8c; and c) Chemical structure of MCR5 7.

Ia, R = H, previous synthetic work, **8**
Ib, R = Ph, this work, **9**

α-iminophosphonate moiety

8a

8c

MCR5 **7**
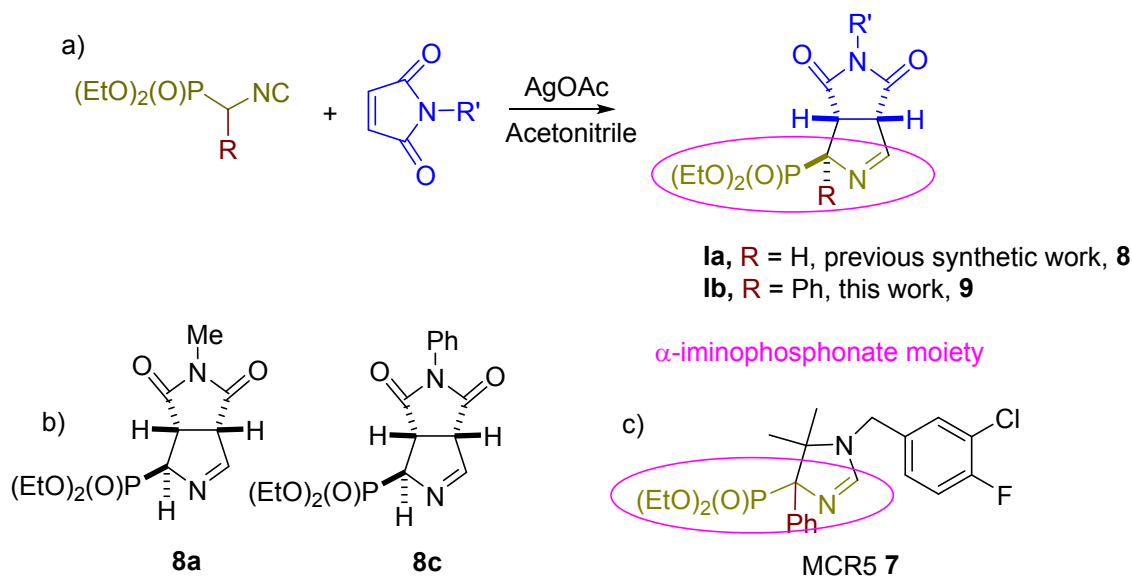
^{a}*Reagents and conditions*, (a) *N*-substituted maleimide derivative (1.5 mmol), PhosMic

(1 mmol), AgOAc (0.06 mmol), acetonitrile, room temperature, overnight.

Herein, we explore the synthetic scope of the [3+2] cycloaddition reaction of α-

substituted PhosMic derivatives and diversely substituted maleimides. Particular attention

was given to derivatives including a phenyl substituent in the α-position of the phosphonate

leading to general structures **9** depicted as **Ib** in the Scheme 1a, in order to resemble

the structure of MCR5 **7** (Scheme 1c). We also assessed the pharmacological profile

and selectivity of a wide range of bicyclic α-iminophosphonates through competition

binding studies against the selective I_2-IR radioligand [³H]-2-[(2-benzofuranyl)-2-

imidazoline] (2-BFI).[29] Selectivity versus two related targets, the I_1-IR and the α_2-adrenergic receptor (α_2-AR) was evaluated through competition studies using the selective radioligands [^{3}H]clonidine and [^{3}H]RX821002 (2-methoxyidazoxan), respectively. Complementary, we performed 3D-QSAR studies. Compound **9d**, endowed with outstanding I_2-IR affinity and excellent selectivity index regarding I_1-IR and α_2-AR, was selected for further studies. We first compared the affinity for the human I_2-IR of **9d** with those of the standards shown in Figure 1. Additionally, the affinity for I_2-IR from different species was considered for idazoxan **4** and **9d**. Next, we performed preliminary DMPK studies for **9d**, including chemical stability, PAMPA-BBB permeability assay, solubility, cytotoxicity, microsomal stability, cytochromes inhibition, and safety. Finally, we characterized its *in vivo* neuroprotective effects in the 5xFAD murine model of AD.

RESULTS AND DISCUSSION

Chemistry

Synthesis and structural characterization

Considering the previously described compounds **8a** and **8c** as promising starting points for designing potent I_2-IR ligands, we resolved to prepare bicyclic compounds functionally close to MCR5 **7** by including a α-phenyliminophosphonate moiety in their structure. To this end, we decided to increase the scope of the original [3+2] cycloaddition by using diversely α-substituted PhosMic derivatives (Figure 2).

10a, R = phenyl
10b, R = 4-fluorophenyl
10c, R = 4-methoxyphenyl
10d, R = benzyl
10e, R = 4-fluorobenzyl
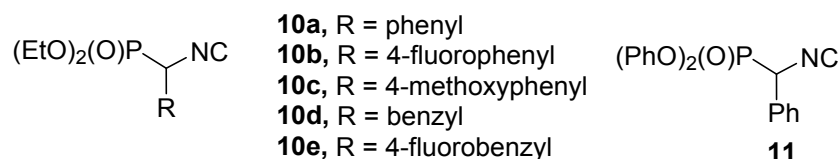
Figure 2. α-Substituted PhosMic derivatives used in this work.

The preparation of the α-substituted PhosMic derivatives was performed adapting previously described procedures (for references and experimental procedures, see Supporting Information). Briefly, the four phenylisocyanomethylphosphonates **10a**, **10b**, **10c** and **11** were prepared by conversion of the required (α-aminophenyl)phosphonate derivative to the corresponding formamide followed by dehydration with phosphorus oxychloride. While diethyl (α-aminophenyl)phosphonate is a commercially available compound, the other three precursors were synthesized according to published procedures. A different approach was followed for the α-benzylisocyano derivatives **10d** and **10e**. Alkylation of commercially available PhosMic with either benzylbromide or 4-fluorobenzylbromide, using potassium *tert*-butoxide furnished diethyl benzylisocyanomethylphosphonate **10d** and diethyl 4-fluorobenzylisocyanomethylphosphonate **10e**, respectively.

11

The maleimides used in the cycloaddition reaction were commercially available or were prepared following previously described procedures.

Gratifyingly, although the targeted compounds feature increased steric hindrance in the α-phosphonate position, our previously optimized set of conditions for the [3+2] cycloaddition reaction of maleimides with PhosMic also worked for the current set of α-substituted PhosMic derivatives.[28] In this way, 36 new bicycloderivatives (Schemes 2 and 3) having a quaternary stereocenter, were synthesized in medium to high yields (experimental section). The products were purified by column chromatography and, when solids, analytical samples were obtained by recrystallization. For the sake of clarity in the section I_2-IR binding activity and structure-activity relationships the new α-substituted bicycles, depicted in Schemes 2 and 3, were ordered and numbered attending to the SAR discussion.

Analogously to our previous work,[28] all the [3+2] cycloaddition reactions occurred in a diastereoselective manner and only one of the two possible diastereoisomers was formed. The relative configuration of the three stereocenters in the new compounds was unambiguously confirmed by X-ray crystallographic analysis for five examples and the stereochemistry of the other compounds was assigned by comparison of their ^{1}H and ^{13}C-NMR spectra (Tables S12 and S13).

Scheme 2. General procedure for the synthesis of bicyclic α-iminophosphonates.[a] Compounds prepared in previous work (R = H)[28] and compounds prepared in this work (R = Ph, 4FPh, 4-MeOPh, PhCH$_2$, 4FPhCH$_2$).
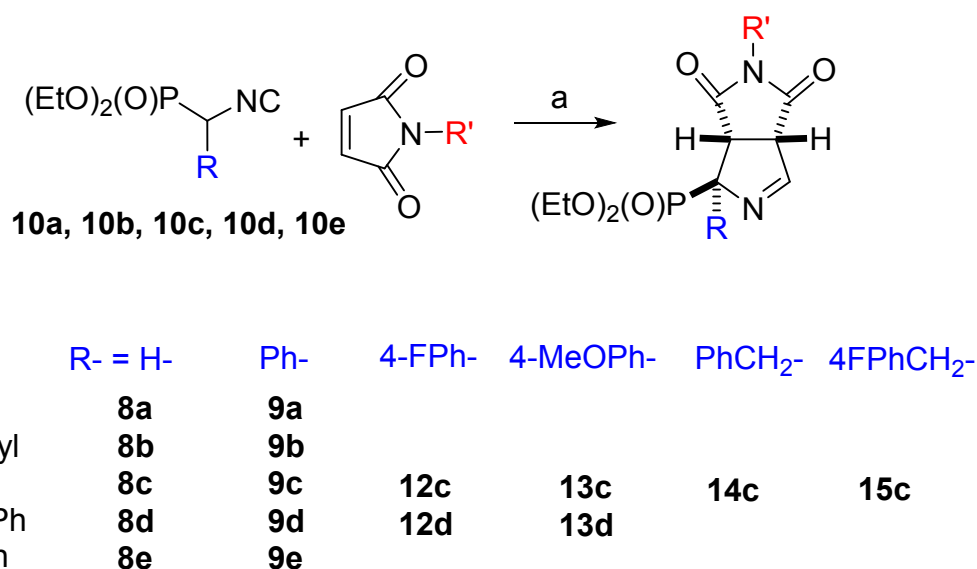
(EtO)$_2$(O)P—NC + N–R' →[a] (product structure)

R

10a, 10b, 10c, 10d, 10e

R'-	R- = H-	Ph-	4-FPh-	4-MeOPh-	PhCH$_2$-	4FPhCH$_2$-
Me	**8a**	**9a**				
cyclohexyl	**8b**	**9b**				
Ph	**8c**	**9c**	**12c**	**13c**	**14c**	**15c**
3-Cl,4-FPh	**8d**	**9d**	**12d**	**13d**		
4-MeOPh	**8e**	**9e**				

[a]*Reagents and conditions*, (a) *N*-substituted maleimide derivative (1.5 mmol), α-substituted PhosMic (**10a**, **10b**, **10c**, **10d**, **10e**, 1 mmol), AgOAc (0.06 mmol), acetonitrile, room temperature, overnight.

Scheme 3. Second-round of compounds synthesized, featuring modified *N*-maleimide substituents inspired by compounds 9a and 9b, R' = alkyl and 9c and 9d, R' =aryl.[a]

(EtO)$_2$(O)P—NC + N–R' →[a] (product structure)

Ph

10a
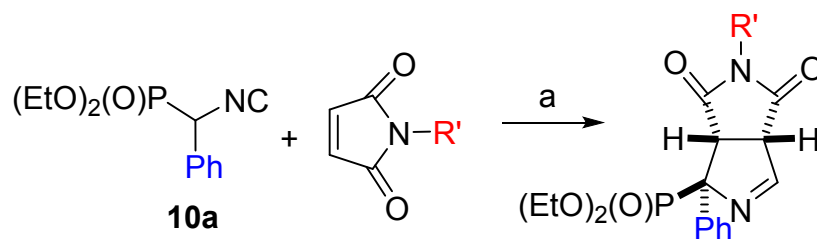
R'- = alkyl, 9a 9b

9f, ethyl
9g, propyl
9h, *t*-butyl
9i, (1-adamantyl)methyl-

9j, PhCH$_2$-
9k, PhCH$_2$CH$_2$-
9l, 4-FPhCH$_2$CH$_2$-
9m, Ph(CH$_2$)$_2$CH-

R'- = aryl, 9c 9d

9n, 4-CF$_3$Ph-
9o, 3-CF$_3$Ph-
9p, 4-FPh-
9q, 4-ClPh-
9r, 2-ClPh-
9s, 3-ClPh-
9t, 4-BrPh-
9u, 3,5-diClPh-
9v, 3,4-diClPh-
9w, 2,4,6-triClPh-
9x, 3-NO$_2$Ph-
9y, 3-NO$_2$,6-CH$_3$Ph-

9z, 4-PhPh-
9aa, 4-CH$_3$Ph-
9ab, 4-PhOPh-

9ac, 1-naphthyl
9ad, 2-Cl,3-pyridyl

[a]*Reagents and conditions*, (a) *N*-alkyl or aryl substituted maleimide derivative (1.5 mmol), α-PhenylPhosMic (**10a**, 1 mmol), AgOAc (0.06 mmol), acetonitrile, room temperature, overnight.

As previously noted the [3+2] cycloaddition reaction between α-substituted PhosMic derivatives and diversely substituted maleimides was completely diastereoselective, only one of the two possible diastereoisomers was observed. Iminophosphonates **9b, 9c, 9d, 9v** and **9ab** were recrystallized as monocrystals from ethyl acetate. Their relative configuration was unambiguously confirmed by X-ray crystallographic analysis, indicating a *trans* relationship

between the hydrogen atoms on the bridged positions and the substituent at the α phosphonate

carbon atom (Figure 3).
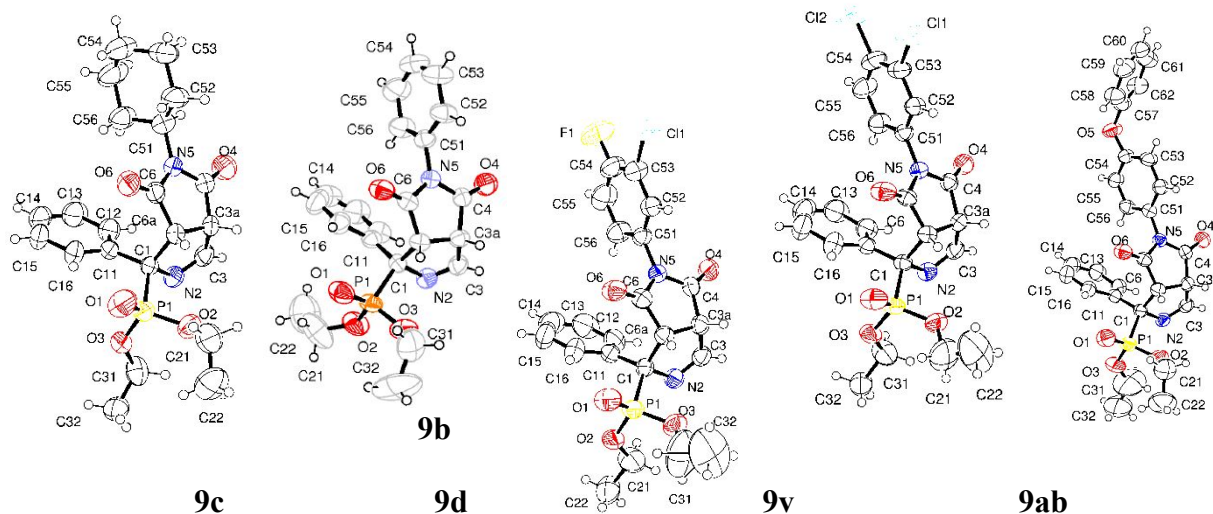
Figure 3. X-Ray structures of **9b, 9c, 9d, 9v** and **9ab** .

Finally, the origin of the diastereoselective [3+2] cycloaddition was investigated by

quantum mechanical (QM) calculations that were performed for the addition of *N*-

methylmaleimide to α-phenylPhosMic (in this latter case the ethyl groups were replaced

by methyl in order to reduce the cost of QM computations). In addition, a silver cation

bound to acetonitrile was introduced to account for the catalytic effect on the chemical

reaction. Reactants, transition states and products for the *cis* and *trans* [3+2]

cycloadditions were determined from geometry optimizations at the B3LYP/6-31+G(d)

(LANL2DZ for silver) level, and the nature of the stationary points was verified from the

analysis of the vibrational frequencies. The geometries of the transition states point out

that the cycloaddition occurs via an asynchronous concerted process as the length of the

bond that is formed by carbon atom 3*a* is shorter than the bond formed by carbon atom

6a by 0.51 and 0.23 Å in the *cis* and *trans* addition, respectively (Figure 4). Moreover, a

significant deviation from linearity is observed in the isocyano group, as the C-N-C angle

is close to 144 degrees in the two transition states. The results also point out that the

transition state leading to the *trans* addition was more stable by 2.3 kcal mol^{-1} relative to

the *cis* cycloaddition (Table S1), presumably due to the destabilizing electrostatic

interactions between the oxygen atoms of the phosphonate and maleimide moieties. The

preferred stability of the *trans* transition state was further checked by geometry

optimizations performed the *cis* and *trans* cycloadditions with the MN15L density

functional, leading to a free energy difference of 1.2 kcal mol^{-1} favoring the *trans*

cycloaddition. The contribution due to the solvation effects in acetonitrile was determined

by means of continuum solvation calculations (see Methods). The results (Table S1)

reveal that solvation leads to a slight destabilization of the transition state relative to the

reactants. Nevertheless, this effect cancels out for the *cis* and *trans* addition, which can

be understood from the similar structural features of the two transition states. Overall,

these results justify the preferential formation of the diastereoselective compound

originated from the *trans* cycloaddition (Figure 4).

16
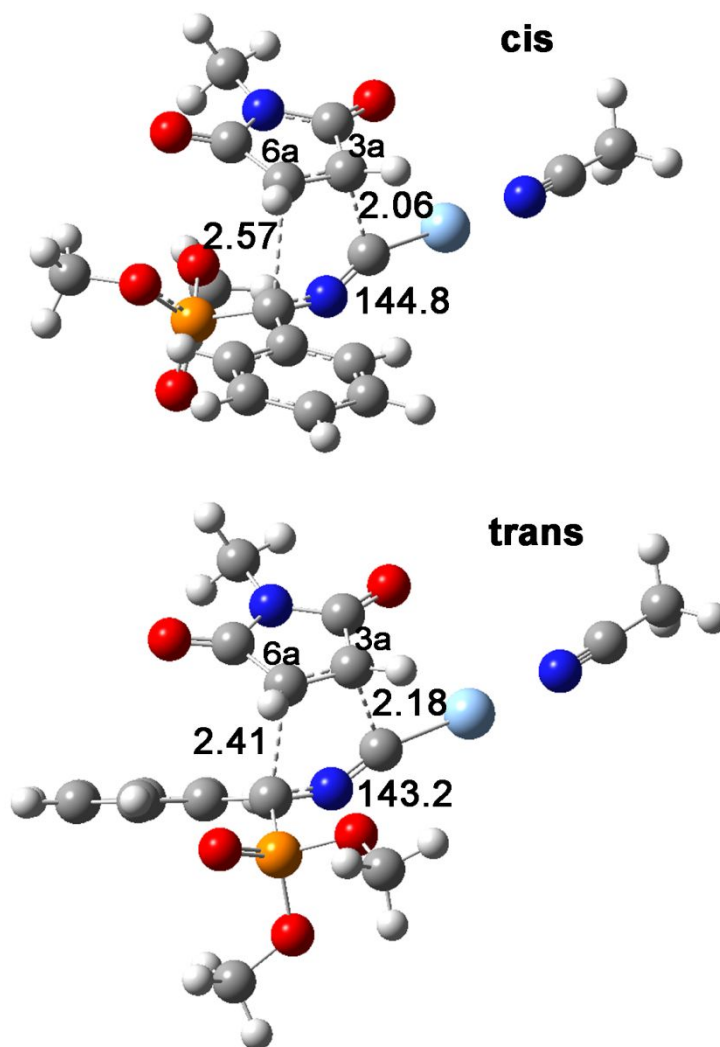
Figure 4. Representation of the transition states for the *cis* and *trans* [3+2] cycloaddition between *N*-methylmaleimide and α-phenylPhosMic (ethyl groups substituted by methyl) located from B3LYP calculations (C$\cdots$C distances in a; C-N-C angle in degrees).

I$_2$-IR binding activity and Structure-Activity Relationships

The pharmacological activity of the compounds depicted in Schemes 2 and 3 was evaluated through competition binding studies against the selective I$_2$-IR radioligand [^{3}H]-2-BFI and the

selective α_2-AR radioligand [^{3}H]RX821002. The studies were performed in membranes from post-mortem human frontal cortex, a brain area that shows an important density of I_2-IR and α_2-AR.[30] Idazoxan **4**, a compound with well-established affinity for I_2-IR (pKi = 7.27 ± 0.07) and α_2-AR (pKi = 7.51 ± 0.07) was used as reference. The inhibition constant (K_i) for each compound was obtained and is expressed as the corresponding pKi (Table 1). The selectivity for these two receptors was expressed by the I_2/α_2 index, calculated as the antilogarithm of the ratio between pKi values for I_2-IR and pKi values for α_2-AR (Table 1). Competition experiments against [^{3}H]2-BFI were monophasic for most of the compounds (for a few exceptions, see below).

Among the set of ten bicycles of general structure **Ia** (Scheme 1a) already reported[28] five representative compounds, **8a**, **8b**, **8c**, **8d** and **8e**, were selected for evaluation as potential I_2-IR ligands considering the substitution in the *N*-maleimide by an alkyl (**8a**), cycloalkyl (**8b**), unsubstituted phenyl (**8c**), electron withdrawing-disubstituted phenyl (**8d**) and electron donating-substituted phenyl (**8e**) groups.

Pleasantly, **8a** and **8c** displayed pKi I_2 affinity of 6.79 and 7.73, respectively, in the range of that of idazoxan **4** (7.41). However, no promising results were found for **8b**, **8d** and **8e** (Table 1). As a first structural approximation, we turned our attention to compounds bearing a quaternary center in the α-position by including a phenyl group. In this manner, the new compounds would resemble the α-phenyliminophosphonate moiety of MCR5 **7** (in pink color in Scheme 1a and 1c). In order to maintain the homology with the first series of evaluated compounds (Scheme 2, R = H), analogous maleimide derivatives were considered to give access to compounds **9a**, **9b**, **9c**, **9d**, and **9e** (Scheme 2, R = phenyl). Indeed, this change was highly positive for the whole

series, increasing the pKi I_2 affinity for all the phenyl-substituted derivatives compared to their unsubstituted congeners, with the added benefit, in three cases (**9a**, **9d** and **9e**), of an enhanced I_2/α_2 selective ratio up to 195. A remarkably benefit in the I_2-IR affinity, pKi I_2 9.74 (Ki = 18 nM) was observed in *N*-cyclohexyl derived **9b**, 4-fold compared with analogous **8b** with an I_2/α_2 selectivity of 5. The rise in the affinity was also conserved in compounds bearing an *N*-arylimide substitution. In particular, the presence of an *N*-phenyl group led to **9c**, with an outstanding activity binding pKi I_2 10.28 (Ki = 63.0 pM), but not I_2/α_2 selectivity. Gratifyingly, introduction of halogen atoms (3-chloro-4-fluoro) in the *N*-phenyl ring of **9c** led to congener **9d** that kept a nice affinity, with a pKi I_2 8.56. Of note, **9d** fitted significantly better to a two-sites binding model, with a high pKi I_2 8.61 (Ki_H= 2.45 nM) and a low pKi I_2 4.29 (Ki_L= 51.2 μM), with the high-affinity site representing a calculated 37% of the specific binding of [^{3}H]2-BFI at 2 nM concentration.

The enhancement, both in terms of affinity and of selectivity, observed when moving from the α-unsubstituted to the α-substituted phosphonates prompted us to briefly consider additional variations. The introduction in the α-phosphonate position of *p*-fluorophenyl (**12c**) or *p*-methoxyphenyl (**13c**), benzyl (**14c**), and *p*-fluorobenzyl (**15c**) groups was highly deleterious for the affinity (pKi I_2 = 6.59 for **14c** and pKi I_2 < 3 up to 5.35 for **12c**, **13c** and **15c**, respectively). However, for the *p*-substituted phenyl derivatives, the further introduction of halogen atoms (3-chloro-4-fluoro) in the *N*-phenyl ring (compounds **12d** and **13d**), nicely restored the affinity (pKi I_2 7.55 for **12d** and pKi I_2 7.87 for **13d**). Additionally, due to the lack of binding of **12d** and **13d** to α_2-AR, their I_2/α_2 selectivity was outstanding, 14791 and 74131, respectively.

Taking into account the aforementioned results, for a second round of compounds the general structure depicted in Scheme 3 was conserved, featuring the unsubstituted phenyl group in the α-position of the phosphonate, and modifying the substituents in the maleimide. New compounds were classified in two groups taking into consideration whether an alkyl or an aryl substituent was introduced in the *N*-maleimide.
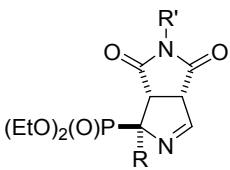
Inspired by **9a** and **9b**, compounds bearing an alkyl substituents with different length, **9f** and **9g**, ramified alkyl, **9h**, and polycycloalkane, **9i**, were prepared. From **9a**, the elongation of the *N*-alkyl chain, from methyl to ethyl, led to **9f**, with an increase in the affinity to pKi I_2 = 8.37 (Ki = 4.3 nM) and I_2/α_2 selectivity to 331, while the *n*-propyl derivative, **9g**, was much less affine pKi I_2 = 4.02. For **9f**, the best fit was a two-site model of binding with a high pKi I_2 = 8.95 and a low pK$_i$ I_2 = 5.86, high affinity site occupancy is 62%. Further increase of the size of the *N*-alkyl substituent to a *tert*-butyl, **9h**, or an adamantylmethyl, **9i**, did not improve the affinity. Taking together the affinity values for **9a**, **9b**, **9f**, **9g**, **9h** and **9i**, it seems that small and large substituents are compatible with good affinity values, but that conformational freedom, as in **9g**, is deleterious.

Compounds **9j**, **9k**, **9l** and **9m**, with *N*-benzyl, *N*-phenethyl, *N*-4-fluorophenethyl, and *N*-phenylpropyl substituents, respectively, were accessed to increase the examples in the SAR study. However, their affinities revealed a remarkable decrease in the biological properties, leading to pKi I_2 = 5.26, 6.35 <3 and 3.84 values, respectively.

Taking into account that **9c** displayed an outstanding affinity for I_2-IR, but lacked selectivity over α_2-AR, further R'= aryl derivatives were explored. As we knew that **9d** (pKi I_2 = 8.56, I_2/α_2 = 195) was endowed with excellent affinity and remarkable selectivity, we mainly focused on

electron withdrawing groups (**9n**, **9o**, **9p**, **9q**, **9r**, **9s**, **9t**, **9u**, **9v**, **9w**, **9x** and **9y**), although a few

electron donating substituents were briefly examined (**9z**, **9aa**, and **9ab**). Overall, neither these

new phenyl derivatives nor the *N*-naphthyl derivative **9ac**, outperformed the excellent affinity of

9c (Table 1), although **9z** (pK$_i$ I$_2$ = 7.90) had an improved I$_2$/α_2 ratio of 602. Finally, **9ad** with an

N-(2-chloro-3-pyridyl) substituent gave a pKi I$_2$ = 7.96, in the range of standard idazoxan **4**, but

it offered as an outstanding advantage a null affinity upon α_2-AR, leading to an I$_2$/α_2 selectivity

of 91201.

Table 1. I$_2$-IR and α_2-AR Binding Affinities (pKi) of five previously reported compounds

8[28] and new compounds.

Compound General structure	R-	R'-	[³H]-2-BFI, I$_2$ one site ª[³H]-2-BFI, I$_2$ two sites H/L; High affinity site %	[³H]-RX821002, α_2	ªSelectivity I$_2$/α_2
			pKi		
Idazoxan			7.41 ± 0.63	8.35 ± 0.16	-
8a	H	Me	6.79 ± 0.51	9.49 ± 0.18	5
8b	H	cyclohexyl	5.74 ± 0.51	5.02 ± 0.58	-
8c	H	Ph	7.73 ± 0.19	8.49 ± 0.36	-
8d	H	3-Cl,4-FPh	<3	10.27 ± 0.32	-
8e	H	4-MeOPh	5.11 ± 0.13	6.14 ± 0.85	

9a	Ph	Me	7.97 ± 0.55	5.93 ± 0.41	110
9b	Ph	cyclohexyl	9.74 ± 0.29	9.01 ± 0.51	5
9c	Ph	Ph	10.28 ± 0.37	10.38 ± 0.22	1
9d	Ph	3-Cl,4-FPh	8.56 ± 0.32	6.27 ± 0.56	195
			$8.61 \pm 0.28/$ $4.29 \pm 0.20;$ 37 ± 4		219
9e	Ph	4-MeOPh	6.65 ± 1.27	4.59 ± 0.22	115
12c	4-FPh	Ph	<3	6.77 ± 0.64	-
12d	4-FPh	3-Cl,4-FPh	7.55 ± 0.32	3.38 ± 0.33	14791
13c	4-MeOPh	Ph	3.39 ± 0.62	3.85 ± 0.31	-
13d	4-MeOPh	3-Cl,4-FPh	7.87 ± 0.40	<3	74131
14c	CH_2Ph	Ph	6.59 ± 0.77	3.94 ± 0.16	447
15c	4-FCH_2Ph	Ph	5.35 ± 0.35	7.20 ± 1.02	-
9f	Ph	Et	8.37 ± 0.27	5.85 ± 0.53	331
			$8.95 \pm 0.36/$ $5.86 \pm 0.66;$ 62 ± 11		1259
9g	Ph	propyl	4.02 ± 0.41	$\pm$	-
9h	Ph	*t*-butyl	7.35 ± 0.43	6.77 ± 0.66	3
9i	Ph	(1-adamantyl)methyl	7.01 ± 0.76	4.31 ± 0.29	501
9j	Ph	$PhCH_2$	5.26 ± 0.22	8.11 ± 0.28	-
9k	Ph	$PhCH_2CH_2$	6.35 ± 0.38	3.77 ± 0.09	380
9l	Ph	4-$FPhCH_2CH_2$	<3	5.65 ± 0.39	-
9m	Ph	$Ph(CH_2)_2CH_2$	3.84 ± 0.31	3.44 ± 0.28	2

			6.87 ± 0.81/ 3.20 ± 0.99; 22 ± 2		2691
9n	Ph	4-CF$_3$Ph	<3	4.73 ± 0.60	-
9o	Ph	3-CF$_3$Ph	<3	±	-
9p	Ph	4-FPh	<3	5.34 ± 0.35	-
9q	Ph	4-ClPh	<3	±	-
9r	Ph	2-ClPh	5.09 ± 0.16	6.15 ± 0.44	-
			7.53 ± 0.66/ 4.74 ± 0.23; 25 ± 7		24
9s	Ph	3-ClPh	<3	±	-
9t	Ph	4-BrPh	<3	±	-
9u	Ph	3,5-diClPh	5.81 ± 0.37	6.22 ± 0.26	-
9v	Ph	3,4-diClPh	<3	±	-
9w	Ph	2,4,6-triClPh	<3	5.16 ± 0.19	-
9x	Ph	3-NO$_2$Ph	6.81 ± 0.27	10.18 ± 0.41	-
9y	Ph	3-NO$_2$,6-CH$_3$Ph	<3	±	-
9z	Ph	4-PhPh	7.90 ± 0.46	5.12 ± 0.14	602
9aa	Ph	4-CH$_3$Ph	5.44 ± 0.16	±	-
9ab	Ph	4-PhOPh	6.96 ± 0.30	5.43 ± 0.21	34
9ac	Ph	1-naphthyl	3.11 ± 0.7	<3	-
9ad	Ph	2-Cl,3-pyridyl	7.96 ± 0.41	<3	91201

[a] Selectivity I$_2$-IR/α_2-AR expressed as the antilog (pKi I$_2$-IR-pKi α_2-AR). [b] The best fit of

the data for **9d**, **9f**, **9m** and **9r** was to a two-site binding model of binding with high pKi

(pKi$_H$) and low pKi (pKi$_L$) affinities for both binding sites respectively.

Selectivity I$_2$-IR *versus* I$_1$-IR

After evaluating the affinity of the indicated compounds for α_2-AR, we assessed the affinity of some representative compounds for I$_1$-IR. To this end, I$_1$-IR binding site assays were conducted in membranes obtained from the rat kidney using moxonidine, a known I$_1$-IR selective compound, as reference. The results are summarized in Table 2 and only **8e** deserves a mention with a pKi I$_1$ 8.09. Gratifyingly, the values for the rest of the assessed compounds led to the conclusion that there was not a significant interaction with I$_1$-IR highlighting the I$_2$-IR selective behavior of this family of ligands.

Table 2. I$_1$-IR potencies (pIC$_{50}$) of representative compounds

Compound	pIC$_{50}$
	[^{3}H]-Clonidine
Moxonidine	8.45 ± 0.85
8a	5.13 ± 0.44
8b	5.14 ± 0.54
8c	5.47 ± 0.31
8d	<3
8e	8.09 ± 0.34
9a	6.19 ± 0.27
9b	7.54 ± 0.79
9c	6.74 ± 0.74
9d	3.04 ± 0.45
9e	3.22 ± 0.67
14c	5.12 ± 0.85

9j	5.87 ± 0.19
9k	7.98 ± 0.31
9x	5.26 ± 0.43
9z	7.19 ± 0.33

Overall, considering their excellent I_2-IR affinity (Ki = 2.8 nM) and the remarkable selectivity versus α_2-AR (Ki = 53 µM) and I_1-IR (Ki = 91 mM), we identified **9d** as the most promising compound for performing further studies.

Comparison of I_2-IR human receptor binding affinities (pKi) of 9d and other ligands, and across species

A problem typically encountered when working with I_2-IR ligands is that the binding experiments reported in the bibliography have been performed in a variety of non-human species and using tissues from different anatomical parts (e.g., kidney, whole brain, cortex). Another factor of potential discrepancies is that different radioligands have been used. Overall, this makes difficult the comparison amongst studies. For this reason, and in order to better place **9d** as a new I_2-IR ligand, unprecedented experiments of displacement of [³H]2-BFI[31] in samples from post-mortem human brains were performed with clinical candidates BU99008 **2**[32] and CR4056 **1**[33] and the widely used I_2-IR ligands tracizoline, LSL60101 **3** and 2-BFI **6** (Table 3).

As previously observed with **9d**, the affinity data found for BU99008 **2** and CR4056 **1** fitted best to a two-site model of binding. In particular, BU99008 **2** showed a pK_{iH} I_2 = 6.89 (K_{iH} = 128 nM) and pKi_L I_2 = 3.82 (Ki_H = 15.1 mM), and a good I_2/α_2 selectivity ratio of 331. CR4056 **1** showed

a pKi_H I_2 = 7.72 (Ki_H = 19.0 nM) and pKi_L I_2 = 5.45 (Ki_H = 3.5 µM) with an excellent I_2/α_2 selectivity of 117490. The percentage of occupancy for the high affinity site was different for BU99008 **2** (51%) compared with CR4056 **1** (29%). Other well-stablished I_2-IR ligands, tracizoline **5**, LSL60101 **3** and 2-BFI **6** also resulted in clearly biphasic curves. Tracizoline **5** displayed a pKi_H I_2 = 8.48 (Ki_H = 3.3 nM) and pKi_L I_2 = 6.48 with an excellent I_2/α_2 selectivity of 14125. 2-BFI **6** had a pKi_H I_2 = 9.87 (Ki_H = 0.13 nM) and pKi_L I_2 = 7.94, with a good I_2/α_2 selectivity of 1698 and LSL60101 **3** a pKi_H I_2 = 9.03 (Ki_H = 0.9 nM) and pKi_L I_2 = 5.25 (Ki_L = 5.6 µM), with a good I_2/α_2 selectivity of 7244. The high-affinity site represented 38, 21 and 49% occupancy for tracizoline **5**, 2-BFI **6** and LSL60101 **3**, respectively (Table 3). Previous studies have reported [^{3}H]2-BFI identifying two binding sites in rabbit,[34] rat[35,36] and human brain.[31] It remains unclear whether these two sites observed represent distinct receptors or interconvertible conformational states of the I_2-IR. For tracizoline **5** a single binding site of pKi I_2 = 8.72, similar to the affinity described for human tissues, was described in the rabbit kidney membranes.[37] In the rat cerebral cortex, LSL60101 **3** is less affine than in human tissues, with a Ki_H = 350 nM and Ki_L = 116 µM.[38]

Therefore, compounds BU99008 **2**, tracizoline **5** and 2-BFI **6**, that have a non-substituted 2-(imidazolin-2-yl) group, CR4056 **1** and LSL60101 **3**, that feature an imidazole ring, and the structurally dissimilar **9d**, have similar affinity profiles upon I_2-IR in human brain.

Table 3. I_2-IR and α_2-AR binding affinities (pKi) of BU99008 2, CR4056 1, tracizoline 5 and LSL60101 3 and 9d in postmortem human brain cortical membranes.

Compound	[^{3}H]-2-BFI I$_2$ pKi two sites		High-affinity site %	[^{3}H]-RX821002 α$_2$ pKi	Selectivity I$_2$/α$_2$ for [^{3}H]-2-BFI (high-affinity site)
BU99008, 2	6.89 ± 0.21	3.82 ± 0.30	51 ± 6	4.37 ± 0.17	331
CR4056, 1	7.72 ± 0.31	5.45 ± 0.15	29 ± 6	2.65 ± 1.24	117490
Tracizoline, 5	8.48 ± 0.51	6.48 ± 0.32	38 ± 13	4.33 ± 0.22	14125
2-BFI, 6	9.87 ± 0.33	7.94 ± 0.11	21 ± 5	6.64 ± 0.38	1698
LSL60101, 3	9.03 ± 0.21	5.25 ± 0.24	49 ± 4	5.17 ± 1.32	7244
9d	8.61 ± 0.28	4.29 ± 0.20	37 ± 4	6.27 ± 0.56	219

Of note, the ability of BU99008 **2** to displace [^{3}H]2-BFI from I$_2$-IR in rat brain was described to fit to a two-site model of binding, with a Ki$_H$ = 1.4 ± 0.6 nM and Ki$_L$ = 238.6 ± 63.3 nM, and with a percentage % fraction of high occupancy of 58 ± 7. That is, an enhanced affinity by 100 times in rat brain, compared with human brain, being the % of occupancy similar in the high site. Regarding selectivity, a good I$_2$/α$_2$ ratio of 909 was reported in rat, 4.5 times higher than that found in human. Of note, the opposite trend was found for CR4056 **1**, the inhibition recorded in rat whole-brain for [^{3}H]2-BFI binding was IC$_{50}$ of 596 ± 76 nM, with an improved affinity to 19 nM showed in human brain.[39] Therefore, significant differences between species occur within the two I$_2$-IR ligands in clinical trials, BU99008 **2** and CR4056 **1**.

In an attempt to incorporate additional data regarding the differences in I$_2$-IR binding affinities between species, idazoxan **4** and **9d** were investigated (Table 4). In our hands, idazoxan **4** gave similar results in human frontal cortex, pKi 7.74, as compared to rat brain cortex, pKi 7.17, and was considerably less affine in mouse brain cortical membranes, pKi 5.68. Importantly, differences for **9d** were not only found among species but also in its binding

characteristics. As previously mentioned, the binding to I_2-IR in human frontal cortex displayed a biphasic curve, whereas a monophasic one was observed in rat and mouse brain cortex with affinity values of pKi 6.92 and 6.41, respectively.

Table 4. I_2-IR binding affinities (pKi) of idazoxan 4 and 9d in the brain cortex of different species.

	Human		Rat	Mice
Idazoxan, 4	7.74 ± 0.10		7.17 ± 0.11	5.68 ± 0.31
9d	8.61 ± 0.28	4.29 ± 0.20	6.92 ± 0.35	6.41 ± 0.39

Finally, in order to verify if the high affinity site observed for **9d** in competition experiments against [^{3}H]2-BFI corresponded to the I_2-IR, we performed additional experiments in the presence of MCR5 **7**, a high-affinity I_2-IR selective compound previously reported by our group.[25] Interestingly, in the presence of MCR5 **7** (10^{-5} M) the **9d** competition curve against [^{3}H]2-BFI became monophasic (pKi = 6.96 ± 0.46), and the high-affinity site recognized by **9d** was completely blocked. These results confirm that the high affinity site bound by **9d** is the I_2-IR.

3D-QSAR study

3D-QSAR studies were performed to rationalize the differences in activity and gain

insights for improved bicyclic α-iminophosphonates-based I_2-IR ligands. 3D-QSAR

models were created using Pentacle program,[40] which calculates GRIND independent

descriptors (GRIND and GRIND2) from molecular interaction fields, and were evaluated

by internal and external validation parameters (Tables S2 and S3). The data set

included structurally diverse bicyclic α-iminophosphonates (Schemes 2 and 3) with a

wide range of binding activity on I_2-IR (pKi I_2 = 3.11-10.28) and $α_2$-AR (pKi $α_2$ = 3.38-

10.27) ensuring the good quality and applicability of the 3D-QSAR models. Additionally,

we added four I_2-IR standard ligands (tracizoline **5**, idazoxan **4**, BU99008 **2** and

LSL60101 **3**), in both data sets to compare and validate our results. Created 3D-QSAR

models were used to analyse statistically significant variables which describe distance

between chemical groups in the examined compounds. These variables are presented

as interactions between two same (e.g. DRY-DRY) or different (e.g. DRY-TIP) MIF

probes in PLS coefficients plots (Figures S1 and S2).

Describing most significant GRIND variables with positive and negative influence on I_2-IR and α_2-AR binding activity gave us the deeper insight into crucial interactions for enhancing activity and selectivity on I_2-IR against α_2-AR. Based on comprehensive 3D-QSAR analysis presented in Supporting Information we can conclude that presence of two steric hot spots (var183: TIP-TIP), such as halogen atoms (3-chloro-4-fluoro) in the *N*-phenyl ring at the distance range 6.00-6.40 Å may be crucial for enhancing I_2-IR binding activity and selectivity. The highest values are calculated for compounds **13d** and **12d** which possess high selectivity towards I_2-IR (Figure 5B). Likewise, var19 (DRY-DRY: 7.60-8.00 Å) implies that introduction of hydrophobic regions such as phenyl ring in the *N*-maleimide group may be crucial for establishing favourable Van der Waals interactions with aromatic amino acids of the active pocket of I_2-IR (Figure 5A and 5B). Comparing to compounds which possess *N*-alkyl substituents instead of *N*-phenyl, such as **8a** or **9a**, we can conclude that introduction of this aromatic ring positively correlates with I_2-IR binding activity. Contrary, α_2-AR model pointed out negative DRY-DRY variable (var25: 10.00-10.40 Å) which suggests that introduction of phenyl substituent in the *α*-phosphonate position negatively correlates with α_2-AR activity. This is in

agreement with experimental findings which show that α-substituted ligands possess

higher affinity and selectivity towards I_2-IR (**8a**, **8c**, **8d** and **8e**). Additionally, analysis of

negative variables var200 (TIP-TIP: 12.80-13.20 Å), var314 (DRY-N1: 13.60-14.00 Å)

and var377 (DRY-TIP: 16.40-16.80 Å) emphasizes that introduction of bulkier

substituents in the *N*-maleimide group unfavourably fit in the binding site of I_2-IR and

may decrease the potency of I_2 ligands (Figure 6A and 6B). The highest values of these

variables are pronounced in compounds **9z**, **9m**, **9k**, **9j**, **9ab** and **9ac**.
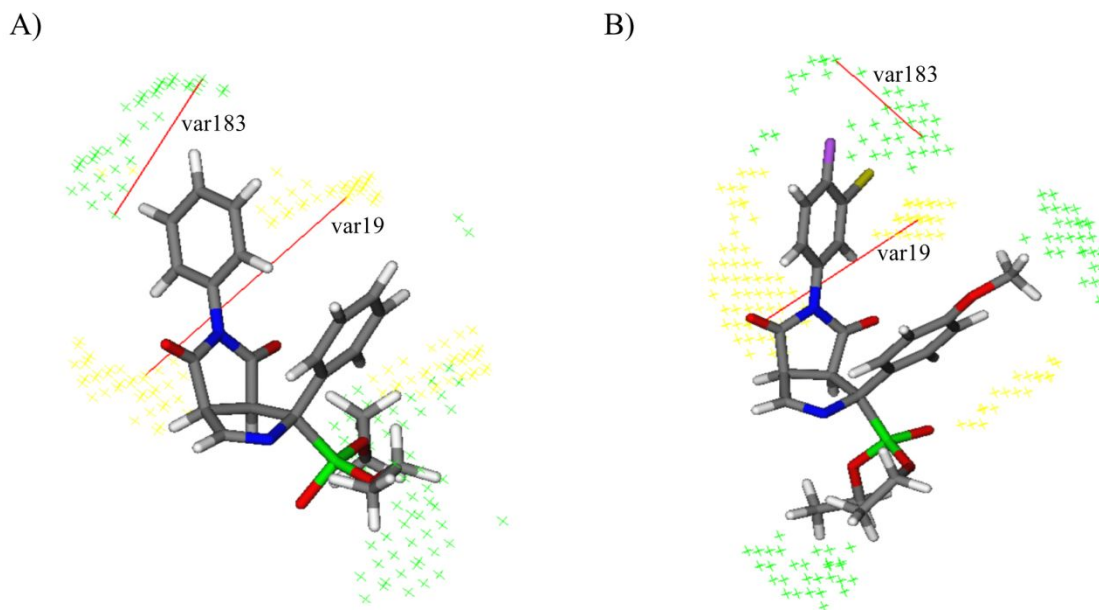
Figure 5. Representation of positive (in red) interactions of **9c** (A) and **13d** (B) in I_2-IR

3D-QSAR model. The steric hot spots (TIP) are presented in green and hydrophobic

regions (DRY) in yellow.

A)   B)
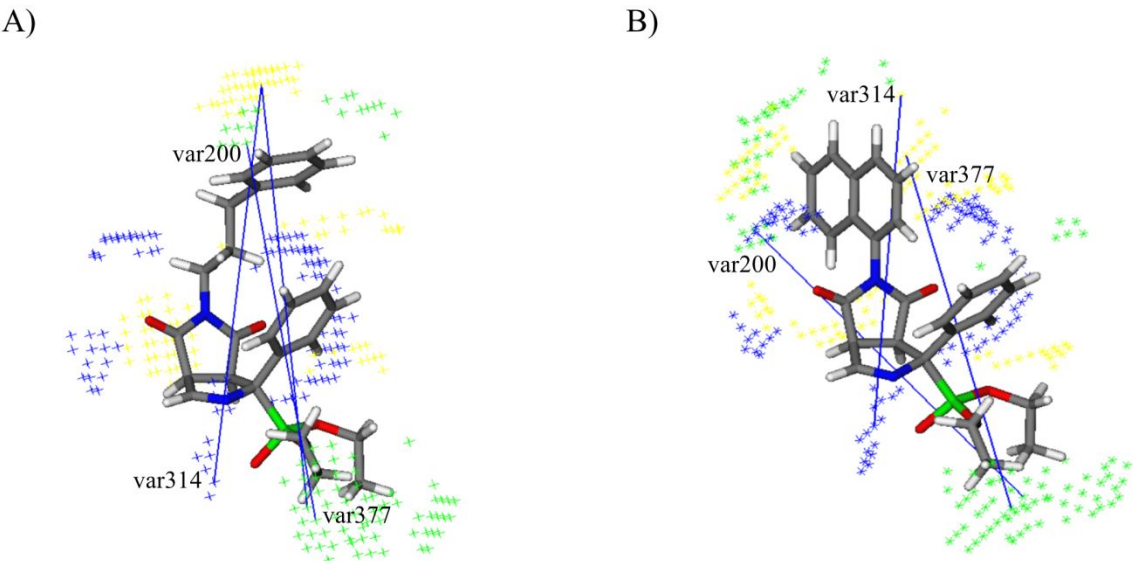
Figure 6. Representation of negative (in blue) interactions of **9m** (A) and **9ac** (B) in I_2-IR

3D-QSAR model. The steric hot spots (TIP) are presented in green, hydrophobic

regions (DRY) in yellow and H-bond acceptor regions (N1) in blue.

In silico analysis of physico-chemical and pharmacokinetic parameters

In silico analysis of key parameters is one of the most important steps in drug discovery

processes.[41] Thus, ADMET Predictor software 9.5,[42] and SwissADME web tool[43] were

used to foresee ADMET and physico-chemical properties on most potent bicyclic α-iminophosphonate I_2-IR ligands (pKi>7) and four standards. The obtained results are presented in the Supporting information (Table S4 and S5) including solubility and lipophilicity, BBB-penetration, elimination rate, as well as interactions with targets. Note, that introduction of aromatic rings increases log P values and affinity for albumin, while it decreases the water solubility (**9d**, **9z**, **12d**, **13d**). Based on results obtained from different computational methods we can conclude that all examined compounds possess good water solubility and lipophilicity. Furthermore, calculated values of topological polar surface area (TPSA) descriptor revealed acceptable polarity of all molecules. The Lipinski's Rule of 5 was used to describe drug-likeness properties of compounds based on physico-chemical analysis (Mlog P≤4.15; MW≤500; N or O≤10 OH or NH≤5). Because of the slightly higher molecular weight, **9z** and **13d** violated only one rule. Analysis of pharmacokinetic parameters shows that all compounds possess high BBB permeation. Compared to standards, bicyclic α-iminophosphonates have lower percentage of unbound drug in plasma. Also, it is estimated lower metabolic CYP risk comparing to idazoxan. Only three compounds, **9z**, **12d** and **13d** were identified as

P-gp inhibitors. Performed calculations also show that bicyclic α-iminophosphonates

possess lower toxicity risk, while compound **13d** have no predicted toxicity.

The theoretical effort paved the way to continue with *in vitro* crucial experiments (drug-

like) due to the lack of warnings that had stopped the progress of this family of α-

iminophosphonates as I_2-IR ligands.

BBB permeation assay

Considering the localization of I_2-IR in the CNS, a good ability to cross the BBB is an essential

requirement for developing effective I_2-IR ligands with potential therapeutic applications in the

neuroprotective field. For this reason, the *in vitro* permeability (P_e) of all the novel compounds

was determined by using the PAMPA-BBB permeability assay (Table S6). In particular, our

representative compound **9d** had a P_e value of $9.7 \pm 0.7 \times 10^{-6}$ cm s^{-1}, well above the threshold

established for high BBB permeation ($P_e > 5.198 \times 10^{-6}$ cm s^{-1}). Thus, compounds were

considered suitable to envisage further *in vitro* and *in vivo* studies oriented to in-depth the

pharmacological profile of the new family of I_2-IR ligands.

Cytotoxicity

All the synthesized compounds were devoid of cytotoxicity in human embryonic lung fibroblast

cell cultures (highest concentration tested: 100 μM). Further evaluation of eight selected

compounds, including the outstanding I_2-IR ligands **9d**, **9b** and **9c**, and representative

compounds **8d**, **9e**, **8b**, **9x** and **9j** was performed in different mammalian cell lines, such as HeLa

(human cervix carcinoma), Vero (African green monkey kidney), MDCK (Mandin-Darby canine kidney) and MT4 (human T-lymphocyte). Serial compound dilutions were added to semi-confluent cell cultures and after three to five days incubation at 37 ºC, cytotoxicity was estimated by microscopic inspection of cell morphology and by colorimetric cell viability assay cells. Neither of the compounds produced any cytotoxicity at 100 μM, the highest concentration tested. Additionally, the cytotoxicity of **9d** was tested in MRC-5 (human embryonic lung fibroblast) cells ($CC_{50} > 100$ μM).

ADME-DMPK profiling of 9d

In order to further progress **9d** to *in vivo* assays and with the confidence that offered the *in silico* studies (see above), we evaluated its physico-chemical properties, such as solubility and chemical stability, microsomal stability, cytochromes inhibition, hERG inhibition and plasma protein binding.
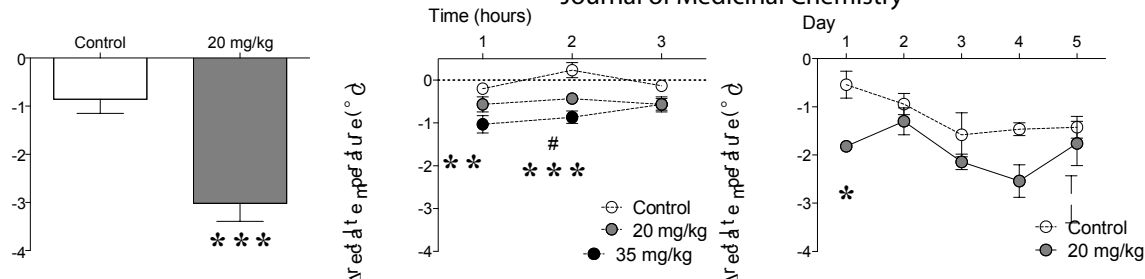
The solubility of **9d** was determined in several media. An excellent solubility of 92 μM was found in 1% DMSO and 99% PBS buffer. Additional solvents, methanol, acetonitrile and water were also evaluated with good solubility.[44] To evaluate the stability of **9d**, forced degradation studies were performed under various stress conditions for a period of nine weeks, with HPLC and ^{1}H-NMR monitoring every week.[45] Particularly, **9d** was subjected to the effect of daylight with temperatures between 0-23 ºC and a relative humidity of 25-85 %, to the effect of high temperature (thermal stability at 75 ºC), and to the continuous light of a 100W (230V) bulb. Analysis by HPLC showed that the compound was completely stable under all the

aforementioned conditions. Overall, these studies confirmed that **9d** is sufficiently stable to undertake further experiments.

Selected compound **9d** was further studied *in vitro* for ascertaining their microsomal stability, CYP inhibition, and protein plasma binding. The microsomal stability was assessed in three species (human, mouse, rat), considering that the affinity and selectivity studies were performed in human samples, the cognition studies were envisaged in mice and the hypothermia in mice and rats (see below). **9d** showed good microsomal stability (Table S7) and neither inhibited cytochromes [CYP1A2, CYP2C9, CYP2C19, CYP3A4 (BFC and DBF) and CYP2D6] nor hERG. Plasma protein binding was measured in mice and human species (Table S8) with a slight difference that should be taken into consideration if **9d** progress through additional preclinical studies.

Receptor characterization panel

A. Acute B06 treatmEnt in mice (1 h, i.p.)
B. Acute B06 treatment in rats (i.p.)
C. Repeated B06 treatment in mice (i.p., 5 d)

In a Lead Profiling Screen (Eurofins)[46] of 44 potential off targets, **9d** showed a clean ancillary pharmacology (Table S9). Only one target, the cholecystokinin type A receptor (CCK_A), was inhibited more than 50% at the tested concentration of 10 μM. CCK receptors belong to the G-protein-coupled receptors superfamily and are involved in a range of biological actions mediated by two distinct receptor types, CCK_A (present in gastrointestinal tract and discrete regions of the brain) and CCK_B (present in the CNS). Compound **9d** exhibited an IC_{50} of 5.94 μM upon CCK_A and an $IC_{50} > 10$ μM for CCK_B. Taking into account the relative high IC_{50} of **9d** for CCK_A and the lack of significant interaction with the other off targets evaluated, we conclude that **9d** shows a very selective profile.

Hypothermic effects of 9d

It is known that I_2-IR ligands as idazoxan **4** or 2-(4,5-dihydroimidazol-2-yl)quinoline (BU224) induce hypothermia in rats.[48,49] We have also found hypothermic effects with compound MCR5 **7** in mice.[25, 27]

In the same line, acute **9d** (20 mg/kg) induced hypothermia in adult CD1 mice as observed by reductions of core body temperature (ranging from -1.8 to - 3.0 ºC) measured 1 h post-injection (Figures 7A and 7C, day 1). To test for differences between species, a pilot study was performed in adult rats, which showed that acute **9d** (20 and 35 mg/kg) induced moderate drops in temperature (-0.4 to -1.0 ºC) as measured 1 and 2 h post-injection (Figure 7B). Repeated administration of **9d** (20 mg/kg, 5 days) in mice revealed the induction of tolerance to the acute

hypothermic effect of this drug from day 2 of treatment (Figure 7C), effects previously observed

for other I_2-IR compounds.[25, 27]

Figure 7. Hypothermic effects of **9d** in rodents. (A) Acute effect of **9d** (20 mg/kg, i.p.) in mice. Columns are means ± SEM of the difference (Δ, 1 h minus basal value) in body temperature (°C) for each treatment group. ***$p < 0.001$ vs. control group (Student's *t*-test). (B) Acute effect of **9d** (20 or 35 mg/kg, i.p.) in rats. Columns are means ± SEM of the difference (Δ, 1, 2 or 3 h minus basal value) in body temperature (°C) for each treatment group. #$p < 0.05$ for dose of 20 mg/kg and **$p < 0.01$ and ***$p < 0.001$ for dose of 35 mg/kg vs. control group (repeated measures ANOVA followed by Sidak's comparison test). (C) Repeated (5 days) effect of **9d** (20 mg/kg, i.p.) in mice. Circles are means ± SEM of the daily difference (Δ, 1 h minus basal value) in body temperature (ºC) for each treatment group. *$p < 0.05$ vs. control group (repeated measures ANOVA followed by Sidak's comparison test).

Of note, hypothermia is well established as having a neuroprotective effect in cerebral ischemia and even mild temperature drops cause significant neuroprotection.[50] Also, hypothermia has been clinically used to improve the neurological outcome under various pathological conditions, including stroke and traumatic brain injury.[51,52] Thus, the hypothermic effects showed by **9d** might be a relevant feature that could mediate neuroprotection.

Effects of acute and repeated treatments with 9d on hippocampal FADD protein content in mice

FADD multifunctional protein is an adaptor of cell death receptors that can also mediate antiapoptotic and/or neuroprotective actions in rodents.[25,53.54] Acute treatment with **9d** significantly decreased (- 30 %) the content of FADD protein in the hippocampus when compared to vehicle-treated mice (Figure 8, left panel). Following repeated (5 days) administration, no effects were observed on FADD modulation (Figure 8, right panel). The significant decrease in hippocampal FADD following acute **9d** treatment suggests that this compound might be mediating some of its neuroplastic and/or neuroprotective actions through the regulation of this key brain marker, similarly with other I_2-IR compounds.[25]
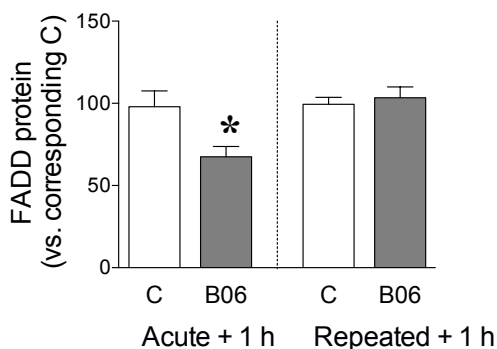
Figure 8. Effects of acute (20 mg/kg, i.p.) and repeated (20 mg/kg, i.p., 5 days) treatments with **9d** on the contents of FADD protein in the hippocampus of mice. Columns are means ± SEM of FADD in **9d**- and vehicle-treated groups. *$p < 0.05$ vs. control group (Student's *t*-test).

## 5xFAD *In Vivo* Behavioral Studies on Selected Compound 9d

Recently, we reported the first *in vivo* study that validates I_2-IR as a target for cognitive impairment using a mice model of age-related cognitive decline and late-onset AD, the SAMP8,

a murine model that displays a phenotype of accelerated aging.[27] To further support the effect of I$_2$-IR ligands as a putative treatment for neurodegenerative diseases, herein we evaluate **9d** in the 5xFAD, a well-stablished murine model of early on-set AD.[55]

Because one of the signs of AD is memory loss (cognitive decline), the effect of orally administered **9d** (5 mg/kg/day, for 28 days) on cognitive performance was evaluated in the novel object recognition test (NORT). The NORT is a widely used behavioral task to assess visual recognition memory.[56] This brain activity relies on the hippocampus and involves cortex to

remember and recognize new and old objects. Then NORT is based on an animal's innate preference for novelty. The task consists of three parts: a habituation phase; a training phase, where mice are presented with two identical objects; and, a trial phase, following an interval time (2 or 24 h) memory was assessed by presenting the mice with a trained object and a novel. Mice with cognitive ability preserved preferentially explore the novel object in the different time exposition studied. After a 2 h acquisition trial, one of the familiar objects was replaced with a novel object, and the time spent investigating each of the objects was recorded, and the discrimination index (DI) was calculated as the percentage of novel object interaction time relative to total interaction time during the retention trial. As expected, untreated 5xFAD did not exhibit differences between exploration times for the familiar and novel objects (DI close to 0), indicating deterioration or loss of memory for the familiar object. As shown in Figure 9A, the oral administration of **9d** to 5xFAD enhanced recognition memory at short term, reaching DI values of WT mice (Figure 9A). Of note, 24 h after the retention trial, **9d** treated 5xFAD mice, explored the novel object for a longer time, obtaining a higher DI, indicative of preserved

memory for the familiar object presented during the acquisition trial (Figure 9B). These results

suggest that compound **9d** enhanced recognition memory during the NORT in 5xFAD mice.
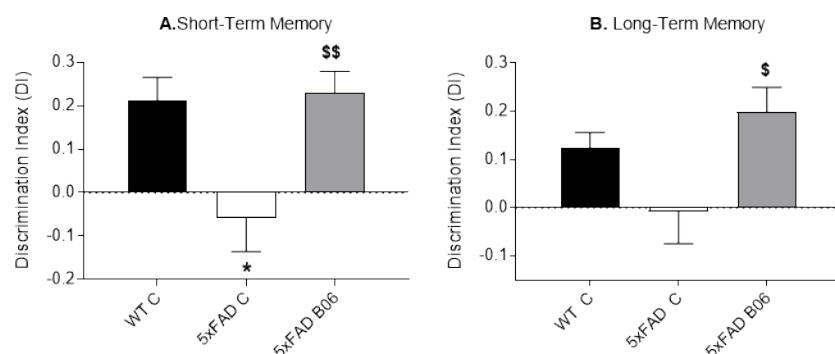
Figure 9. DI of NORT in 6-month-old (WT C, n=12), 5xFAD (C, n=14) control mice and

5xFAD mice after treatment with **9d** at 5mg/Kg for 4 weeks (n=25). Summary from (A)

Short-Term Memory (B) Long-Term Memory Values represented are mean ± Standard

error of the mean (SEM). One-way ANOVA followed by (Tukey post-hoc test); P-value:

*$p<0.05$ vs WT-Control, $^{\$}$ $p<0.05$; $^{\$\$}$ $p<0.01$ vs 5xFAD-Control.

**Effects of Selected Compound 9d in 5xFAD hippocampus: neuroinflammation and
oxidative stress parameters**

Inflammation is an omnipresent sign in neurodegeneration and can act as a propagation way to

the deleterious effects for the characteristic event in AD.[57] Oxidative stress (OS) is another key

risk factor that can promote ignition for degenerative processes.[58] The reduction in the memory

impairment of the **9d** treated animals prompted us to determine indicators of brain neuroinflammation and OS by comparison of WT and 5xFAD mice (vehicle and **9d** treated). 5xFAD had higher gene expression of *Cxcl10* (C-X-C motif chemokine 10) and *Tnf-α* (Tumor necrosis factor α) compared to WT mice (Figure 10A) that reduced after treatment of 5xFAD mice with **9d** (5 mg/kg/day). Of note, it is described that TNF-α contributes to amyloidogenesis via β-secretase regulation, apart from to be involved in AD-related brain neuroinflammation.[59] In fact, when amyloid precursor protein (APP) processing was studied in treated 5xFAD mice, an increase in sAPPα, correlating with a significant decrease in sAPPβ protein levels were determined compared with untreated mice (Figure 10B).

In reference to OS, 5xFAD showed no changes in gene expression for *iNOS* (inducible Nitric Oxide Synthase, a pro-oxidant key driver)[60] and *Hmox1* (an enzyme implicated in antioxidant defense) (Figure 10A).[61] Those results correlated with published results in 5xFAD, and in agreement, **9d** treatment did not modify neither *iNOS* nor *Hmox1* (Figure 10A). Nonetheless, total levels of hydrogen peroxide (H_2O_2), although not significant, were higher in 5xFAD than in the WT, and were reduced after **9d** treatment (Figure 10C). The increase of OS, without increases in *iNOS* expression, was also described in 5xFAD, concretely the increase in 4-HNE (4-hydroxy-2-nonenal), a protein derivative obtained when reactive species of oxygen ROS (as H_2O_2) increase is significant in 6-month-old 5xFAD compared to WT mice.[62] All the evaluated parameters are consistent with a mild reduction in the oxidative environment in 5xFAD treated mice.
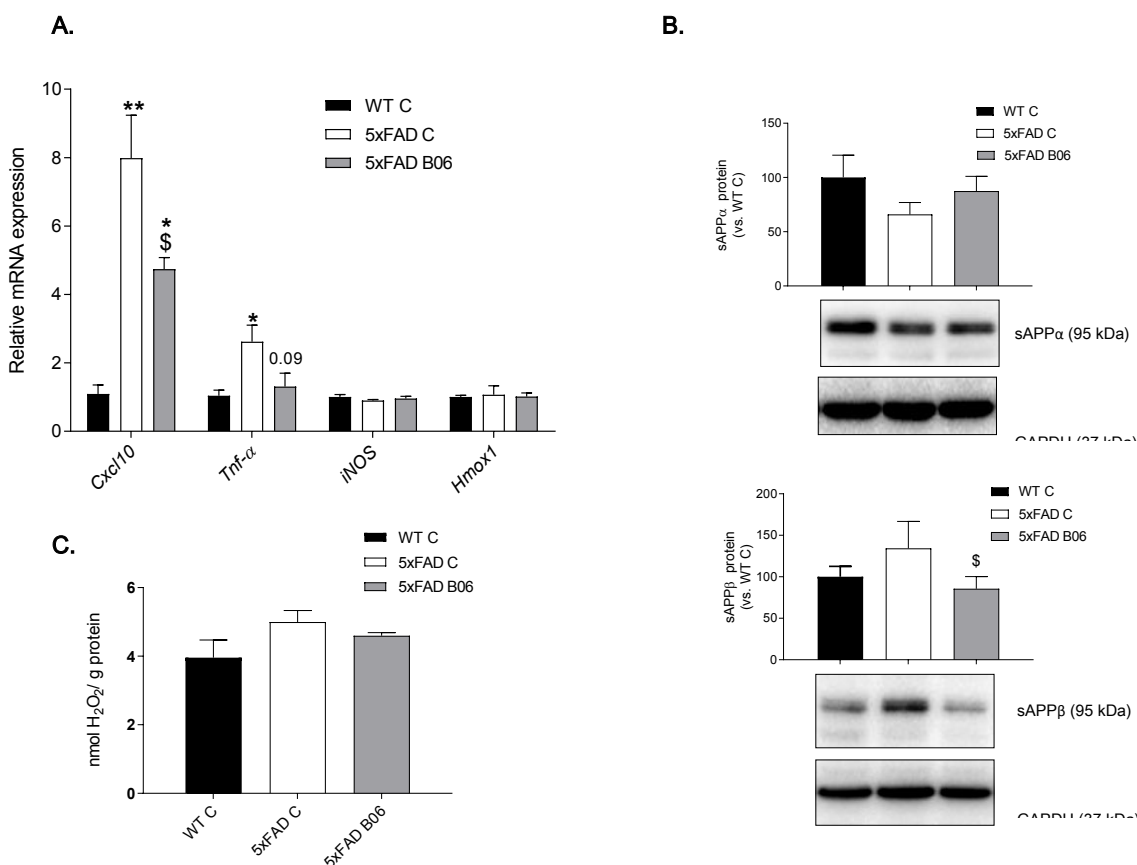
Figure 10. (A) Gene expression of inflammatory markers *Cxcl10, Tnf-α,* and OS markers *iNOS, Hmox1*(n=4 for each group) (B) H_2O_2 concentration (n=3 for each group) and (C) Representative Western blot and bar chart sAPPα and sAPPα, (n=4-6 for each group) in the hippocampus of 6-month-old female WT, 5xFAD Control mice and 5xFAD mice after treatment with **9d** at 5mg/Kg for 4 weeks. Bars represent mean ± Standard error of the mean (SEM);

CONCLUSIONS

To sum up, we have explored the scope of diastereoselective [3+2] cycloaddition reaction of α-substituted-PhosMic derivatives with diversely substituted maleimides leading to a family of

43

bicyclic α-iminophosphonates. A combination of X-ray crystallographic analyses and NMR studies allowed a full stereochemical characterization, and theoretical calculations provided a basis to justify the excellent diastereoselectivity observed. The pharmacological profiling of the new compounds led to the identification of high affine and selective I_2-IR ligands devoid to α_2-AR and I_1-IR affinities. 3D-QSAR study revealed key structural parameters for the designing of future promising structures and theoretical DMPK and physico-chemical parameters were calculated in order to rule out warnings to continue the medicinal chemistry program. DMPK and cytotoxicity assays and a safety panel were carried out for the selected compound **9d**. Taking in account the improvement in the cognitive impairment in a 5xFAD model treated with **9d**, modulation of I_2-IR can be proposed as a new therapeutic strategy for AD treatment.

EXPERIMENTAL SECTION

Chemistry

General Information. Reagents, solvents and starting products were acquired from commercial sources. The term "concentration" refers to the vacuum evaporation using a Büchi rotavapor. When indicated, the reaction products were purified by "flash" chromatography on silica gel (35-70 μm) with the indicated solvent system. The melting points were measured in a MFB 59510M Gallenkamp instruments. IR spectra were performed in a spectrophotometer Nicolet Avantar 320

FTR-IR or in a Spectrum Two FT-IR Spectrometer, and only noteworthy IR absorptions (cm^{-1}) are listed. NMR spectra were recorded in CDCl$_3$ at 400 MHz (^{1}H) and 100.6 MHz (^{13}C), and 162 MHz (^{31}P). Chemical shifts are reported in δ values downfield from TMS or relative to residual chloroform (7.26 ppm, 77.0 ppm) as an internal standard. Data are reported in the following manner: chemical shift, multiplicity, coupling constant (J) in hertz (Hz), integrated intensity and assignment (when possible). Multiplicities are reported using the following abbreviations: s, singlet; d, doublet; dd, doublet of doublets; ddd, double double of doublets; dq, doble quadrupet; t, triplet; qu, quintet; m, multiplet; br s, broad signal, app, apparent. Assignments and stereochemical determinations are given only when they are derived from definitive two-dimensional NMR experiments (g-HSQC-COSY). The accurate mass analyses were carried out using a LC/MSD-TOF spectrophotometer. The elemental analyses were carried out in a Flash 1112 series Thermofinnigan elemental microanalyzator (A5) to determine C, H, and N. HPLC-MS (Agilent 1260 Infinity II) analysis was conducted on a Poroshell 120 EC-C15 (4.6 mm x50 mm, 2.7 μm) at 40 ºC. Mobile phase (A: H$_2$0 + 0.05% formic acid and B: ACN + 0.05% formic acid) using a gradient elution. Flow rate 0.6 mL/min. The DAD detector was set at 254 nm and the injection volume was 5 μL and oven temperature 40 ºC. All tested compounds possess a purity of at least 95%.

General Procedure for the [3 + 2] cycloaddition reaction. To a solution of silver acetate (0.06 or 0.1 mmol) and maleimide (1.0 or 1.5 mmol) in acetonitrile was added diethyl α-methylisocyanomethylphosphonate, diethyl α-phenylisocyanomethylphosphonate, diphenyl α-phenylisocyanomethylphosphonate, diethyl α-(4-fluorophenyl)isocyanomethylphosphonate, diethyl α-(4-methoxyphenyl)isocyanomethylphosphonate, or diethyl α-

benzylisocyanomethylphosphonate (1.0 mmol). The reaction mixture was stirred at room temperature overnight, concentrated and the resulting residue was purified by column chromatography to afford pure products.

Diethyl (1*RS*,3a*SR*,6a*SR*)-5-methyl-4,6-dioxo-1-phenyl-1,3a,4,5,6,6a-hexahydropyrrolo[3,4-*c*]pyrrole-1-phosphonate (9a). Following the general procedure, AgOAc (13 mg, 0.08 mmol), *N*-methylmaleimide (133 mg, 1.2 mmol), acetonitrile (6 mL) and diethyl α-phenylisocyanomethylphosphonate (202 mg, 0.8 mmol) gave **9a** (184 mg, 64%) as a yellowish oil, after column chromatography (EtOAc/hexane 95:5). IR (NaCl) 3472, 2981, 1709, 1432, 1281, 1248, 1051, 967 cm^{-1}.^{1}H NMR (400 MHz, CDCl$_3$, HETCOR) δ 1.15 (t, J = 7.0 Hz, 3H, CH$_2$C*H$_3$*), 1.27 (t, J = 7.0 Hz, 3H, CH$_2$C*H$_3$*), 2.70 (s, 3H, NCH$_3$), 3.83 (m, 1H, C*H$_2$*CH$_3$), 4.01-4.18 (m, 4H, H-6a and C*H$_2$*CH$_3$), 4.34 (ddd, J = 8.5, 4.0, 1.0 Hz, 1H, H-3a), 7.29-7.37 (m, 3H, ArH), 7.68-7.70 (m, 2H, ArH), 7.95 (dd, J = 5.5, 1.0 Hz, 1H, H-3).^{13}C NMR (100.6 MHz) δ 16.1 (d, J = 5.0 Hz, CH$_2$*C*H$_3$), 16.2 (d, J = 5.0 Hz, CH$_2$*C*H$_3$), 25.0 (NCH$_3$), 47.7 (d, J = 2.0 Hz, C-6a), 60.5 (C-3a), 63.4 (d, J = 7.0 Hz, *C*H$_2$CH$_3$), 64.6 (d, J = 7.0 Hz, *C*H$_2$CH$_3$), 85.6 (d, J = 154.0 Hz, C-1), 127.6 (d, J = 2.0 Hz, 2CHAr), 128.4 (d, J = 2.5 Hz, CHAr), 128.5 (d, J = 6.0 Hz, 2CHAr), 133.2 (d, J = 4.5 Hz, C-*ipso*), 162.5 (d, J = 11.5 Hz, C-3), 172.1 (d, J = 5.5 Hz, CO), 172.5 (d, J = 14.0 Hz, CO). MS-EI m/z 364 M$^+$ (36), 255 (31), 227 (73), 199 (23), 170 (41), 143 (21), 142 (100), 115 (58). HRMS C$_{17}$H$_{22}$N$_2$O$_5$P [M+H]$^+$ 365.1262; found, 365.1261. Purity 97.0 % (t_R= 3.89 min).

Diethyl (1*RS*,3a*SR*,6a*SR*)-5-cyclohexyl-4,6-dioxo-1-phenyl-1,3a,4,5,6,6a-hexahydropyrrolo[3,4-*c*]pyrrole-1-phosphonate (9b). Following the general procedure, AgOAc (15 mg, 0.09 mmol), *N*-cyclohexylmaleimide (403 mg, 2.3 mmol), acetonitrile (12 mL) and diethyl α-phenylisocyanomethylphosphonate (380 mg, 1.5 mmol) gave **9b** (494 mg, 76%) as

a white solid, after column chromatography (EtOAc). M.p. 128-132 °C (EtOAc). IR (NaCl) 3467, 2934, 2858, 1705, 1370, 1249, 1191, 1025, 971, 755 cm^{-1}.^{1}H NMR (400 MHz, CDCl$_3$, HETCOR) δ 1.06-1.13 (m, 3H, CH$_2$cycl), 1.16 (t, J = 7.0 Hz, 3H, CH$_2$CH_3), 1.21 (m, 1H, CH$_2$cycl), 1.25 (t, J = 7.0 Hz, 3H, CH$_2$CH_3), 1.51-1.54 (m, 2H, CH$_2$cycl), 1.57-1.69 (m, 3H, CH$_2$cycl), 1.85 (m, 1H, CH$_2$cycl), 3.60 (m, 1H, CHcycl), 3.90 (m, 1H, CH_2CH$_3$), 4.03 (dd, J = 18.5, 8.5 Hz, 1H, H-6a), 4.06-4.18 (m, 3H, CH_2CH$_3$), 4.25 (ddd, J = 8.5, 3.0, 1.5 Hz, 1H, H-3a), 7.29-7.35 (m, 3H, ArH), 7.61-7.63 (m, 2H, ArH), 8.00 (dd, J = 5.0, 1.5 Hz, 1H, H-3); ^{13}C NMR (100.6 MHz) δ 16.1 (d, J = 5.5 Hz, CH$_2$CH_3), 16.2 (d, J = 5.5 Hz, CH$_2$CH_3), 24.7 (CH$_2$cycl), 25.6 (2CH$_2$cycl), 27.8 (CH$_2$cycl), 28.6 (CH$_2$cycl), 47.5 (d, J = 2.5 Hz, C-6a), 51.9 (CHcycl), 59.9 (C-3a), 63.3 (d, J = 7.5 Hz, CH$_2$CH$_3$), 64.6 (d, J = 7.5 Hz, CH$_2$CH$_3$), 85.7 (d, J = 156.0 Hz, C-1), 127.7 (d, J = 1.6 Hz, 2CHAr), 128.2 (CHAr), 128.3 (CHAr), 128.4 (CHAr), 133.6 (d, J = 4.0 Hz, C-$ipso$), 162.8 (d, J = 12.0 Hz, C-3), 172.1 (d, J = 5.5 Hz, CO), 172.5 (d, J = 12.0 Hz, CO). MS-EI m/z 432 M$^+$ (60), 323 (30), 295 (95), 223 (12), 170 (78), 142 (100), 115 (35), 81 (15). HRMS C$_{22}$H$_{30}$N$_2$O$_5$P [M+H]$^+$ 433.1892; found, 433.1887. Anal. Cald. for C$_{22}$H$_{30}$N$_2$O$_5$P: C, 61.10%; H, 6.76%; N, 6.48%; found: C, 61.42%; H, 6.81%; N, 6.47%.

Diethyl (1RS,3aSR,6aSR)-4,6-dioxo-1,5-diphenyl-1,3a,4,5,6,6a-hexahydropyrrolo[3,4-c]pyrrole-1-phosphonate (9c). Following the general procedure, AgOAc (4 mg, 0.02 mmol), N-phenylmaleimide (104 mg, 0.6 mmol), acetonitrile (3 mL) and diethyl α-phenylisocyanomethylphosphonate (101 mg, 0.4 mmol) gave **9c** (108 mg, 64%) as a white solid, after column chromatography (EtOAc). M.p. 158-160 °C (EtOAc). IR (NaCl) 3479, 2969, 1713, 1496, 1390, 1239, 1021, 969 cm^{-1}. ^{1}H NMR (400 MHz, CDCl$_3$, HETCOR) δ 1.10 (t, J = 7.0 Hz, 3H, CH$_2$CH_3), 1.19 (t, J = 7.0 Hz, 3H, CH$_2$CH_3), 3.85 (m, 1H, CH_2CH$_3$), 3.99-4.14 (m, 3H, CH_2CH$_3$), 4.17 (dd, J = 18.5, 9.0 Hz, 1H, H-6a), 4.40 (ddd, J = 8.5, 3.0, 1.6 Hz, 1H, H-3a), 6.62-

6.65 (m, 2H, ArH), 7.15-7.30 (m, 6H, ArH), 7.61-7.63 (m, 2H, ArH), 7.97 (dd, J = 4.5, 1.6 Hz, 1H, H-3).^{13}C NMR (100.6 MHz) δ 16.2 (d, J = 4.0 Hz, CH$_2$CH$_3$), 16.3 (d, J = 4.0 Hz, CH$_2$CH$_3$), 48.2 (d, J = 2.0 Hz, C-6a), 60.2 (C-3a), 63.4 (d, J = 7.0 Hz, CH$_2$CH$_3$), 64.6 (d, J = 7.0 Hz, CH$_2$CH$_3$), 86.2 (d, J = 157.0 Hz, C-1), 126.0 (2CHAr), 127.9 (CHAr), 128.0 (CHAr), 128.4 (d, J = 6.0 Hz, CHAr), 128.5 (CHAr), 128.6 (CHAr), 128.7 (CHAr), 129.0 (2CHAr), 131.1 (C-*ipso*), 133.5 (d, J = 4.0 Hz, C-*ipso*), 162.5 (d, J = 12.0 Hz, C-3), 170.9 (d, J = 5.5 Hz, CO), 171.6 (d, J = 11.5 Hz, CO). MS-EI *m/z* 426 M$^+$ (43), 317 (20), 289 (47), 244 (11), 170 (43), 142 (100), 115 (43), 81 (11). HRMS C$_{22}$H$_{24}$N$_2$O$_5$P [M+H]$^+$ 427.1418; found, 427.1417. Anal. Cald. for C$_{22}$H$_{23}$N$_2$O$_5$P: C, 61.97%; H, 5.44%; N, 6.57%; found: C, 62.18%; H, 5.36%; N, 6.43%.

Diethyl (1*RS*,3a*SR*,6a*SR*)-5-(3-chloro-4-fluorophenyl)-4,6-dioxo-1-phenyl-1,3a,4,5,6,6a-hexahydropyrrolo[3,4-*c*]pyrrole-1-phosphonate (9d). Following the general procedure, AgOAc (8 mg, 0.05 mmol), *N*-(3-chloro-4-fluorophenyl)maleimide (250 mg, 1.1 mmol), acetonitrile (6 mL) and diethyl α-phenylisocyanomethylphosphonate (187 mg, 0.7 mmol) gave **9d** (189 mg, 54%) as a white needles, after column chromatography (EtOAc). M.p. 185-186 ºC (EtOAc). IR (NaCl) 3437, 2956, 1718, 1499, 1256, 1050, 980 cm^{-1}.^{1}H NMR (400 MHz, CDCl$_3$, HETCOR) δ 1.20 (t, J = 7.0 Hz, 3H, CH$_2$CH_3), 1.28 (t, J = 7.0 Hz, 3H, CH$_2$CH_3), 3.95 (m, 1H, CH_2CH$_3$), 4.09-4.20 (m, 3H, CH_2CH$_3$), 4.25 (dd, J = 18.0, 8.0 Hz, 1H, H-6a), 4.47 (m, 1H, H-3a), 6.63 (ddd, J = 9.0, 4.0, 3.0 Hz, 1H, ArH), 6.72 (dd, J = 6.5, 2.5 Hz, 1H, ArH), 7.05 (t, J = 8.5 Hz, 1H, ArH), 7.35-7.39 (m, 3H, ArH), 7.67 (m, J = 5.0 Hz, 2H, ArH), 8.05 (d, J = 4.5 Hz, 1H, H-3).^{13}C NMR (100.6 MHz) δ 16.3 (t, J = 5.5 Hz, 2CH$_2$CH$_3$), 48.5 (C-6a), 60.1 (C-3a), 63.7 (d, J = 7.0 Hz, CH$_2$CH$_3$), 64.8 (d, J = 7.0 Hz, CH$_2$CH$_3$), 86.2 (d, J = 156.0 Hz, C-1), 116.8 (d, J = 22.5 Hz, CHAr), 121.5 (d, J = 19.5 Hz, C-*ipso*), 126.1 (d, J = 8.0 Hz, CHAr), 127.4 (d, J = 4.0 Hz, C-*ipso*), 128.1 (2CHAr), 128.3 (d, J = 5.5 Hz, 2CHAr), 128.6 (CHAr), 128.8 (CHAr), 133.5

(d, J = 3.0 Hz, C-*ipso*), 157.7 (d, J = 251.0 Hz, C-*ipso*), 162.0 (d, J = 12.5 Hz, C-3), 170.6 (d, J = 5.5 Hz, CO), 171.3 (d, J = 11.0 Hz, CO). ^{31}P NMR (162 MHz) δ 19.71. MS-EI *m/z* 478 M$^+$ (2), 341 (12), 281 (41), 207 (100), 191 (11), 147 (14), 73 (31). HRMS C$_{22}$H$_{22}$ClFN$_2$O$_5$P [M+H]$^+$ 479.0935; found, 479.0933. Anal. Cald. for C$_{22}$H$_{21}$ClFN$_2$O$_5$P: C, 55.18%; H, 4.42%; N, 5.85%; found: C, 55.28%; H, 4.49%; N, 5.56%.

Diethyl (1*RS*,3a*SR*,6a*SR*)-5-(4-methoxyphenyl)-4,6-dioxo-1-phenyl-1,3a,4,5,6,6a-hexahydropyrrolo[3,4-*c*]pyrrole-1-phosphonate (9e). Following the general procedure, AgOAc (4 mg, 0.02 mmol), *N*-(4-methoxyphenyl)maleimide (122 mg, 0.6 mmol), acetonitrile (3 mL) and diethyl α-phenylisocyanomethylphosphonate (102 mg, 0.4 mmol) gave **9e** (119 mg, 65%) as a white solid, after column chromatography (EtOAc). M.p. 167 °C (EtOAc). IR (NaCl) 3477, 2981, 2930, 1715, 1513, 1384, 1251, 1024, 970, 755 cm^{-1}.^{1}H NMR (400 MHz, CDCl$_3$, HETCOR) δ 1.18 (t, J = 7.0 Hz, 3H, CH$_2$C*H$_3$*), 1.28 (t, J = 7.0 Hz, 3H, CH$_2$C*H$_3$*), 3.73 (s, 3H, OCH$_3$), 3.92 (m, 1H, C*H$_2$*CH$_3$), 4.09-4.19 (m, 3H, C*H$_2$*CH$_3$), 4.25 (dd, J = 18.0, 8.5 Hz, 1H, H-6a), 4.45 (ddd, J = 8.5, 3.0, 1.5 Hz, 1H, H-3a), 6.60-6.64 (m, 2H, ArH), 6.77-6.81 (m, 2H, ArH), 7.30-7.39 (m, 3H, ArH), 7.68-7.70 (m, 2H, ArH), 8.04 (dd, J = 5.0, 1.5 Hz, 1H, H-3).^{13}C NMR (100.6 MHz) δ 16.2 (d, J = 3.5 Hz, CH$_2$*C*H$_3$), 16.3 (d, J = 3.5 Hz, CH$_2$*C*H$_3$), 48.1 (d, J = 2.0 Hz, C-6a), 55.4 (OCH$_3$), 60.1 (C-3a), 63.5 (d, J = 7.5 Hz, *C*H$_2$CH$_3$), 64.6 (d, J = 7.5 Hz, *C*H$_2$CH$_3$), 86.2 (d, J = 157.5 Hz, C-1), 114.3 (2CHAr), 123.6 (C-*ipso*), 127.2 (2CHAr), 127.9 (2CHAr), 128.3 (CHAr), 128.4 (CHAr), 128.5 (CHAr), 133.5 (d, J = 4.0 Hz, C-*ipso*), 159.5 (C-*ipso*), 162.4 (d, J = 12.0 Hz, C-3), 171.1 (d, J = 5.0 Hz, CO), 171.8 (d, J = 11.5 Hz, CO). HRMS C$_{23}$H$_{26}$N$_2$O$_6$P [M+H]$^+$ 457.1519; found, 457.1523. Anal. Cald. for C$_{23}$H$_{25}$N$_2$O$_6$P: C, 60.52%; H, 5.52%; N, 6.14%; found: C, 60.71%; H, 5.75%; N, 5.98%.

Diethyl (1*RS*,3a*SR*,6a*SR*)-1-(4-fluorophenyl)-4,6-dioxo-5-phenyl-1,3a,4,5,6,6a-

hexahydropyrrolo[3,4-*c*]pyrrole-1-phosphonate (12c). Following the general procedure, AgOAc (10 mg, 0.06 mmol), *N*-phenylmaleimide (156 mg, 0.9 mmol), acetonitrile (4 mL) and diethyl α-(4-fluorophenyl)isocyanomethylphosphonate (164 mg, 0.6 mmol) gave **12c** (159 mg, 60%) as a white solid, after column chromatography (EtOAc/hexane 4:1). M.p. 191-193 ºC (EtOAc). IR (ATR) 3491, 2991, 2909, 1775, 1718, 1598, 1506, 1377, 1242, 1189, 1016, 982, 742, 598 cm^{-1}. ^{1}H NMR (400 MHz, CDCl$_3$, HETCOR) δ 1.20 (t, *J* = 7.0 Hz, 3H, CH$_2$C*H$_3$*), 1.29 (t, *J* = 7.0 Hz, 3H, CH$_2$C*H$_3$*), 3.93 (m, 1H, C*H$_2$*CH$_3$), 4.08-4.19 (m, 3H, C*H$_2$*CH$_3$), 4.25 (dd, *J* = 18.0, 8.5 Hz, 1H, H-6a), 4.49 (dq, *J* = 8.5, 1.5 Hz, 1H, H-3a), 6.79-6.81 (m, 2H, ArH), 7.03-7.08 (m, 2H, ArH), 7.29-7.35 (m, 3H, ArH), 7.70-7.73 (m, 2H, ArH), 8.04 (dd, *J* = 5.0, 1.5 Hz, 1H, H-3). ^{13}C NMR (100.6 MHz) δ 16.4 (d, *J* = 5.5 Hz, CH$_2$*C*H$_3$), 16.5 (d, *J* = 5.0 Hz, CH$_2$*C*H$_3$), 48.1 (d, *J* = 3.0 Hz, C-6a), 60.5 (C-3a), 63.8 (d, *J* = 8.0 Hz, *C*H$_2$CH$_3$), 64.9 (d, *J* = 8.0 Hz, *C*H$_2$CH$_3$), 85.9 (d, *J* = 156.0 Hz, C-1), 114.9 (d, *J* = 2.0 Hz, CHAr), 115.1 (d, *J* = 2.0 Hz, CHAr), 126.2 (2CHAr), 129.0 (CHAr), 129.3 (2CHAr), 129.4 (dd, *J* = 4.0, 3.5 Hz, C-ipso), 130.6 (d, *J* = 6.0 Hz, CHAr), 130.7 (d, *J* = 6.0 Hz, CHAr), 131.1 (C-*ipso*), 162.8 (d, *J* = 12.0 H, C-3), 162.9 (dd, *J* = 246.0, 2.5 Hz, C-*ipso*), 171.0 (d, *J* = 6.0 Hz, CO), 171.8 (d, *J* =12.0 Hz, CO). HRMS C$_{22}$H$_{23}$FN$_2$O$_5$P [M+H]$^+$ 445.1323; found, 445.1324. Anal. Cald. for C$_{22}$H$_{22}$FN$_2$O$_5$P: C, 59.46%; H, 4.99%; N, 6.30%; found: C, 59.90%; H, 5.13%; N, 6.20%.

Diethyl (1*RS*,3a*SR*,6a*SR*)-5-(3-chloro-4-fluorophenyl)-1-(4-fluorophenyl)-4,6-dioxo-1,3a,4,5,6,6a-hexahydropyrrolo[3,4-*c*]pyrrole-1-phosphonate (12d). Following the general procedure, AgOAc (7 mg, 0.04 mmol), *N*-(3-chloro-4-fluorophenyl)maleimide (135 mg, 0.6 mmol), acetonitrile (3 mL) and diethyl α-(4-fluorophenyl)isocyanomethylphosphonate (108 mg, 0.4 mmol) **12d** (124 mg, 62%) as a white solid, after column chromatography (EtOAc). M.p. 179-181 ºC (EtOAc). IR (ATR) 3483, 2962, 2903, 1719, 1504, 1236, 1051, 1012, 978, 739, 593

cm^{-1}. ^{1}H NMR (400 MHz, CDCl$_3$, HETCOR) δ 1.20 (t, *J* = 7.0 Hz, 3H, CH$_2$C*H$_3$*), 1.28 (t, *J* = 7.0 Hz, 3H, CH$_2$C*H$_3$*), 3.94 (m, 1H, C*H$_2$*CH$_3$), 4.08-4.19 (m, 3H, C*H$_2$*CH$_3$), 4.25 (dd, *J* = 18.0, 8.5 Hz, 1H, H-6a), 4.49 (ddd, *J* = 8.5, 3.0, 1.5 Hz, 1H, H-3a), 6.71 (m, 1H, ArH), 6.87 (dd, *J* = 6.5, 2.5 Hz, 1H, ArH), 7.04-7.09 (m, 3H, ArH), 7.68-7.71 (m, 2H, ArH), 8.02 (dd, *J* = 5.0, 1.5 Hz, 1H, H-3). ^{13}C NMR (100.6 MHz) δ 16.4 (d, *J* = 5.5 Hz, CH$_2$*C*H$_3$), 16.5 (d, *J* = 5.5 Hz, CH$_2$*C*H$_3$), 48.2 (d, *J* = 3.0 Hz, C-6a), 60.3 (C-3a), 63.9 (d, *J* = 7.0 Hz, *C*H$_2$CH$_3$), 64.9 (d, *J* = 8.0 Hz, *C*H$_2$CH$_3$), 86.0 (d, *J* = 156.0 Hz, C-1), 115.1 (dd, *J* = 21.0, 2.0 Hz, 2CHAr), 117.1 (d, *J* = 22.0 Hz, CHAr), 121.8 (d, *J* = 19.0 Hz, C-*ipso*), 126.1 (CHAr), 127.4 (d, *J* = 3.0 Hz, C-*ipso*), 128.7 (CHAr), 129.2 (dd, *J* = 4.0, 3.0 Hz, C-*ipso*), 130.6 (dd, *J* = 7.0, 2.0 Hz, 2CHAr), 157.9 (d, *J* = 251.0 Hz, C-*ipso*)*, 162.4 (d, *J* = 12.0 Hz, C-3), 163.0 (d, *J* = 249.5, 3.0 Hz, C-*ipso*), 170.5 (d, *J* = 5.0 Hz, CO), 171.5 (d, *J* = 13.0 Hz, CO). HRMS C$_{22}$H$_{21}$ClF$_2$N$_2$O$_5$P [M+H]$^+$ 497.0839; found, 497.0840. Anal. Cald. for C$_{22}$H$_{20}$ClF$_2$N$_2$O$_5$P: C, 53.19%; H, 4.06%; N, 5.64%; found: C, 53.45%; H, 4.24%; N, 5.46%.

Diethyl (1*RS*,3a*SR*,6a*SR*)-1-(4-methoxyphenyl)-4,6-dioxo-5-phenyl-1,3a,4,5,6,6a-hexahydropyrrolo[3,4-*c*]pyrrole-1-phosphonate (13c). Following the general procedure, AgOAc (8 mg, 0.05 mmol), *N*-phenylmaleimide (138 mg, 0.8 mmol), acetonitrile (4 mL) and diethyl α-(4-methoxyphenyl)isocyanomethylphosphonate (142 mg, 0.5 mmol) gave **13c** (155 mg, 69%) as a white solid, after column chromatography (EtOAc/hexane 4:1). M.p. 184-186 ºC (EtOAc). IR (ATR) 3481, 2986, 2914, 1785, 1713, 1607, 1511, 1386, 1247, 1189, 1021, 737, 694, 598 cm^{-1}. ^{1}H NMR (400 MHz, CDCl$_3$, HETCOR) δ 1.20 (t, *J* = 7.0 Hz, 3H, CH$_2$C*H$_3$*), 1.28 (t, *J* = 7.0 Hz, 3H, CH$_2$C*H$_3$*), 3.79 (s, 3H, OCH$_3$), 3.92 (m, 1H, C*H$_2$*CH$_3$), 4.08-4.18 (m, 3H, C*H$_2$*CH$_3$), 4.23 (dd, *J* = 18.0, 8.5 Hz, 1H, H-6a), 4.46 (ddd, *J* = 8.5, 3.0, 1.5 Hz, 1H, H-3a), 6.76-6.78 (m, 2H, ArH), 6.88 (d, *J* = 9.0 Hz, 2H, ArH), 7.27-7.32 (m, 3H, ArH), 7.60-7.63 (m, 2H,

ArH), 8.02 (dd, J = 5.5, 1.5 Hz, 1H, H-3). ^{13}C NMR (100.6 MHz) δ 16.4 (d, J = 5.0 Hz, 2CH$_2$CH$_3$), 48.3 (d, J = 3.0 Hz, C-6a), 55.3 (OCH$_3$), 60.3 (C-3a), 63.5 (d, J = 8.0 Hz, *C*H$_2$CH$_3$), 64.8 (d, J = 8.0 Hz, *C*H$_2$CH$_3$), 86.0 (d, J = 157.0 Hz, C-1), 113.4 (d, J = 2.0 Hz, 2CHAr), 125.5 (d, J = 4.0 Hz, C-*ipso*), 126.3 (2CHAr), 128.8 (CHAr), 129.2 (2CHAr), 129.9 (d, J = 6.0 Hz, 2CHAr), 131.2 (C-*ipso*), 159.7 (d, J = 2.0 Hz, C-*ipso*), 162.3 (d, J = 12.0 Hz, C-3), 171.2 (d, J = 6.0 Hz, CO), 171.9 (d, J =12.0 Hz, CO). HRMS C$_{23}$H$_{26}$N$_2$O$_6$P [M+H]$^+$ 457.1523; found, 457.1520. Anal. Cald. For C$_{23}$H$_{25}$N$_2$O$_6$P: C, 60.52%; H, 5.52%; N, 6.14%; found: C, 60.85%; H, 5.51%; N, 5.94%.

Diethyl (1*RS*,3a*SR*,6a*SR*)-5-(3-chloro-4-fluorophenyl)-1-(4-methoxyphenyl)-4,6-dioxo-1,3a,4,5,6,6a-hexahydropyrrolo[3,4-*c*]pyrrole-1-phosphonate (13d). Following the general procedure, AgOAc (8 mg, 0.05 mmol), *N*-(3-chloro-4-fluorophenyl)maleimide (181 mg, 0.8 mmol), acetonitrile (4 mL) and diethyl α-(4-methoxyphenyl)isocyanomethylphosphonate (142 mg, 0.5 mmol) gave **13d** (170 mg, 67%) as a white solid, after column chromatography (EtOAc). M.p. 227-228 ºC (EtOAc). IR (ATR) 3481, 2986, 2905, 1771, 1718, 1612, 1497, 1386, 1237, 1184, 1026, 968, 752, 656 cm^{-1}. ^{1}H NMR (400 MHz, CDCl$_3$, HETCOR) δ 1.21 (t, J = 7.0 Hz, 3H, CH$_2$C*H*$_3$), 1.28 (t, J = 7.0 Hz, 3H, CH$_2$C*H*$_3$), 3.81 (s, 3H, OCH$_3$), 3.94 (m, 1H, C*H*$_2$CH$_3$), 4.09-4.18 (m, 3H, C*H*$_2$CH$_3$), 4.22 (dd, J = 18.0, 8.5 Hz, 1H, H-6a), 4.46 (ddd, J = 8.5, 3.0, 1.5 Hz, 1H, H-3a), 6.69-6.73 (m, 2H, ArH), 6.89 (d, J = 9.0 Hz, 2H, ArH), 7.07 (m, 1H, ArH), 7.59 (d, J = 7.5 Hz, 2H, ArH), 8.02 (dd, J = 5.0, 1.5 Hz, 1H, H-3). ^{13}C NMR (100.6 MHz) δ 16.4 (d, J = 5.0 Hz, CH$_2$*C*H$_3$), 16.5 (d, J = 5.0 Hz, CH$_2$*C*H$_3$), 48.6 (d, J = 3.0 Hz, C-6a), 55.3 (OCH$_3$), 60.1 (C-3a), 63.7 (d, J = 8.0 Hz, *C*H$_2$CH$_3$), 64.8 (d, J = 7.0 Hz, *C*H$_2$CH$_3$), 86.0 (d, J = 158.0 Hz, C-1), 113.5 (d, J = 1.0 Hz, 2CHAr), 117.0 (d, J = 22.0 Hz, CHAr), 121.7 (d, J = 19.0 Hz, C-*ipso*), 125.3 (d, J = 4.0 Hz, C-*ipso*), 126.2 (d, J = 8.0 Hz, CHAr), 127.5 (d, J = 4.0 Hz, C-

ipso), 128.7 (CHAr), 129.8 (d, *J* = 6.0 Hz, 2CHAr), 157.9 (d, *J* = 250.0 Hz, C-*ipso*), 159.9 (d, *J* = 2.0 Hz, C-*ipso)*, 161.8 (d, *J* = 13.0 Hz, C-3), 170.7 (d, *J* = 5.0 Hz, CO), 171.6 (d, *J* =11.0 Hz, CO). HRMS $C_{23}H_{24}ClFN_2O_6P$ $[M+H]^+$ 509.1039; found, 509.1037. Anal. Cald. for $C_{23}H_{23}ClFN_2O_6P$: C, 54.29%; H, 4.56%; N, 5.51%; found: C, 54.66%; H, 4.63%; N, 5.36%.

Diethyl (1*RS*,3a*SR*,6a*SR*)-1-benzyl-4,6-dioxo-5-phenyl-1,3a,4,5,6,6a-hexahydropyrrolo[3,4-c]pyrrole-1-phosphonate (14c). Following the general procedure, AgOAc (8 mg, 0.05 mmol), *N*-phenylmaleimide (139 mg, 0.8 mmol), acetonitrile (6 mL) and diethyl α-benzylisocyanomethylphosphonate (213 mg, 0.8 mmol) gave **14c** (32 mg, 9%) as a yellowish oil, after column chromatography (EtOAc/hexane 1:1). IR (ATR) 3738, 2926, 2843, 1730, 1492, 1385, 1220, 1181, 1059, 1020, 782, 700 cm^{-1}. ^{1}H NMR (400 MHz, CDCl$_3$, HETCOR) δ 1.29 (t, *J* = 7.0 Hz, 3H, CH$_2$C*H$_3$*), 1.40 (t, *J* = 7.0 Hz, 3H, CH$_2$C*H$_3$*), 3.29 (dd, *J* = 15.0, 12.5 Hz, 1H, C*H$_2$*-Ar), 3.86 (dd, *J* = 15.0, 9.5 Hz, 1H, C*H$_2$*-Ar), 3.97 (dd, *J* = 19.0, 9.0 Hz, 1H, H-6a), 4.11-4.26 (m, 4H, C*H$_2$*CH$_3$), 4.39 (dq, *J* = 9.0, 1.5 Hz, 1H, H-3a), 6.73-6.75 (m, 2H, ArH), 7.10-7.12 (m, 3H, ArH), 7.21-7.23 (m, 2H, ArH), 7.33-7.36 (m, 3H, ArH), 7.82 (dd, *J* = 5.0, 1.5 Hz, 1H, H-3). ^{13}C NMR (100.6 MHz) δ 16.3 (d, *J* = 6.0 Hz, CH$_2$*C*H$_3$), 16.5 (d, *J* = 6.0 Hz, CH$_2$*C*H$_3$), 36.8 (d, *J* = 2.0 Hz, CH$_2$-Ar), 45.9 (d, *J* = 3.0 Hz, C-6a), 59.9 (C-3a), 63.4 (d, *J* = 7.0 Hz, *C*H$_2$CH$_3$), 64.0 (d, *J* = 6.0 Hz, *C*H$_2$CH$_3$), 83.7 (d, *J* =158.0 Hz, C-1), 126.5 (2CHAr), 126.7 (CHAr), 127.8 (2CHAr), 128.7 (CHAr), 128.8 (2CHAr), 131.0 (C-*ipso*), 131.8 (2CHAr), 134.9 (d, *J* = 12.0 Hz, C-*ipso*), 161.3 (d, *J* = 13.0 Hz, C-3), 171.1 (d, *J* = 6.0 Hz, CO), 173.1 (d, *J* = 8.0 Hz, CO). HRMS $C_{23}H_{26}N_2O_5P$ $[M+H]^+$ 441.1574; found, 441.1580. Additional column chromatography led to sample for testing. Purity 95.7% (t_R= 4.50 min).

Diethyl (1*RS*,3a*SR*,6a*SR*)-1-(4-fluorobenzyl)-4,6-dioxo-5-phenyl-1,3a,4,5,6,6a-hexahydropyrrolo[3,4-c]pyrrole-1-phosphonate (15c). Following the general procedure,

AgOAc (12 mg, 0.07 mmol), *N*-phenylmaleimide (121 mg, 0.7 mmol), acetonitrile (5 mL) and

diethyl α-(4-fluorobenzyl)isocyanomethylphosphonate (200 mg, 0.7 mmol) gave **15c** (67 mg,

21%) as an oil, after column chromatography (EtOAc). IR (ATR) 3471, 2924, 2853, 1780, 1711,

1509, 1378, 1221, 1049, 1017, 968, 691 cm^{-1}. ^{1}H NMR (400 MHz, CDCl$_3$, HETCOR) δ 1.30 (td,

J = 7.0, 0.5 Hz, 3H, CH$_2$C*H*$_3$), 1.40 (td, *J* = 7.0, 0.5 Hz, 3H, CH$_2$C*H*$_3$), 3.25 (dd, *J* = 14.5, 12.5

Hz, 1H, C*H*$_2$-Ar), 3.81 (dd, *J* = 14.5, 9.0 Hz, 1H, C*H*$_2$-Ar), 3.96 (dd, *J* = 19.0, 9.5 Hz, 1H, H-6a),

4.11-4.27 (m, 4H, C*H*$_2$CH$_3$), 4.39 (ddd, *J* = 9.5, 3.5, 1.5 Hz, 1H, H-3a), 6.76-6.82 (m, 3H, ArH),

7.14-7.19 (m, 2H, ArH), 7.33-7.47 (m, 4H, ArH), 7.82 (dd, *J* = 5.0, 1.5 Hz, 1H, H-3). ^{13}C NMR

(100.6 MHz) δ 16.3 (d, *J* = 6.0 Hz, CH$_2$C*H*$_3$), 16.5 (d, *J* = 5.5 Hz, CH$_2$C*H*$_3$), 36.0 (CH$_2$Ar), 45.9

(d, *J* = 2.5 Hz, C-6a), 59.9 (C-3a), 63.4 (d, *J* = 7.5 Hz, C*H*$_2$CH$_3$), 64.4 (d, *J* = 7.0 Hz, C*H*$_2$CH$_3$),

83.7 (d, *J* =159.5 Hz, C-1), 114.5 (d, *J* = 2.0 Hz, 2CHAr), 126.3 (2CHAr), 128.9 (CHAr), 129.0

(2CHAr), 130.5 (d, *J* = 12.5. Hz, C-*ipso*), 130.9 (C-*ipso*), 133.4 (d, *J* = 8.0 Hz, 2CHAr), 161.5

(d, *J* = 12.5 Hz, C-3), 161.8 (d, *J* = 245.5 Hz, C-*ipso*), 171.0 (d, *J* = 6.0 Hz, CO), 173.2 (d, *J* =

12.5 Hz, CO). HRMS C$_{23}$H$_{25}$FN$_2$O$_5$P [M+H]$^+$ 459.1480; found, 459.1483. Purity 96.4% (t_R=

4.56 min).

Diethyl   (1*RS*,3a*SR*,6a*SR*)-5-ethyl-4,6-dioxo-1-phenyl-1,3a,4,5,6,6a-hexahydropyrrolo[3,4-

***c*]pyrrole-1-phosphonate (9f).** Following the general procedure, AgOAc (11 mg, 0.07 mmol),

N-ethylmaleimide   (213   mg,   1.7   mmol),   acetonitrile   (8   mL)   and   diethyl   α-

phenylisocyanomethylphosphonate (279 mg, 1.1 mmol) gave **9f** (130 mg, 31%) as a yellowish

oil, after column chromatography (EtOAc). IR (ATR) 3476, 2981, 2929, 1780, 1698, 1626,

1396, 1251, 1055, 1026, 968, 766 cm^{-1}. ^{1}H NMR (400 MHz, CDCl$_3$, HETCOR) δ 0.75 (t, *J* = 7.0

Hz, 3H, NCH$_2$C*H*$_3$), 1.15 (t, *J* = 7.0 Hz, 3H, CH$_2$C*H*$_3$), 1.25 (t, *J* = 7.0 Hz, 3H, CH$_2$C*H*$_3$), 3.21-

3.27 (m, 2H, NC*H*$_2$CH$_3$), 3.88 (m, 1H, C*H*$_2$CH$_3$), 4.06-4.15 (m, 4H, C*H*$_2$CH$_3$ and H-6a), 4.29

(ddd, J = 8.5, 3.5, 1.5 Hz, 1H, H-3a), 7.31-7.34 (m, 3H, ArH), 7.65 (dbr, J = 11.6 Hz, 2H, ArH), 7.96 (dd, J = 5.0, 1.5 Hz, 1H, H-3). ^{13}C NMR (100.6 MHz) δ 12.6 (NCH$_2$CH$_3$), 16.4 (d, J = 5.5 Hz, CH$_2$CH$_3$), 16.4 (d, J = 5.5 Hz, CH$_2$CH$_3$), 34.0 (NCH$_2$CH$_3$), 47.9 (d, J = 2.0 Hz, C-6a), 60.5 (C-3a), 63.6 (d, J = 8.0 Hz, CH$_2$CH$_3$), 64.8 (d, J = 8.0 Hz, CH$_2$CH$_3$), 85.8 (d, J =155.0 Hz, C-1), 127.9 (d, J = 1.0 Hz, 2CHAr), 128.6 (d, J = 2.0 Hz, 2CHAr), 128.6 (CHAr), 133.6 (d, J = 4.0 Hz, C-*ipso*), 162.7 (d, J = 12.0 Hz, C-3), 171.0 (d, J = 6.0 Hz, CO), 172.5 (d, J =12.0 Hz, CO). HRMS C$_{18}$H$_{24}$N$_2$O$_5$P [M+H]$^+$ 379.1417; found, 379.1418. Additional column chromatography led to sample for testing. Purity 95.5% (t_R=4.06 min).

Diethyl (1*RS*,3a*SR*,6a*SR*)-4,6-dioxo-1-phenyl-5-propyl-1,3a,4,5,6,6a-hexahydropyrrolo[3,4-*c*]pyrrole-1-phosphonate (9g). Following the general procedure, AgOAc (8 mg, 0.05 mmol), *N*-propylmaleimide (200 mg, 1.4 mmol), acetonitrile (7 mL) and diethyl α-phenylisocyanomethylphosphonate (228 mg, 0.9 mmol) gave **9g** (314 mg, 89%) as a yellowish oil, after column chromatography (EtOAc/hexane 1:1 to 3:2). IR (ATR) 3464, 2976, 2928, 1719, 1631, 1451, 1402, 1202, 1056, 1027, 963, 705, 583 cm^{-1}. ^{1}H NMR (400 MHz, CDCl$_3$, HETCOR) δ 0.59 (t, J = 7.0 Hz, 3H, CH$_2$CH$_2$C*H$_3$*), 1.13-1.19 (m, 2H, CH$_2$C*H$_2$*CH$_3$), 1.14 (t, J = 7.0 Hz, 3H, CH$_2$C*H$_3$*), 1.25 (t, J = 7.0 Hz, 3H, CH$_2$C*H$_3$*), 3.16 (m, 2H, C*H$_2$*CH$_2$CH$_3$), 3.85 (m, 1H, C*H$_2$*CH$_3$), 4.02-4.14 (m, 4H, C*H$_2$*CH$_3$ and H-6a), 4.30 (ddd, J = 8.5, 3.5, 1.5 Hz, 1H, H-3a), 7.29-7.34 (m, 3H, ArH), 7.65 (br d, J = 8.0 Hz, 2H, ArH), 7.95 (dd, J = 5.0, 1.5 Hz, 1H, H-3). ^{13}C NMR (100.6 MHz) δ 11.0 (CH$_2$CH$_2$CH$_3$), 16.3 (d, J = 4.0 Hz, CH$_2$CH$_3$), 16.4 (d, J = 6.0 Hz, CH$_2$CH$_3$), 20.7 (CH$_2$CH$_2$CH$_3$), 40.6 (CH$_2$CH$_2$CH$_3$), 47.8 (d, J = 3.0 Hz, C-6a), 60.5 (C-3a), 63.5 (d, J = 7.0 Hz, CH$_2$CH$_3$), 64.7 (d, J = 7.0 Hz, CH$_2$CH$_3$), 85.9 (d, J =154.0 Hz, C-1), 127.8 (d, J = 2.0 Hz, 2CHAr), 128.5 (d, J = 3.0 Hz, CHAr), 128.6 (d, J = 6.0 Hz, 2CHAr), 133.5 (d, J = 4.0 Hz, C-*ipso*), 162.8 (d, J = 12.0 Hz, C-3), 172.2 (d, J = 6.0 Hz, CO), 172.7 (d, J =12.0 Hz, CO). HRMS

$C_{19}H_{26}N_2O_5P$ $[M+H]^+$ 393.1574; found, 393.1572. Additional column chromatography led to sample for testing. Purity 95.6% (t_R=4.24 min).

Diethyl (1RS,3aSR,6aSR)-5-(tert-butyl)-4,6-dioxo-1-phenyl-1,3a,4,5,6,6a-hexahydropyrrolo[3,4-c]pyrrole-1-phosphonate (9h). Following the general procedure, AgOAc (9 mg, 0.05 mmol), N-$tert$-butylmaleimide (215 mg, 1.4 mmol), acetonitrile (7 mL) and diethyl α-phenylisocyanomethylphosphonate (229 mg, 0.9 mmol) gave **9h** (202 mg, 55%) as a yellowish oil, after column chromatography (EtOAc). IR (ATR) 3454, 2981, 2923, 1777, 1709, 1348, 1265, 1241, 1173, 1061, 973, 744, 710, 588 cm^{-1}. ^{1}H NMR (400 MHz, CDCl$_3$, HETCOR) δ 1.13 [s, 9H, C(CH_3)$_3$], 1.17 (t, J = 7.0 Hz, 3H, CH$_2$CH_3), 1.24 (t, J = 7.0 Hz, 3H, CH$_2$CH_3), 3.88-3.95 (m, 2H, CH_2CH$_3$ and H-6a), 4.07-4.15 (m, 4H, CH_2CH$_3$ and H-3a), 7.28-7.33 (m, 3H, ArH), 7.59 (dbr, J = 8.0 Hz, 2H, ArH), 7.93 (dd, J = 5.0, 1.5 Hz, 1H, H-3). ^{13}C NMR (100.6 MHz) δ 16.4 (d, J = 6.0 Hz, CH$_2$CH_3), 16.4 (d, J = 6.0 Hz, CH$_2$CH_3), 27.7 (C(CH_3)$_3$), 48.1 (d, J = 2.0 Hz, C-6a), 58.6 [C(CH$_3$)$_3$], 60.2 (C-3a), 63.5 (d, J = 8.0 Hz, CH$_2$CH$_3$), 64.6 (d, J = 8.0 Hz, CH$_2$CH$_3$), 86.6 (d, J =158.0 Hz, C-1), 127.9 (d, J = 2.0 Hz, 2CHAr), 128.4 (d, J = 2.0 Hz, CHAr), 128.5 (d, J = 6.0 Hz, 2CHAr), 134.1 (d, J = 4.0 Hz, C-$ipso$), 163.3 (d, J = 12.0 Hz, C-3), 172.6 (d, J = 5.0 Hz, CO), 173.6 (d, J =10.0 Hz, CO). HRMS $C_{20}H_{28}N_2O_5P$ $[M+H]^+$ 407.1730; found, 407.1733. Additional column chromatography led to sample for testing. Purity 98.3% (t_R= 4.46 min).

Diethyl (1RS,3aSR,6aSR)-5-(adamantan-1-yl)methyl)-4,6-dioxo-1-phenyl-1,3a,4,5,6,6a-hexahydropyrrolo[3,4-c]pyrrole-1-phosphonate (9i). Following the general procedure, AgOAc (12 mg, 0.07 mmol), N-(adamantan-1-methylphenyl)maleimide (270 mg, 1.1 mmol), acetonitrile (5 mL) and diethyl α-phenylisocyanomethylphosphonate (177 mg, 0.7 mmol) gave

9i (220 mg, 63%) as a white solid, after column chromatography (EtOAc/hexane 7:3). M.p. 107-

108 ºC (EtOAc). IR (ATR) 3469, 2908, 2850, 1714, 1446, 1392, 1226, 1158, 1012, 978, 758,

700, 573 cm^{-1}. ^{1}H NMR (400 MHz, CDCl$_3$, HETCOR) δ 0.95 (dd, J = 52.0, 12.0 Hz, 6H, 3CH$_2$),

1.12 (t, J = 7.0 Hz, 3H, CH$_2$CH_3), 1.25 (t, J = 7.0 Hz, 3H, CH$_2$CH_3), 1.47 (dd, J = 53.0, 12.0 Hz,

6H, 3CH$_2$), 1.72 (s, 3H, 3CH), 2.95 (s, 2H, NCH$_2$), 3.81 (m, 1H, CH_2CH$_3$), 3.99-3.15 (m, 3H,

CH_2CH$_3$), 4.11 (dd, J = 19.0, 8.5 Hz, 1H, H-6a), 4.29 (ddd, J = 8.5, 3.0, 1.0 Hz, 1H, H-3a), 7.25-

7.33 (m, 3H, ArH), 7.72 (d, J = 7.0 Hz, 2H, ArH), 7.95 (dd, J = 5.0, 1.0 Hz, 1H, H-3). ^{13}C NMR

(100.6 MHz) δ 16.3 (d, J = 5.5 Hz, CH$_2$CH$_3$), 16.4 (d, J = 6.0 Hz, CH$_2$CH$_3$), 28.1 (3CH), 34.9

(C), 36.5 (3CH$_2$), 40.0 (3CH$_2$), 47.7 (d, J = 2.0 Hz, C-6a), 50.2 (NCH$_2$), 60.6 (C-3a), 63.6 (d, J =

7.5 Hz, CH$_2$CH$_3$), 64.7 (d, J = 7.5 Hz, CH$_2$CH$_3$), 86.0 (d, J = 155.0 Hz, C-1), 127.8 (d, J = 2.0

Hz, 2CHAr), 128.5 (d, J = 3.0 Hz, CHAr), 129.0 (d, J = 4.5 Hz, 2CHAr), 133.5 (d, J = 5.0 Hz,

C-*ipso*), 162.6 (d, J = 12.0 Hz, C-3), 172.7 (d, J = 5.0 Hz, CO), 173.2 (d, J = 13.0 Hz, CO);

HRMS C$_{27}$H$_{36}$N$_2$O$_5$P [M+H]$^+$ 499.2356; found, 499.2359. Purity 97.8% (t_R= 5.27 min).

Diethyl (1*RS*,3a*SR*,6a*SR*)-5-benzyl-4,6-dioxo-1-phenyl-1,3a,4,5,6,6a-hexahydropyrrolo[3,4-

***c*]pyrrole-1-phosphonate (9j).** Following the general procedure, AgOAc (4 mg, 0.02 mmol), *N*-

benzylmaleimide (112 mg, 0.6 mmol), acetonitrile (3 mL) and diethyl α-

phenylisocyanomethylphosphonate (101 mg, 0.4 mmol) gave **9j** (139 mg, 79%) as a yellowish

oil, after column chromatography (EtOAc/hexane 9:1). IR (NaCl) 3472, 3068, 2984, 1778, 1698,

1632, 1495, 1249, 1172, 1021, 750, 615 cm^{-1}. ^{1}H NMR (400 MHz, CDCl$_3$, HETCOR)δ 1.14 (t, J

= 7.0 Hz, 3H, CH$_2$CH_3), 1.25 (t, J = 7.0 Hz, 3H CH$_2$CH_3), 3.86 (m, 1H, CH_2CH$_3$), 4.00-4.18 (m,

4H, CH_2CH$_3$ and H-6a), 4.33 (ddd, J = 8.5, 3.5, 1.5 Hz, 1H, H-3a), 4.36 (dd, J = 53.5, 14.5 Hz,

2H, CH$_2$Ar), 6.94-6.96 (m, 2H, ArH), 7.14-7.22 (m, 3H, ArH), 7.23-7.30 (m, 3H, ArH), 7.61-

7.63 (m, 2H, ArH), 7.92 (dd, J = 5.0, 1.5 Hz, 1H, H-3).^{13}C NMR (100.6 MHz) δ 16.1 (d, J = 5.0

Hz, CH$_2$CH$_3$), 16.2 (d, J = 5.0 Hz, CH$_2$CH$_3$), 42.4 (CH$_2$Ar), 47.8 (d, J = 2.0 Hz, C-6a), 60.4 (C-

3a), 63.4 (d, J = 7.5 Hz, CH$_2$CH$_3$), 64.6 (d, J = 7.5 Hz, CH$_2$CH$_3$), 85.7 (d, J = 155.0 Hz, C-1),

127.7 (d, J = 1.0 Hz, 2CHAr), 127.8 (CHAr), 128.3 (br s, 4CHAr), 128.4 (CHAr), 128.5

(2CHAr), 133.2 (d, J = 4.0 Hz, C-$ipso$), 135.0 (C-$ipso$), 162.3 (d, J = 11.5 Hz, C-3), 171.6 (d, J =

5.5 Hz, CO), 172.2 (d, J = 13.5 Hz, CO). HRMS C$_{23}$H$_{25}$N$_2$O$_5$P [M+H]$^+$ 441.1574; found,

441.1579. Additional column chromatography led to sample for testing. Purity 95.4% (t_R= 4.43

min).

Diethyl (1RS,3aSR,6aSR)-4,6-dioxo-5-phenethyl-1-phenyl-1,3a,4,5,6,6a-hexahydropyrrolo[3,4-c]pyrrole-1-phosphonate (9k). Following the general procedure,

AgOAc (7 mg, 0.04 mmol), N-phenethylmaleimide (200 mg, 1.0 mmol) acetonitrile (5 mL) and

diethyl α-phenylisocyanomethylphosphonate (170 mg, 0.7 mmol) gave **9k** (110 mg, 36%) as an

oil, after column chromatography (EtOAc/hexane 1:1). IR (NaCl) 3468, 3027, 2981, 1709, 1627,

1394, 1250, 1162, 1052, 1025, 968, 792, 750 cm^{-1}.^{1}H NMR (400 MHz, CDCl$_3$, HETCOR) δ 1.14

(t, J = 7.0 Hz, 3H, CH$_2$CH_3), 1.25 (t, J = 7.0 Hz, 3H, CH$_2$CH_3), 2.40-2.53 (m, 2H, CH$_2$), 3.46 (t,

J = 7.5 Hz, 2H, CH$_2$), 3.83 (m, 1H, CH_2CH$_3$), 3.99-4.16 (m, 4H, CH_2CH$_3$ and H-6a), 4.24 (ddd, J

= 8.5, 4.0, 1.0 Hz, 1H, H-3a), 6.97-6.99 (m, 2H, ArH), 7.16-7.25 (m, 3H, ArH), 7.30-7.38 (m,

3H, ArH), 7.68-7.70 (m, 2H, ArH), 7.85 (dd, J = 5.0, 1.0 Hz, 1H, H-3).^{13}C NMR (100.6 MHz) δ

16.1 (d, J = 4.0 Hz, CH$_2$CH$_3$), 16.2 (d, J = 4.5 Hz, CH$_2$CH$_3$), 33.0 (CH$_2$), 39.9 (CH$_2$), 47.5 (d, J =

2.5 Hz, C-6a), 60.2 (C-3a), 63.4 (d, J = 7.5 Hz, CH$_2$CH$_3$), 64.6 (d, J = 7.5 Hz, CH$_2$CH$_3$), 126.6

(CHAr), 127.6 (CHAr), 127.7 (CHAr), 128.4 (d, J = 2.5 Hz, CHAr), 128.5 (2CHAr), 128.6

(CHAr), 128.7 (CHAr), 128.8 (2CHAr), 133.2 (d, J = 4.5 Hz, C-$ipso$), 137.1 (C-$ipso$), 162.6 (d, J

= 11.5 Hz, C-3), 171.6 (d, J = 5.5 Hz, CO), 172.3 (d, J = 13.5 Hz, CO). HMRS C$_{24}$H$_{28}$N$_2$O$_5$P

[M+H]$^+$ 455.1730; found: 455.1731. Additional column chromatography led to sample for

testing. Purity 98.0% (t_R= 4.54 min).

Diethyl (1RS,3aSR,6aSR)-5-(4-fluorophenethyl)-4,6-dioxo-1-phenyl-1,3a,4,5,6,6a-hexahydropyrrolo[3,4-c]pyrrole-1-phosphonate (9l). Following the general procedure, AgOAc (8 mg, 0.05 mmol), *N*-(4-fluorophenethyl)maleimide (263 mg, 1.2 mmol), acetonitrile (6 mL) and diethyl α-phenylisocyanomethylphosphonate (202 mg, 0.8 mmol) gave **9l** (201 mg, 53%) as a white solid, after column chromatography (EtOAc). M.p. 94-95 ºC (EtOAc). IR (NaCl) 3466, 3050, 2976, 1779, 1702, 1632, 1507, 1257, 1153, 1013, 763, 583 cm^{-1}. ^{1}H NMR (400 MHz, CDCl$_3$, HETCOR) δ 1.23 (t, *J* = 7.0 Hz, 3H, CH$_2$C*H*$_3$), 1.25 (t, *J* = 7.0 Hz, 3H, CH$_2$C*H*$_3$), 2.40-2.52 (m, 2H, CH$_2$), 3.41-3.46 (m, 2H, CH$_2$), 3.80 (m, 1H, C*H*$_2$CH$_3$), 3.97-4.15 (m, 4H, C*H*$_2$CH$_3$ and H-6a), 4.24 (ddd, *J* = 8.0, 4.0, 1.5 Hz, 1H, H-3a), 6.86-6.92 (m, 4H, ArH), 7.31-7.37 (m, 3H, ArH), 7.67 (m, 2H, ArH), 7.83 (dd, *J* = 5.5, 1.5 Hz, 1H, H-3). ^{13}C NMR (100.6 MHz) δ 16.1 (d, *J* = 5.0 Hz, CH$_2$*C*H$_3$), 16.2 (d, *J* = 5.0 Hz, CH$_2$*C*H$_3$), 32.1 (CH$_2$), 39.9 (CH$_2$), 47.5 (d, *J* = 2.0 Hz, C-6a), 60.3 (C-3a), 63.4 (d, *J* = 7.0 Hz, *C*H$_2$CH$_3$), 64.6 (d, *J* = 7.0 Hz, *C*H$_2$CH$_3$), 85.7 (d, *J* = 153.0 Hz, C-1), 115.3 (d, *J* = 2.0 Hz, 2CHAr), 127.6 (d, *J* = 2.0 Hz, 2CHAr), 128.4 (d, *J* = 3.0 Hz, CHAr), 128.6 (d, *J* = 6.0 Hz, 2CHAr), 130.1 (d, *J* = 8.0 Hz, 2CHAr), 132.7 (d, *J* = 3.0 Hz, C-*ipso*), 133.1 (d, *J* = 5.0 Hz, C-*ipso*), 160.4 (d, *J* = 244.5 Hz, C-*ipso*), 162.5 (d, *J* = 12.0 Hz, C-3), 171.6 (d, *J* = 6.0 Hz, CO), 172.3 (d, *J* = 14.0 Hz, CO). HRMS C$_{24}$H$_{27}$FN$_2$O$_5$P [M+H]$^+$ 473.1636; found, 473.1640. Anal. Cald. for C$_{24}$H$_{26}$FN$_2$O$_5$P: C, 61.01%; H, 5.55%; N, 5.93%; found: C, 61.14%; H, 5.74%; N, 5.83%.

Diethyl (1RS,3aSR,6aSR)-5-(2,3-dihydro-1H-inden-2-yl)-4,6-dioxo-1-phenyl-1,3a,4,5,6,6a-hexahydropyrrolo[3,4-c]pyrrole-1-phosphonate (9m). Following the general procedure, AgOAc (7 mg, 0.04 mmol), *N*-(2,3-dihydro-1*H*-inden-2-yl)maleimide (126 mg, 0.6 mmol), acetonitrile (3 mL) and diethyl α-phenylisocyanomethylphosphonate (100 mg, 0.4 mmol) gave

9m (158 mg, 85%) as a beige solid, after column chromatography (EtOAc). M.p. 124-126 ºC

(EtOAc). IR (ATR) 3457, 2986, 2943, 2866, 1766, 1698, 1623, 1377, 1252, 1170, 1055, 1021,

790, 704, 574 cm^{-1}. ^{1}H NMR (400 MHz, CDCl$_3$, HETCOR) δ 1.18 (t, J = 7.0 Hz, 3H, CH$_2$CH_3),

1.26 (t, J = 7.0 Hz, 3H, CH$_2$CH_3), 2.69 (dd, J = 15.0, 9.0 Hz, 1H, CH$_2$), 2.75 (dd, J = 15.0, 9.0

Hz, 1H, CH$_2$), 2.77 (dd, J = 15.0, 9.0 Hz, 1H, CH$_2$), 3.23 (dd, J = 15.0, 9.0 Hz, 1H, CH$_2$), 3.92

(m, 1H, CH_2CH$_3$), 4.08-4.17 (m, 4H, CH_2CH$_3$ and H-6a), 4.31 (ddd, J = 9.0, 3.0, 1.5 Hz, 1H, H-

3a), 4.62 (qu, J = 9,2 Hz, 1H, CH), 7.09 (m, 1 H, ArH), 7.07-7.11 (m, 3H, ArH), 7.32-7.37 (m,

3H, ArH), 7.64 (br d, J = 7.5 Hz, 2H, ArH), 8.00 (dd, J = 5.0, 1.5 Hz, 1H, H-3). ^{13}C NMR (100.6

MHz) δ 16.4 (d, J = 2.0 Hz, CH$_2$CH_3), 16.5 (d, J = 3.0 Hz, CH$_2$CH_3), 34.6 (CH$_2$), 35.1 (CH$_2$),

48.0 (d, J = 2.0 Hz, C-6a), 50.8 (CH), 60.2 (C-3a), 63.6 (d, J = 7.0 Hz, CH$_2$CH$_3$), 64.7 (d, J = 8.0

Hz, CH$_2$CH$_3$), 86.1 (d, J = 157.0 Hz, C-1), 124.4 (d, J = 2.0 Hz, 2CHAr), 126.8 (d, J = 2.0 Hz,

2CHAr), 128.0 (d, J = 1.0 Hz, 2CHAr), 128.5 (d, J = 8.0 Hz, 2CHAr), 128.6 (CHAr), 133.7 (C-

ipso), 133.8 (C-*ipso)*, 140.5 (d, J = 9.0 Hz, C-*ipso*), 162.7 (d, J = 12.0 Hz, C-3), 172.1 (d, J =

5.0 Hz, CO), 172.7 (d, J =12.0 Hz, CO). HRMS C$_{25}$H$_{28}$N$_2$O$_5$P [M+H]$^+$ 467.1730; found,

467.1728. Anal. Cald. for C$_{25}$H$_{27}$N$_2$O$_5$P: C, 64.37%; H, 5.83%; N, 6.01%; found: C,64.55%;

H,6.11%; N,5.76%.

Diethyl (1*RS*,3a*SR*,6a*SR*)-4,6-dioxo-1-phenyl-5-[4-(trifluoromethyl)phenyl]-1,3a,4,5,6,6a-hexahydropyrrolo[3,4-*c*]pyrrole-1-phosphonate (9n). Following the general procedure,

AgOAc (4 mg, 0.03 mmol), *N*-(4-trifluoromethylphenyl)maleimide (144mg, 0.6 mmol),

acetonitrile (3 mL) and diethyl α-phenylisocyanomethylphosphonate (101 mg, 0.4 mmol) gave

9n (133 mg, 67%) as a white solid, after column chromatography (EtOAc). M.p. 184-185 ºC

(EtOAc). IR (NaCl) 3492, 3050, 2984, 1723, 1616, 1378, 1326, 1249, 1170, 1067, 758, 580 cm^{-1}.

^{1}H NMR (400 MHz, CDCl$_3$, HETCOR) δ 1.19 (t, J = 7.0 Hz, 3H, CH$_2$CH_3), 1.28 (t, J = 7.0 Hz,

3H, CH$_2$CH_3), 3.95 (m, 1H, CH_2CH$_3$), 4.10-4.20 (m, 3H, CH_2CH$_3$), 4.28 (dd, J = 18.0, 9.0, 1H, H-6a), 4.51 (ddd, J = 8.5, 3.0, 1.5 Hz, 1H, H-3a), 6.85-6.87 (m, 2H, ArH), 7.34-7.38 (m, 3H, ArH), 7.54-7.56 (m, 2H, ArH), 7.67-7.69 (m, 2H, ArH), 8.05 (dd, J = 5.0, 1.5 Hz, 1H, H-3). ^{13}C NMR (100.6 MHz) δ 16.2 (d, J = 5.0 Hz, CH$_2$CH$_3$), 16.3 (d, J = 5.0 Hz, CH$_2$CH$_3$), 48.3 (d, J = 3.0 Hz, C-6a), 60.1 (C-3a), 63.6 (d, J = 7.0 Hz, CH$_2$CH$_3$), 64.7 (d, J = 7.0 Hz, CH$_2$CH$_3$), 86.3 (d, J =157.0 Hz, C-1), 123.5 (q, J = 272.5 Hz, CF$_3$), 126.0 (q, J = 4.0 Hz, 2CHAr), 126.3 (2CHAr), 128.0 (d, J = 1.0 Hz, 2CHAr), 128.4 (d, J = 6.0 Hz, 2CHAr), 128.7 (d, J = 2.0 Hz, CHAr), 137.5 (q, J = 33.0 Hz, CCF$_3$), 133.4 (d, J = 4.0 Hz, C-$ipso$), 134.1 (d, J = 1.5 Hz, C-$ipso$), 162.0 (d, J = 13.0 Hz, C-3), 170.4 (d, J = 5.0 Hz, CO), 171.2 (d, J = 12.0 Hz, CO). HRMS C$_{23}$H$_{23}$F$_3$N$_2$O$_5$P [M+H]$^+$ 495.1291; found, 495.1288. Anal. Cald. for C$_{23}$H$_{22}$F$_3$N$_2$O$_5$P: C, 55.88%; H, 4.49%; N, 5.67%; found: C, 56.04%; H, 4.71%; N, 5.56%.

Diethyl (1RS,3aSR,6aSR)-4,6-dioxo-1-phenyl-5-[3-(trifluoromethyl)phenyl]-1,3a,4,5,6,6a-hexahydropyrrolo[3,4-c]pyrrole-1-phosphonate (9o). Following the general procedure, AgOAc (10 mg, 0.06 mmol), N-(3-trifluoromethylphenyl)maleimide (362 mg, 1.5 mmol), acetonitrile (8 mL) and diethyl α-phenylisocyanomethylphosphonate (253 mg, 1.0 mmol) gave **9o** (218 mg, 44%) as a white solid, after column chromatography (EtOAc). M.p. 179-180 ºC (EtOAc). IR (ATR) 3483, 3084, 2957, 2036, 1719, 1446, 1382, 1329, 1168, 1027, 978, 739, 573 cm^{-1}. ^{1}H NMR (400 MHz, CDCl$_3$, HETCOR) δ 1.21 (t, J = 7.0 Hz, 3H, CH$_2$CH_3), 1.28 (t, J = 7.0 Hz, 3H, CH$_2$CH_3), 3.98 (m, 1H, CH_2CH$_3$), 4.11-4.20 (m, 3H, CH_2CH$_3$), 4.27 (dd, J = 18.0, 9.0 Hz, 1H, H-6a), 4.50 (ddd, J = 9.0, 2.5, 1.5 Hz, 1H, H-3a), 6.86 (s, 1H, ArH), 6.96 (d, J = 9.5 Hz, 1H, ArH), 7.36-7.39 (m, 3H, ArH), 7.42 (t, 7.5 Hz, 1H, ArH), 7.53 (d, J = 8.0 Hz, 1H, ArH), 7.67 (br d, J = 7.0 Hz, 2H, ArH), 8.06 (dd, J = 5.0, 1.5 Hz, 1H, H-3). ^{13}C NMR (100.6 MHz) δ 16.4 (d, J = 5.5 Hz, CH$_2$CH$_3$), 16.4 (d, J = 5.5 Hz, CH$_2$CH$_3$), 48.6 (d, J = 2.0 Hz, C-6a), 60.2 (C-

3a), 63.8 (d, J = 7.5 Hz, CH_2CH_3), 64.9 (d, J = 7.5 Hz, CH_2CH_3), 86.4 (d, J =158.0 Hz, C-1), 123.3 (q, J = 4.0 Hz, CHAr), 123.4 (q, J = 272.5 Hz, CF_3), 125.6 (q, J = 4.0 Hz, CHAr), 128.2 (d, J = 2.0 Hz, 2CHAr), 128.5 (d, J = 6.0 Hz, 2CHAr), 128.9 (d, J = 2.0 Hz, CHAr), 129.5 (d, J = 1.0 Hz, CHAr), 129.7 (CHAr), 131.6 (q, J = 33.5 Hz, CCF_3), 131.7 (C-*ipso*), 133.5 (d, J = 4.0 Hz, C-*ipso*), 162.1 (d, J = 12.0 Hz, C-3), 170.6 (d, J = 5.0 Hz, CO), 171.5 (d, J =11.0 Hz, CO). HRMS $C_{23}H_{23}F_3N_2O_5P$ [M+H]$^+$ 495.1291; found, 495.1287. Anal. Cald. for $C_{23}H_{22}F_3N_2O_5P$: C, 55.88%; H, 4.49%; N, 5.67%; found: C, 56.00%; H, 4.63%; N, 5.46%.

Diethyl (1*RS*,3a*SR*,6a*SR*)-5-(4-fluorophenyl)-4,6-dioxo-1-phenyl-1,3a,4,5,6,6a-hexahydropyrrolo[3,4-*c*]pyrrole-1-phosphonate (9p). Following the general procedure, AgOAc (7 mg, 0.04 mmol), *N*-(4-fluorophenyl)maleimide (211mg, 1.1mmol), acetonitrile (5mL) and diethyl α-phenylisocyanomethylphosphonate (177 mg, 0.7 mmol) gave **9p** (198 mg, 64%) as a white solid, after column chromatography (EtOAc). M.p. 200-201 ºC (EtOAc). IR (NaCl) 3481, 3061, 2980, 1787, 1717, 1511, 1385, 1245, 1017, 969, 700, 583 cm^{-1}. ^{1}H NMR (400 MHz, CDCl$_3$, HETCOR) δ 1.19 (t, J = 7.5 Hz, 3H, CH$_2$CH_3), 1.28 (t, J = 7.5 Hz, 3H, CH$_2$CH_3), 3.93 (m, 1H, CH_2CH$_3$), 4.10-4.20 (m, 3H, CH_2CH$_3$), 4.26 (dd, J = 18.0, 9.0, 1H, H-6a), 4.48 (ddd, J = 8.5, 3.0, 1.5 Hz, 1H, H-3a), 6.67-6.72 (m, 2H, ArH), 6.96-7.00 (m, 2H, ArH), 7.33-7.39 (m, 3H, ArH), 7.68-7.70 (m, 2H, ArH), 8.05 (dd, J = 5.0, 1.5 Hz, 1H, H-3). ^{13}C NMR (100.6 MHz) δ 16.2 (d, J = 4.0 Hz, CH$_2$CH_3), 16.3 (d, J = 4.0 Hz, CH$_2$CH_3), 48.2 (d, J = 3.0 Hz, C-6a), 60.1 (C-3a), 63.6 (d, J = 8.0 Hz, CH_2CH$_3$), 63.7 (d, J = 7.0 Hz, CH_2CH$_3$), 86.2 (d, J =157.0 Hz, C-1), 116.1 (d, J = 23.0 Hz, 2CHAr), 126.9 (d, J = 3.0 Hz, C-*ipso*), 127.9 (2CHAr), 128.0 (2CHAr), 128.4 (d, J = 6.0 Hz, 2CHAr), 128.6 (d, J = 2.0 Hz, CHAr), 133.4 (d, J = 4.0 Hz, C-*ipso*), 160.9 (d, J = 248.5 Hz, C-*ipso*), 162.2 (d, J = 12.0 Hz, C-3), 170.9 (d, J = 5.0 Hz, CO), 171.6 (d, J =

11.0 Hz, CO). HRMS $C_{22}H_{23}FN_2O_5P$ [M+H]$^+$445.1323; found, 445.1322. Anal. Cald. for $C_{22}H_{22}FN_2O_5P$: C, 59.46%; H, 4.99%; N, 6.30%; found: C,59.73%; H,5.13%; N,6.19%.

Diethyl (1RS,3aSR,6aSR)-5-(4-chlorophenyl)-4,6-dioxo-1-phenyl-1,3a,4,5,6,6a-hexahydropyrrolo[3,4-c]pyrrole-1-phosphonate (9q). Following the general procedure, AgOAc (5 mg, 0.03 mmol), *N*-(4-chlorophenyl)maleimide (150 mg, 0.7 mmol), acetonitrile (4 mL) and diethyl α-phenylisocyanomethylphosphonate (118 mg, 0.5 mmol) gave **9q** (136 mg, 59%) as a white solid, after column chromatography (EtOAc). M.p. 211-212 ºC (EtOAc). IR (ATR) 3078, 2981, 2923, 2855, 1713, 1499, 1377, 1187, 1022, 773, 583 cm^{-1}. ^{1}H NMR (400 MHz, CDCl$_3$, HETCOR) δ 1.19 (t, *J* = 7.0 Hz, 3H, CH$_2$C*H$_3$*), 1.28 (t, *J* = 7.0 Hz, 3H, CH$_2$C*H$_3$*), 3.94 (m, 1H, C*H$_2$*CH$_3$), 4.11-4.19 (m, 3H, C*H$_2$*CH$_3$), 4.25 (dd, *J* = 18.0, 9.0 Hz, 1H, H-6a), 4.47 (ddd, *J* = 8.5, 3.0, 1.0 Hz, 1H, H-3a), 6.65-6.67 (m, 2H, ArH), 7.24-7.27 (m, 2H, ArH), 7.33-7.37 (m, 3H, ArH), 7.67 (br d, *J* = 7.5 Hz, 2H, ArH), 8.04 (dd, *J* = 5.5, 1.0 Hz, 1H, H-3). ^{13}C NMR (100.6 MHz) δ 16.4 (d, *J* = 3.0 Hz, CH$_2$*C*H$_3$), 16.4 (d, *J* = 4.0 Hz, CH$_2$*C*H$_3$), 48.4 (d, *J* = 2.0 Hz, C-6a), 60.2 (C-3a), 63.7 (d, *J* = 7.0 Hz, *C*H$_2$CH$_3$), 64.8 (d, *J* = 7.0 Hz, *C*H$_2$CH$_3$), 86.4 (d, *J* =157.0 Hz, C-1), 127.4 (2CHAr), 128.1 (d, *J* = 1.0 Hz, 2CHAr), 128.5 (d, *J* = 6.0 Hz, 2CHAr), 128.7 (d, *J* = 2.0 Hz, CHAr), 129.4 (2CHAr), 129.6 (C-*ipso*), 133.6 (d, *J* = 4.0 Hz, C-*ipso*), 134.7 (C-*ipso*), 162.2 (d, *J* = 12.0 Hz, C-3), 170.8 (d, *J* = 5.0 Hz, CO), 171.5 (d, *J* =12.0 Hz, CO). HRMS $C_{22}H_{23}ClN_2O_5P$ [M+H]$^+$ 461.1028; found, 461.1026. Anal. Cald. for $C_{22}H_{22}ClN_2O_5P$: C, 57.34%; H, 4.81%; N, 6.08%; found: C, 57.71%; H, 4.92%; N, 5.96%.

Diethyl (1RS,3aSR,6aSR)-5-(2-chlorophenyl)-4,6-dioxo-1-phenyl-1,3a,4,5,6,6a-hexahydropyrrolo[3,4-c]pyrrole-1-phosphonate (9r). Following the general procedure, AgOAc (6 mg, 0.04 mmol), *N*-(2-chlorophenyl)maleimide (180 mg, 0.9 mmol), acetonitrile (5 mL) and diethyl α-phenylisocyanomethylphosphonate (152 mg, 0.6 mmol) gave **9r** (200 mg,

72%) as a white solid, after column chromatography (EtOAc/hexane 7:3). M.p. 172-174 °C (EtOAc). IR (ATR) 3496, 2981, 2866, 1790, 1718, 1482, 1386, 1237, 1194, 1045, 1021, 973, 757, 579 cm^{-1}. ^{1}H NMR (400 MHz, CDCl$_3$, HETCOR) δ 1.14 (t, J = 7.0 Hz, 3H, CH$_2$CH_3-rotamer A), 1.19 (t, J = 7.0 Hz, 3H, CH$_2$CH_3-rotamer B), 1.29 (t, J = 7.0 Hz, 3H, CH$_2$CH_3-rotamer A), 1.30 (t, J = 7.0 Hz, 3H, CH$_2$CH_3-rotamer B), 3.82 (m, 1H, CH_2CH$_3$-rotamer A), 3.93 (m, 1H, CH_2CH$_3$-rotamer B), 4.05-4.20 (m, 6H, CH_2CH$_3$-rotamer A and B), 4.35 (dd, J = 18.0, 8.5 Hz, 1H, H-6a rotamer A), 4.36 (dd, J = 18.0, 8.5 Hz, 1H, H-6a rotamer B), 4.52 (ddd, J = 8.5, 4.5, 1.5 Hz, 1H, H-3a rotamer A), 4.56 (ddd, J = 8.5, 3.0, 1.5 Hz, 1H, H-3a rotamer B), 6.30 (dd, J = 8.0, 1.5 Hz, 1H, ArH rotamer B), 7.10 (m, 1H, ArH rotamer B), 7.13 (ddd, J = 16.0, 8.0, 2.0 Hz, 1H, ArH rotamer A), 7.25-7.43 (m, 10H, 6ArH rotamer A and 4ArH rotamer B), 7.42 (dd, J = 8.0, 1.5 Hz, 1H, ArH rotamer B), 7.71 (d, J = 8.0 Hz, 2H, ArH rotamer B), 7.78 (d, J = 8.0 Hz, 2H, ArH rotamer A), 8.03 (dd, J = 5.5 Hz, 1.5 Hz, 1H, H-3 rotamer A), 8.08 (dd, J = 5.0, 1.5 Hz, 1H, H-3 rotamer B). ^{13}C NMR (100.6 MHz) δ 16.2 (d, J = 6.0 Hz, CH$_2$CH_3 rotamer A or B), 16.2 (d, J = 6.0 Hz, CH$_2$CH_3 rotamer A or B), 16.3 (d, J = 6.0 Hz, CH$_2$CH_3 rotamer A or B), 16.3 (d, J = 5.5 Hz, CH$_2$CH_3 rotamer A or B), 48.0 (d, J = 2.5 Hz, C-6a rotamer A), 48.6 (d, J = 2.5 Hz, C-6a rotamer B), 60.3 (C-3a rotamer B), 60.1 (C-3a rotamer A), 63.5 (d, J = 7.5 Hz, CH$_2$CH$_3$ rotamer A), 63.6 (d, J = 7.5 Hz, CH$_2$CH$_3$ rotamer B), 64.7 (d, J = 7.5 Hz, CH$_2$CH$_3$ rotamer B), 64.8 (d, J = 7.5 Hz, CH$_2$CH$_3$ rotamer A), 86.0 (d, J = 157.5, C-1 rotamer A), 86.6 (d, J = 153.5, C-1 rotamer B), 127.6 (CHAr rotamer A or B), 127.7 (d, J = 2.0 Hz, CHAr rotamer A or B), 127.8 (CHAr rotamer A), 127.9 (CHAr rotamer A or B), 128.0 (CHAr rotamer A or B), 128.4 (d, J = 5.0 Hz, 2CHAr rotamer B), 128.5 (2CHAr rotamer A or B), 128.6 (d, J = 2.0 Hz, CHAr rotamer A or B), 128.9 (d, J = 6.0 Hz, CHAr rotamer A), 129.1 (C-$ipso$ rotamer A), 129.2 (C-$ipso$ rotamer B), 129.3 (CHAr rotamer B), 129.6 (CHAr rotamer A), 130.2 (CHAr rotamer B),

130.3 (CHAr rotamer A or B), 130.7 (CHAr rotamer A or B), 130.9 (CHAr rotamer A or B),

132.0 (C-*ipso* rotamer A), 132.2 (C-*ipso* rotamer B), 132.9 (d, J = 4.0 Hz, C-*ipso* rotamer A),

133.5 (d, J = 4.0 Hz, C-*ipso* rotamer B), 162.0 (d, J = 11.5 Hz, C-3 rotamer A), 162.2 (d, J =

12.5 Hz, C-3 rotamer B), 170.2 (d, J = 5.0 Hz, CO rotamer B), 170.3 (d, J = 5.5 Hz, CO rotamer

A), 170.7 (d, J = 11.5 Hz, CO rotamer A or B), 170.8 (d, J = 15.0 Hz, CO rotamer B). HRMS

$C_{22}H_{23}ClN_2O_5P$ [M+H]$^+$ 461.1028; found, 461.1025. Anal. Cald. for $C_{22}H_{22}ClN_2O_5P$: C, 57.34%;

H, 4.81%; N, 6.08%; found: C,57.18%; H,4.86%; N,5.88%.

Diethyl (1*RS*,3a*SR*,6a*SR*)-5-(3-chlorophenyl)-4,6-dioxo-1-phenyl-1,3a,4,5,6,6a-hexahydropyrrolo[3,4-*c*]pyrrole-1-phosphonate (9s). Following the general procedure,

AgOAc (8 mg, 0.05 mmol), *N*-(3-chlorophenyl)maleimide (250 mg, 1.2 mmol), acetonitrile (6

mL) and diethyl α-phenylisocyanomethylphosphonate (203 mg, 0.8 mmol) gave **9s** (167 mg,

45%) as a white solid, after column chromatography (EtOAc). M.p. 186-187 ºC (EtOAc). IR

(ATR) 3488, 3084, 2962, 2928, 1709, 1587, 1475, 1382, 1241, 1183, 1051, 1022, 948, 705 cm^{-1}.

^{1}H NMR (400 MHz, CDCl$_3$, HETCOR) δ 1.19 (t, J = 7.0 Hz, 3H, CH$_2$C*H*$_3$), 1.28 (t, J = 7.0 Hz,

3H, CH$_2$C*H*$_3$), 3.94 (m, 1H, C*H*$_2$CH$_3$), 4.10-4.19 (m, 3H, C*H*$_2$CH$_3$), 4.26 (dd, J = 18.0, 9.0 Hz,

1H, H-6a), 4.48 (ddd, J = 8.5, 3.0, 1.5 Hz, 1H, H-3a), 6.63-6.68 (m, 2H, ArH), 7.22 (m, 1H,

ArH), 7.26 (m, 1H, ArH), 7.35-7.39 (m, 3H, ArH), 7.68 (br d, J = 7.5 Hz, 2H, ArH), 8.05 (dd, J

= 5.0, 1.5 Hz, 1H, H-3). ^{13}C NMR (100.6 MHz) δ 16.4 (d, J = 5.5 Hz, CH$_2$*C*H$_3$), 16.4 (d, J = 5.5

Hz, CH$_2$*C*H$_3$), 48.5 (d, J = 3.0 Hz, C-6a), 60.2 (C-3a), 63.7 (d, J = 7.0 Hz, *C*H$_2$CH$_3$), 64.8 (d, J =

7.0 Hz, *C*H$_2$CH$_3$), 86.4 (d, J =157.0 Hz, C-1), 124.4 (CHAr), 126.5 (CHAr), 128.2 (d, J = 2.0

Hz, 2CHAr), 128.5 (d, J = 6.0 Hz, 2CHAr), 128.9 (d, J = 2.0 Hz, CHAr), 129.0 (CHAr), 130.1

(CHAr), 132.2 (C-*ipso*), 133.5 (d, J = 4.0 Hz, C-*ipso*), 134.7 (C-*ipso*), 162.3 (d, J = 12.0 Hz, C-

3), 170.6 (d, J = 5.0 Hz, CO), 171.4 (d, J = 12.0 Hz, CO). HRMS $C_{22}H_{23}ClN_2O_5P$ [M+H]$^+$

461.1028; found, 461.1029. Anal. Cald. for $C_{22}H_{22}ClN_2O_5P$: C, 57.34%; H, 4.81%; N, 6.08%; found: C, 57.70%; H, 4.96%; N, 5.59%.

Diethyl (1*RS*,3a*SR*,6a*SR*)-5-(4-bromophenyl)-4,6-dioxo-1-phenyl-1,3a,4,5,6,6a-hexahydropyrrolo[3,4-*c*]pyrrole-1-phosphonate (9t). Following the general procedure, AgOAc (7 mg, 0.04 mmol), *N*-(4-bromophenyl)maleimide (275 mg, 1.1 mmol), acetonitrile (5 mL) and diethyl α-phenylisocyanomethylphosphonate (177 mg, 0.7 mmol) gave **9t** (181 mg, 51%) as a white solid, after column chromatography (EtOAc/hexane 1:1). M.p. 180-182 ºC (EtOAc). IR (ATR) 3478, 2918, 2845, 1797, 1714, 1480, 1387, 1236, 1187, 1158, 1022, 973, 744, 578 cm^{-1}. ^{1}H NMR (400 MHz, CDCl$_3$, HETCOR) δ 1.19 (t, *J* = 7.0 Hz, 3H, CH$_2$C*H*$_3$), 1.28 (t, *J* = 7.0 Hz, 3H, CH$_2$C*H*$_3$), 3.93 (m, 1H, C*H*$_2$CH$_3$), 4.10-4.19 (m, 3H, C*H*$_2$CH$_3$), 4.25 (dd, *J* = 18.0, 9.0 Hz, 1H, H-6a), 4.47 (ddd, *J* = 9.0, 3.0, 1.5 Hz, 1H, H-3a), 6.59-6.61 (m, 2H, ArH), 7.34-7.36 (m, 3H, ArH), 7.40-7.42 (m, 2H, ArH), 7.67 (br s, *J* = 7.5 Hz, 2H, ArH), 8.04 (dd, *J* = 5.0, 1.5 Hz, 1H, H-3). ^{13}C NMR (100.6 MHz) δ 16.4 (d, *J* = 3.0 Hz, CH$_2$*C*H$_3$), 16.4 (d, *J* = 4.0 Hz, CH$_2$*C*H$_3$), 48.4 (d, *J* = 3.0 Hz, C-6a), 60.3 (C-3a), 63.7 (d, *J* = 8.0 Hz, *C*H$_2$CH$_3$), 64.8 (d, *J* = 7.0 Hz, *C*H$_2$CH$_3$), 86.4 (d, *J* =157.0 Hz, C-1), 122.7 (C-*ipso*), 127.7 (2CHAr), 128.1 (d, *J* = 2.0 Hz, 2CHAr), 128.5 (d, *J* = 6.0 Hz, 2CHAr), 128.8 (d, *J* = 2.0 Hz, CHAr), 130.2 (C-*ipso*), 132.4 (2CHAr), 133.6 (d, *J* = 4.0 Hz, C-*ipso*), 162.2 (d, *J* = 12.0 Hz, C-3), 170.7 (d, *J* = 5.0 Hz, CO), 171.4 (d, *J* =11.0 Hz, CO). HRMS $C_{22}H_{23}BrN_2O_5P$ [M+H]$^+$ 505.0522; found, 505.0522. Anal. Cald. for $C_{22}H_{22}BrN_2O_5P$: C, 52.99%; H, 4.90%; N, 5.24%; found: C, 53.30%; H, 4.61%; N, 5.10%.

Diethyl (1*RS*,3a*SR*,6a*SR*)-5-(3,5-dichlorophenyl)-4,6-dioxo-1-phenyl-1,3a,4,5,6,6a-hexahydropyrrolo[3,4-*c*]pyrrole-1-phosphonate (9u). Following the general procedure, AgOAc (12 mg, 0.07 mmol), *N*-(3,5-dichlorophenyl)maleimide (267 mg, 1.1 mmol), acetonitrile

(5 mL) and diethyl α-phenylisocyanomethylphosphonate (177 mg, 0.7 mmol) gave **9u** (190 mg, 55%) as a white solid, after column chromatography (EtOAc/hexane 8:2). M.p. 207-209 ºC (EtOAc). IR (ATR) 3483, 3079, 2952, 2928, 1719, 1573, 1441, 1373, 1226, 1183, 1027, 973, 763, 734, 727, 588 cm^{-1}. ^{1}H NMR (400 MHz, CDCl$_3$, HETCOR) δ 1.20 (t, J = 7.0 Hz, 3H, CH$_2$CH_3), 1.28 (t, J = 7.0 Hz, 3H, CH$_2$CH_3), 3.94 (m, 1H, CH_2CH$_3$), 4.10-4.19 (m, 3H, CH_2CH$_3$), 4.25 (dd, J = 18.0, 8.5 Hz, 1H, H-6a), 4.47 (ddd, J = 9.0, 2.5, 1.5 Hz, 1H, H-3a), 6.60 (d, J = 2.0 Hz, 2H, ArH), 7.27 (m, 1H, ArH), 7.37-7.40 (m, 3H, ArH), 7.65 (br d, J = 5.0 Hz, 2H, ArH), 8.04 (dd, J = 5.0, 1.5 Hz, 1H, H-3). ^{13}C NMR (100.6 MHz) δ 16.3 (d, J = 5.5 Hz, CH$_2$CH$_3$), 16.4 (d, J = 5.5 Hz, CH$_2$CH_3), 48.6 (d, J = 3.0 Hz, C-6a), 60.9 (C-3a), 63.8 (d, J = 7.0 Hz, CH_2CH$_3$), 64.9 (d, J = 7.0 Hz, CH_2CH$_3$), 86.5 (d, J = 158.0 Hz, C-1), 124.8 (2CHAr), 128.3 (d, J = 2.0 Hz, 2CHAr), 128.5 (d, J = 5.0 Hz, 2CHAr), 129.0 (d, J = 2.0 Hz, CHAr), 129.1 (CHAr), 132.8 (C-*ipso*), 133.5 (d, J = 3.0 Hz, C-*ipso*), 135.3 (2C-*ipso*), 162.0 (d, J = 13.0 Hz, C-3), 170.2 (d, J = 5.0 Hz, CO), 171.1 (d, J = 11.0 Hz, CO). HRMS C$_{22}$H$_{22}$Cl$_2$N$_2$O$_5$P [M+H]$^+$ 495.0638; found, 495.0638. Anal. Cald. for C$_{22}$H$_{21}$Cl$_2$N$_2$O$_5$P: C, 53.35%; H, 4.27%; N, 5.66%; found: C, 53.69%; H, 4.35%; N, 5.42%.

Diethyl (1*RS*,3a*SR*,6a*SR*)-5-(3,4-dichlorophenyl)-4,6-dioxo-1-phenyl-1,3a,4,5,6,6a-hexahydropyrrolo[3,4-*c*]pyrrole-1-phosphonate (9v). Following the general procedure, AgOAc (8 mg, 0.05 mmol), *N*-(3-chloro-4-chlorophenyl)maleimide (288 mg, 1.2 mmol), acetonitrile (6 mL) and diethyl α-phenylisocyanomethylphosphonate (202 mg, 0.8 mmol) gave **9v** (210 mg, 53%) as a white solid, after column chromatography (EtOAc/hexane 1:1). M.p. 172-174 ºC (EtOAc). IR (ATR) 3480, 3075, 2957, 1790, 1716, 1464, 1251, 1187, 1058, 1024, 737, 579 cm^{-1}. ^{1}H NMR (400 MHz, CDCl$_3$, HETCOR) δ 1.20 (t, J = 7.0 Hz, 3H, CH$_2$CH_3), 1.28 (t, J = 7.0 Hz, 3H, CH$_2$CH_3), 3.95 (m, 1H, CH_2CH$_3$), 4.10-4.20 (m, 3H, CH_2CH$_3$), 4.26 (dd, J = 18.0,

8.5 Hz, 1H, H-6a), 4.47 (ddd, J = 8.5, 3.0, 1.5 Hz, 1H, H-3a), 6.61 (dd, J = 9.0, 2.5 Hz, 1H,

ArH), 6.78 (d, J = 2.5 Hz, 1H, ArH), 7.35-7.38 (m, 4H, ArH), 7.65-7.68 (m, 2H, ArH), 8.04 (dd,

J = 4.5, 1.5 Hz, 1H, H-3). ^{13}C NMR (100.6 MHz) δ 16.2 (d, J = 6.0 Hz, CH$_2$CH$_3$), 16.3 (d, J =

6.0 Hz, CH$_2$CH$_3$), 48.4 (d, J = 3.0 Hz, C-6a), 60.0 (C-3a), 63.6 (d, J = 7.0 Hz, CH$_2$CH$_3$), 64.7 (d,

J = 8.0 Hz, CH$_2$CH$_3$), 86.2 (d, J = 157.0 Hz, C-1), 125.2 (CHAr), 127.9 (CHAr), 128.0 (d, J =

2.0 Hz, 2CHAr), 128,3 (d, J = 6.0 Hz, 2CHAr), 128.7 (d, J = 2.0 Hz, CHAr), 130.2 (C-*ipso*),

130.6 (CHAr), 132.9 (C-*ipso*), 133.0 (C-*ipso*), 133.3 (d, J = 4.0 Hz, C-*ipso*), 161.9 (d, J = 13.0

Hz, C-3), 170.2 (d, J = 5.0 Hz, CO), 171.1 (d, J = 12.0 Hz, CO). HRMS C$_{22}$H$_{22}$Cl$_2$N$_2$O$_5$P

[M+H]$^+$ 495.0638; found, 495.0637. Anal. Cald. for C$_{22}$H$_{21}$Cl$_2$N$_2$O$_5$P: C, 53.35%; H, 4.27%; N,

5.66%; found: C, 53.42%; H, 4.30%; N, 5.48%.

Diethyl (1*RS*,3a*SR*,6a*SR*)-4,6-dioxo-1-phenyl-5-(2,4,6-trichlorophenyl)-1,3a,4,5,6,6a-hexahydropyrrolo[3,4-*c*]pyrrole-1-phosphonate (9w). Following the general procedure,

AgOAc (8.3 mg, 0.05 mmol), *N*-(2,4,6-trichlorophenyl)maleimide (194 mg, 0.7 mmol),

acetonitrile (4 mL) and diethyl α-phenylisocyanomethylphosphonate (127 mg, 0.5 mmol) gave

9w (215 mg, 81%) as a yellowish solid, after column chromatography (EtOAc). M.p. 146-148 ºC

(EtOAc). IR (ATR) 3501, 2976, 2854, 1786, 1727, 1471, 1361, 1253, 1043, 1322, 961, 704 cm^{-1}.

^{1}H NMR (400 MHz, CDCl$_3$, HETCOR) δ 1.14 (t, J = 7.0 Hz, 3H, CH$_2$CH$_3$), 1.28 (t, J = 7.0 Hz,

3H, CH$_2$CH$_3$), 3.84 (m, 1H, CH$_2$CH$_3$), 4.03-4.17 (m, 3H, CH$_2$CH$_3$), 4.41 (dd, J = 18.0, 9.0 Hz,

1H, H-6a), 4.57 (ddd, J = 8.5, 4.0, 1.0 Hz, 1H, H-3a), 7.26 (d, J =3.0 Hz, 1H, ArH), 7.28-7.34

(m, 3H, ArH), 7.36 (d, J = 2.0 Hz, 1H, ArH), 7.75 (br d, J = 8.0 Hz, 2H, ArH), 8.02 (dd, J = 5.0,

1.0 Hz, 1H, H-3). ^{13}C NMR (100.6 MHz) δ 16.3 (d, J = 6.0 Hz, CH$_2$CH$_3$), 16.4 (d, J = 6.0 Hz,

CH$_2$CH$_3$), 48.3 (d, J = 3.0 Hz, C-6a), 61.0 (C-3a), 63.7 (d, J = 7.0 Hz, CH$_2$CH$_3$), 64.9 (d, J = 8.0

Hz, CH$_2$CH$_3$), 86.7 (d, J = 152.0 Hz, C-1), 126.6 (C-*ipso*), 127.8 (d, J = 2.0 Hz, 2CHAr), 128.6

(CHAr), 128.7 (CHAr), 128.8 (CHAr), 129.0 (d, J = 5.0 Hz, 2CHAr), 133.0 (d, J = 5.0 Hz, C-*ipso*), 135.1 (d, J = 10.0 Hz, C-*ipso*), 136.8 (2C-*ipso*), 161.8 (d, J = 11.0 Hz, C-3), 169.3 (d, J = 5.0 Hz, CO), 169.8 (d, J =14.0 Hz, CO). HRMS $C_{22}H_{21}Cl_3N_2O_5P$ $[M+H]^+$ 529.0248; found, 529.0242. Purity 98% (t_R= 5.06 min).

Diethyl (1*RS*,3a*SR*,6a*SR*)-5-(3-nitrophenyl)-4,6-dioxo-1-phenyl-1,3a,4,5,6,6a-hexahydropyrrolo[3,4-*c*]pyrrole-1-phosphonate (9x). Following the general procedure, AgOAc (4 mg, 0.02 mmol), *N*-(3-nitrophenyl)maleimide (131 mg, 0.6 mmol), acetonitrile (3 mL) and diethyl α-phenylisocyanomethylphosphonate (101 mg, 0.4 mmol) gave **9x** (101 mg, 54%) as a white solid, after column chromatography (EtOAc). M.p. 192-195 ºC (EtOAc). IR (NaCl) 2984, 1724, 1537, 1351, 1248, 1176, 1050, 971, 758, 674 cm^{-1}.^{1}H NMR (400 MHz, CDCl$_3$, HETCOR) δ 1.21 (t, J = 7.0 Hz, 3H, CH$_2$C*H*$_3$), 1.29 (t, J = 7.0 Hz, 3H, CH$_2$C*H*$_3$), 3.98 (m, 1H, C*H*$_2$CH$_3$), 4.10-4.24 (m, 3H, C*H*$_2$CH$_3$), 4.30 (dd, J = 18.0, 9.0 Hz, 1H, H-6a), 4.53 (ddd, J = 9.0, 3.0, 1.0 Hz, H-3a), 7.11 (dq, J = 8.0, 1.0 Hz, 1H, ArH), 7.38-7.41 (m, 3H, ArH), 7.49 (t, J = 8.0 Hz, 1H, ArH), 7.58 (t, J = 2.0 Hz, 1H, ArH), 7.67-7.69 (m, 2H, ArH), 8.07 (dd, J = 5.0, 1.0 Hz, 1H, H-3), 8.14 (ddd, J = 8.5, 2.5, 1.0 Hz, 1H, ArH).^{13}C NMR (100.6 MHz) δ 16.2 (d, J = 3.0 Hz, CH$_2$*C*H$_3$), 16.3 (d, J = 3.5 Hz, CH$_2$*C*H$_3$), 48.5 (d, J = 2.0 Hz, C-6a), 60.0 (C-3a), 63.6 (d, J = 7.5 Hz, *C*H$_2$CH$_3$), 64.7 (d, J = 7.5 Hz, *C*H$_2$CH$_3$), 86.2 (d, J = 158.0 Hz, C-1), 121.4 (CHAr), 123.3 (CHAr), 128.1 (2CHAr), 128.2 (CHAr), 128.3 (CHAr), 128.9 (d, J = 1.5 Hz, CHAr), 129.8 (CHAr), 131.9 (CHAr), 132.0 (C-*ipso*), 133.2 (d, J = 4.0 Hz, C-*ipso*), 148.3 (C-*ipso*), 161.7 (d, J = 12.0 Hz, C-3), 170.2 (d, J = 5.5 Hz, CO), 171.1 (d, J = 11.0 Hz, CO). HRMS $C_{22}H_{23}N_3O_7P$ $[M+H]^+$ 472.1268; found, 472.1276. Anal. Cald. for $C_{22}H_{22}N_3O_7P$: C, 56.05%; H, 4.70%; N, 8.91%; found: C, 55.73%; H, 4.74%; N, 8.85%.

Diethyl (1*RS*,3a*SR*,6a*SR*)-5-(2-methyl-5-nitrophenyl)-4,6-dioxo-1-phenyl-1,3a,4,5,6,6a-hexahydropyrrolo[3,4-*c*]pyrrole-1-phosphonate (9y). Following the general procedure, AgOAc (5 mg, 0.03 mmol), *N*-(2-methyl-5-nitrophenyl)maleimide (138 mg, 0.6 mmol), acetonitrile (3 mL) and diethyl α-phenylisocyanomethylphosphonate (101 mg, 0.4 mmol) gave **9y** (111 mg, 57%) as a white solid, after column chromatography (EtOAc). M.p. 196-198 ºC (EtOAc). IR (ATR) 3493, 3079, 2947, 2845, 1724, 1519, 1343, 1192, 1017, 739, 578 cm^{-1}. ^{1}H NMR (400 MHz, CDCl$_3$, HETCOR) δ 1.16 (td, *J* = 7.0, 0.5 Hz, 3H, CH$_2$C*H$_3$* rotamer A), 1.22 (td, *J* = 7.0, 0.5 Hz, 3H, CH$_2$C*H$_3$* rotamer B), 1.29 (td, *J* = 7.0, 0.5 Hz, 3H, CH$_2$C*H$_3$* rotamer B), 1.30 (td, *J* = 7.0, 0.5 Hz, 3H, CH$_2$C*H$_3$* rotamer A), 1.51 (s, 3H, CH$_3$ rotamer A), 2.15 (s, 3H, CH$_3$ rotamer B), 3.85 (m, 1H, C*H$_2$*CH$_3$ rotamer A), 3.99 (m, 1H, C*H$_2$*CH$_3$ rotamer B), 4.03-4.24 (m, 6H, C*H$_2$*CH$_3$ rotamer A and B), 4.35 (dd, *J* = 18.0, 9.0 Hz, 1H, H-6a rotamer B), 4.39 (dd, *J* = 18.5, 9.0 Hz, 1H, H-6a rotamer A), 4.55 (ddd, *J* = 10.0, 2.5, 1.5 Hz, 1H, H-3a rotamer B), 4.59 (ddd, *J* = 9.0, 3.5, 1.5 Hz, 1H, H-3a rotamer A), 6.88 (d, *J* = 2.5 Hz, 1H, ArH rotamer B), 7.47-7.19 (m, 8H, 4ArH rotamer A and 4ArH rotamer B), 7.69 (br s, 2H, ArH rotamer B), 7.77 (d, *J* = 7.5 Hz, 2H, ArH rotamer A), 7.91 (d, *J* = 2.5 Hz, 1H, ArH rotamer A), 8.05 (dd, *J* = 5.0, 1.5 Hz, 1H, C-3 rotamer A), 8.08 (dd, *J* = 5.5, 2.5 Hz, 1H, C-3 rotamer B), 8.08-8.11 (m, 2H, ArH rotamer A and rotamer B). ^{13}C NMR (100.6 MHz) δ 16.3 (d, *J* = 5.5 Hz, CH$_2$*C*H$_3$ rotamer A), 16.3 (d, *J* = 5.5 Hz, CH$_2$*C*H$_3$ rotamer B), 16.4 (d, *J* = 5.5 Hz, CH$_2$*C*H$_3$ rotamer A), 16.4 (d, *J* = 5.5 Hz, CH$_2$*C*H$_3$ rotamer B), 17.5 (CH$_3$ rotamer A), 18.2 (CH$_3$ rotamer B), 48.3 (d, *J* = 2.5 Hz, C-6a rotamer A), 49.2 (d, *J* = 2.5 Hz, C-6a rotamer B), 60.1 (C-3a rotamer B), 61.0 (C-3a rotamer A), 63.7 (d, *J* = 7.5 Hz, CH$_2$*C*H$_3$ rotamer A), 63.8 (d, *J* = 7.5 Hz, CH$_2$*C*H$_3$ rotamer B), 64.9 (d, *J* = 7.5 Hz, CH$_2$*C*H$_3$ rotamer B), 65.0 (d, *J* = 7.5 Hz, CH$_2$*C*H$_3$ rotamer A), 86.3 (d, *J* = 159.0, C-1 rotamer B), 86.6 (d, *J* = 154.5, C-1 rotamer A), 123.5 (CHAr rotamer B), 123.7

(CHAr rotamer A), 124.3 (CHAr rotamer A), 124.5 (CHAr rotamer B), 127.9 (CHAr rotamer A), 128.0 (CHAr rotamer B), 128.3 (d, J = 5.5 Hz, 2CHAr rotamer B), 128.3 (CHAr rotamer A), 128.4 (CHAr rotamer B), 128.8 (d, J = 2.5 Hz, CHAr rotamer A), 128.9 (d, J = 6.5 Hz, 2CHAr rotamer A), 129.4 (d, J = 2.0 Hz, CHAr rotamer B), 131.1 (C-*ipso* rotamer A), 131.2 (C-*ipso* rotamer B), 131.8 (CHAr rotamer B), 131.9 (CHAr rotamer A), 133.3 (d, J = 4.5 Hz, C-*ipso* rotamer A), 133.4 (d, J = 4.0 Hz, C-*ipso* rotamer B), 143.8 (C-*ipso* rotamer A), 143.9 (C-*ipso* rotamer B), 146.6 (C-*ipso* rotamer A), 146.7 (C-*ipso* rotamer B), 161.8 (d, J = 12.5 Hz, C-3 rotamer B), 161.9 (d, J = 11.5 Hz, C-3 rotamer A), 170.4 (d, J = 5.0 Hz, CO rotamer B), 170.6 (d, J = 5.5 Hz, CO rotamer A), 171.0 (d, J = 13.5 Hz, CO rotamer A), 171.3 (d, J = 10.0 Hz, CO rotamer B). HRMS $C_{23}H_{25}N_3O_7P$ [M+H]$^+$ 486.1425; found, 486.1424. Anal. Cald. for $C_{23}H_{24}N_3O_7P$: C, 56.91%; H, 4.98%; N, 8.66%; found: C, 57.33%; H, 5.11%; N, 8.59%.

Diethyl (1RS,3aSR,6aSR)-5-(1,1'-biphenyl)-4-yl-4,6-dioxo-1-phenyl-1,3a,4,5,6,6a-hexahydropyrrolo[3,4-c]pyrrole-1-phosphonate (9z). Following the general procedure, AgOAc (5 mg, 0.03 mmol), *N*-(*p*-phenylphenyl)maleimide (200 mg, 0.8 mmol), acetonitrile (4 mL) and diethyl α-phenylisocyanomethylphosphonate (134 mg, 0.5 mmol) gave **9z** (129 mg, 49%) as a yellowish oil, after column chromatography (EtOAc). IR (NaCl) 3483, 2982, 2928, 1716, 1628, 1487, 1378, 1248, 1182, 1052, 1024, 969, 839, 792 cm^{-1}.^{1}H NMR (400 MHz, CDCl$_3$, HETCOR) δ 1.20 (t, J = 7.0 Hz, 3H, CH$_2$C*H$_3$*), 1.29 (t, J = 7.0 Hz, 3H, CH$_2$C*H$_3$*), 3.97 (m, 1H, C*H$_2$*CH$_3$), 4.09-4.23 (m, 3H, C*H$_2$*CH$_3$), 4.30 (dd, J = 18.5, 9.0 Hz, 1H, H-6a), 4.51 (ddd, J = 9.0, 3.0, 1.5 Hz, 1H, H-3a), 6.80 (m, 2H, ArH), 7.31-7.42 (m, 6H, ArH), 7.47-7.51 (m, 4H, ArH), 7.71 (br d, J = 7.5 Hz, 2H, ArH), 8.08 (dd, J = 5.0, 1.5 Hz, 1H, H-3).^{13}C NMR (100.6 MHz) δ 16.2 (d, J = 5.5 Hz, CH$_2$*C*H$_3$), 16.3 (d, J = 5.5 Hz, CH$_2$*C*H$_3$), 48.2 (d, J = 2.5 Hz, C-6a), 60.2 (C-3a), 63.5 (d, J = 7.0 Hz, *C*H$_2$CH$_3$), 64.6 (d, J = 7.5 Hz, *C*H$_2$CH$_3$), 86.5 (d, J = 157.0 Hz,

C-1), 126.3 (2CHAr), 127.1 (2CHAr), 127.7 (CHAr), 127.8 (2CHAr), 127.9 (d, J = 1.5 Hz, 2CHAr), 128.4 (d, J = 6.0 Hz, 2CHAr), 128.6 (d, J = 2.0 Hz, CHAr), 128.8 (2CHAr), 130.0 (C-$ipso$), 133.4 (d, J = 4.0 Hz, C-$ipso$), 140.0 (C-$ipso$), 141.7 (C-$ipso$), 162.3 (d, J = 12.0 Hz, C-3), 170.9 (d, J = 5.5 Hz, CO), 171.7 (d, J = 11.5 Hz, CO). HRMS $C_{28}H_{28}N_2O_5P$ [M+H]$^+$503.1730; found, 503.1727. Purity 98.5% (t_R= 4.71 min).

Diethyl (1RS,3aSR,6aSR)-4,6-dioxo-1-phenyl-5-(p-tolyl)-1,3a,4,5,6,6a-hexahydropyrrolo[3,4-c]pyrrole-1-phosphonate (9aa). Following the general procedure, AgOAc (6 mg, 0.04 mmol), N-(4-methylphenyl)maleimide (153 mg, 0.9 mmol), acetonitrile (4.5 mL) and diethyl α-phenylisocyanomethylphosphonate (168 mg, 0.6 mmol) gave **9aa** (199 mg, 75%) as a white solid, after column chromatography (EtOAc/hexane 3:2 to 9:1). M.p. 156-158 ºC (EtOAc). IR (ATR) 3476, 2936, 2863, 1711, 1632, 1520, 1368, 1240, 1181, 1025, 971, 740, 583 cm^{-1}; ^{1}H NMR (400 MHz, CDCl$_3$, HETCOR) δ 1.19 (t, J = 7.0 Hz, 3H, CH$_2$CH_3), 1.29 (t, J = 7.0 Hz, 3H, CH$_2$CH_3), 2.28 (s, 3H, CH$_3$-Ar), 3.93 (m, 1H, CH_2CH$_3$), 4.11-4.19 (m, 3H, CH_2CH$_3$), 4.24 (dd, J = 16.5, 9.0, 1H, H-6a), 4.46 (ddd, J = 8.5, 3.0, 1.5 Hz, 1H, H-3a), 6.60 (m, 2H, ArH), 7.09 (m, 2H, ArH), 7.31-7.38 (m, 3H, ArH), 7.68-7.70 (m, 2H, ArH), 8.05 (dd, J = 5.0, 1.5 Hz, 1H, H-3). ^{13}C NMR (100.6 MHz) δ 16.2 (d, J = 5.5 Hz, CH$_2$CH$_3$), 16.3 (d, J = 5.5 Hz, CH$_2$CH$_3$), 21.1 (CH$_3$-Ar), 48.1 (d, J = 3.0 Hz, C-6a), 60.2 (C-3a), 63.5 (d, J = 7.0 Hz, CH$_2$CH$_3$), 64.6 (d, J = 8.0 Hz, CH$_2$CH$_3$), 86.2 (d, J =156.0 Hz, C-1), 125.8 (2CHAr), 127.9 (d, J = 2.0 Hz, 2CHAr), 128.3 (CHAr), 128.4 (CHAr), 128.5 (d, J = 2.0 Hz, CHAr), 128.5 (C-$ipso$), 129.6 (2CHAr), 133.5 (d, J = 4.0 Hz, C-$ipso$), 138.8 (C-$ipso$), 162.4 (d, J = 12.0 Hz, C-3), 171.1 (d, J = 5.0 Hz, CO), 171.7 (d, J = 11.0 Hz, CO). HRMS $C_{23}H_{26}N_2O_5P$ [M+H]$^+$ 441.1574; found, 441.1572. Anal. Cald. for $C_{23}H_{25}N_2O_5P$: C, 62.72%; H, 5.72%; N, 6.36%; found: C, 62.87%; H, 5.82%; N, 6.18%.

Diethyl (1*RS*,3a*SR*,6a*SR*)-4,6-dioxo-5-(4-phenoxyphenyl)-1-phenyl-1,3a,4,5,6,6a-hexahydropyrrolo[3,4-*c*]pyrrole-1-phosphonate (9ab). Following the general procedure, AgOAc (9 mg, 0.05mmol), *N*-(4-phenoxyphenyl)maleimide (371mg, 1.4mmol), acetonitrile (7 mL) and diethyl α-phenylisocyanomethylphosphonate (228 mg, 0.9 mmol) gave **9ab** (302 mg, 65%) as a white solid, after column chromatography (EtOAc). M.p. 165-167ºC (EtOAc).IR (NaCl) 3488, 3057, 2984, 1783, 1715, 1628, 1488, 1242, 1187, 1024, 700, 578 cm^{-1}. ^{1}H NMR (400 MHz, CDCl$_3$, HETCOR) δ 1.19 (t, *J* = 7.0 Hz, 3H, CH$_2$C*H*$_3$), 1.28 (t, *J* = 7.0 Hz, 3H, CH$_2$C*H*$_3$), 3.95 (m, 1H, C*H*$_2$CH$_3$), 4.10-4.19 (m, 3H, C*H*$_2$CH$_3$), 4.25 (dd, *J* = 18.0, 8.5 Hz, 1H, H-6a), 4.46-4,49 (ddd, *J* = 8.5, 3.0, 1.5 Hz, 1H, H-3a), 6.64-6.67 (m, 2H, ArH), 6.87-6.89 (m, 2H, ArH), 6.96-6.98 (m, 2H, ArH), 7.12 (m, 1H, ArH), 7.30-7.38 (m, 5H, ArH), 7.69 (d, *J* = 8.0 Hz, 2H, ArH), 8.01 (dd, *J* = 5.0, 1.5 Hz, 1H, H-3). ^{13}C NMR (100.6 MHz) δ 16.2 (d, *J* = 4.0 Hz, CH$_2$CH$_3$), 16.3 (d, *J* = 4.0 Hz, CH$_2$C*H*$_3$), 48.2 (d, *J* = 3.0 Hz, C-6a), 60.1 (C-3a), 63.5 (d, *J* = 7.0 Hz, *C*H$_2$CH$_3$), 64.6 (d, *J* = 7.0 Hz, *C*H$_2$CH$_3$), 86.2 (d, *J* = 157.0 Hz, C-1), 118.5 (2CHAr), 119.6 (2CHAr), 124.0 (2CHAr), 125.6 (C-*ipso*), 127.5 (2CHAr), 127.9 (d, *J* = 2.0 Hz, 2CHAr), 128.4 (d, *J* = 6.0 Hz, CHAr), 128.6 (d, *J* = 2.0. Hz, CHAr), 129.8 (2CHAr), 133.5 (d, *J* = 4.0 Hz, C-*ipso*), 156.2 (C-*ipso*), 157.6 (C-*ipso*), 162.2 (d, *J* = 12.0 Hz, C-3), 171.0 (d, *J* = 6.0 Hz, CO), 171.7 (d, *J* = 11.0 Hz, CO). HRMS C$_{28}$H$_{28}$N$_2$O$_6$P [M+H]$^+$ 519.1679; found, 519.1675. Anal. Cald. for C$_{28}$H$_{27}$N$_2$O$_6$P: C, 64.86%; H, 5.25%; N, 5.40%; found: C, 65.12%; H, 5.26%; N, 5.41%.

Diethyl (1*RS*,3a*SR*,6a*SR*)-5-(naphth-1-yl)-4,6-dioxo-1-phenyl-1,3a,4,5,6,6a-hexahydropyrrolo[3,4-*c*]pyrrole-1-phosphonate (9ac). Following the general procedure, AgOAc (3 mg, 0.02 mmol), *N*-(naphth-1-yl)maleimide (100 mg, 0.5 mmol), acetonitrile (2 mL) and diethyl α-phenylisocyanomethylphosphonate (76 mg, 0.3 mmol) gave **9ac** (70 mg, 49%) as

a white solid, after column chromatography (EtOAc/hexane 1:1 to 9:1). M.p. 197-198 ℃ (EtOAc). IR (ATR) 3480, 2927, 2853, 1716, 1598, 1446, 1397, 1358, 1240, 1177, 1039, 1025, 961, 775, 706, 583 cm^{-1}. ^{1}H NMR (400 MHz, CDCl$_3$, HETCOR) δ 1.17 (td, J = 7.0, 0.5 Hz, 3H, CH$_2$CH_3 rotamer A), 1.20 (td, J = 7.0, 0.5 Hz, 3H, CH$_2$CH_3 rotamer B), 1.30 (t, J = 7.0 Hz, 3H, CH$_2$CH_3 rotamer A), 1.31 (t, J = 7.0 Hz, 3H, CH$_2$CH_3 rotamer B), 3.90 (m, 1H, CH_2CH$_3$ rotamer A), 3.98 (m, 1H, CH_2CH$_3$ rotamer B), 4.04-4.26 (m, 6H, CH_2CH$_3$ rotamer A and B), 4.43 (dd, J = 18.5, 9.0 Hz, 1H, H-6a rotamer A), 4.46 (dd, J = 18.0, 8.5 Hz, 1H, H-6a rotamer B), 4.63 (ddd, J = 9.0, 3.5, 1.5 Hz, 1H, H-3a rotamer A), 4.67 (ddd, J = 8.5, 3.0, 1.5 Hz, 1H, H-3a rotamer B), 6.33 (dd, J = 8.5, 1.0 Hz, 1H, ArH rotamer A), 6.39 (dd, J = 7.5, 1.0 Hz, 1H, ArH rotamer B), 7.12 (ddd, J = 8.5, 7.0, 1.5 Hz, 1H, ArH rotamer A), 7.21 (dd, J = 7.5, 1.0 Hz, 1H, ArH rotamer A), 7.28-7.49 (m, 12H, ArH rotamer A and B), 7.73-7.90 (m, 8H, ArH rotamer A and B), 8.12 (dd, J = 5.0 Hz, 1.5 Hz, 1H, H-3 rotamer B), 8.13 (dd, J = 5.0, 1.5 Hz, 1H, H-3 rotamer A). ^{13}C NMR (100.6 MHz) δ 16.2 (d, J = 5.0 Hz, CH$_2$CH_3 rotamer A or B), 16.3 (d, J = 5.0 Hz, CH$_2$CH_3 rotamer A or B), 16.3 (d, J = 6.0 Hz, 2CH$_2$CH_3 rotamer A or B), 48.3 (d, J = 2.5 Hz, C-6a rotamer A), 48.6 (d, J = 2.5 Hz, C-6a rotamer B), 60.3 (C-3a rotamer B), 61.0 (C-3a rotamer A), 63.6 (d, J = 7.5 Hz, 2CH_2CH$_3$ rotamer A and B), 64.7 (d, J = 7.0 Hz, CH_2CH$_3$ rotamer B), 64.7 (d, J = 7.5 Hz, CH_2CH$_3$ rotamer A), 86.2 (d, J = 157.5 Hz, C-1 rotamer B), 86.5 (d, J = 155.0 Hz, C-1 rotamer A), 121.2 (CHAr rotamer A), 121.6 (CHAr rotamer B), 125.0 (CHAr rotamer A), 125.1 (CHAr rotamer B), 125.7 (CHAr rotamer B), 126.0 (CHAr rotamer A), 126.3 (CHAr rotamer A), 126.5 (CHAr rotamer B), 127.0 (CHAr rotamer A), 127.2 (CHAr rotamer B), 127.6 (C-*ipso* rotamer A), 127.8 (C-*ipso* rotamer B), 127.9 (d, J = 2.0 Hz, 2CHAr rotamer A), 128.0 (d, J = 2.0 Hz, 2CHAr rotamer B), 128.3 (CHAr rotamer A), 128.4 (d, J = 6.0 Hz, CHAr rotamer B), 128.6 (d, J = 2.0 Hz, 2CHAr rotamer A), 128.7 (d, J = 2.5 Hz, 2CHAr rotamer B), 128.9 (CHAr

rotamer B), 129.0 (CHAr rotamer A), 130.0 (CHAr rotamer A), 130.1 (CHAr rotamer B), 133.4

(d, J = 4.5 Hz, C-*ipso* rotamer A), 133.5 (d, J = 4.0 Hz, C-*ipso* rotamer B), 134.1 (C-*ipso* rotamer

A), 134.2 (C-*ipso* rotamer B), 162.3 (d, J = 11.5 Hz, C-3 rotamer A), 162.4 (d, J = 12.0 Hz, C-3

rotamer B), 171.3 (d, J = 5.5 Hz, CO rotamer B), 171.4 (d, J = 5.5 Hz, CO rotamer A), 171.7 (d,

J = 12.5 Hz, CO rotamer A), 171.9 (d, J = 11.5 Hz, CO rotamer B). HRMS $C_{26}H_{26}N_2O_5P$

[M+H]$^+$ 477.1574; found, 477.1571. Anal. Cald. For $C_{26}H_{25}N_2O_5P$: C, 65.54%; H, 5.29%; N,

5.88%; found: C, 65.34%; H, 5.12%; N, 5.65%.

Diethyl (1*RS*,3a*SR*,6a*SR*)-5-(2-chloropyridin-3-yl)-4,6-dioxo-1-phenyl-1,3a,4,5,6,6a-hexahydropyrrolo[3,4-*c*]pyrrole-1-phosphonate (9ad). Following the general procedure,

AgOAc (12 mg, 0.07 mmol), *N*-(2-chloropyridin-3-yl)maleimide (250 mg, 1.2 mmol),

acetonitrile (6 mL) and diethyl α-phenylisocyanomethylphosphonate (203 mg, 0.8 mmol) gave

9ad (224 mg, 61%) as a white solid, after column chromatography (EtOAc). M.p. 176-178 ºC

(EtOAc). IR (ATR) 3483, 2991, 2948, 1790, 1722, 1564, 1420, 1242, 1050, 752, 699, 574 cm^{-1}.

^{1}H NMR (400 MHz, CDCl$_3$, HETCOR) δ 1.14 (td, J = 7.0, 0.5 Hz, 3H, CH$_2$C*H$_3$* rotamer A),

1.19 (td, J = 7.0, 0.5 Hz, 3H, CH$_2$C*H$_3$* rotamer B), 1.28 (td, J = 7.0, 0.5 Hz, 3H, CH$_2$C*H$_3$* rotamer

A), 1.29 (td, J = 7.0, 0.5 Hz, 3H, CH$_2$C*H$_3$* rotamer B), 3.82 (m, 1H, C*H$_2$*CH$_3$ rotamer A), 3.95

(m, 1H, C*H$_2$*CH$_3$ rotamer B), 4.05-4.20 (m, 6H, C*H$_2$*CH$_3$ rotamer A and B), 4.36 (dd, J = 18.0,

8.5 Hz, 1H, H-6a rotamer A), 4.38 (dd, J = 18.0, 8.5 Hz, 1H, H-6a rotamer B), 4.53 (ddd, J = 8.5,

4.0, 1.5 Hz, 1H, H-3a rotamer A), 4.58 (ddd, J = 8.5, 3.0, 1.5 Hz, 1H, H-3a rotamer B), 6.59 (dd,

J = 8.0, 2.0 Hz, 1H, ArH rotamer B), 7.14 (dd, J = 8.0, 5.0 Hz, 1H, ArH rotamer B), 7.27 (dd, J =

8.0, 5.0 Hz, 1H, ArH rotamer A), 7.31-7.37 (m, 6H, 3ArH rotamer A and 3ArH rotamer B), 7.46

(dd, J = 8.0, 2.0 Hz, 1H, ArH rotamer A), 7.69 (m, 2H, ArH rotamer A), 7.76 (m, 2H, ArH

rotamer B), 8.02 (dd, J = 5.5 Hz, 1.5 Hz, 1H, H-3 rotamer A), 8.07 (dd, J = 5.0, 1.5 Hz, 1H, H-3

rotamer B), 8.36 (dd, *J* = 5.0, 2.0 Hz, 2H, ArH rotamer A and rotamer B). ^{13}C NMR (100.6 MHz) δ 16.3 (d, *J* = 5.5 Hz, CH$_2$*C*H$_3$ rotamer A), 16.4 (d, *J* = 5.5 Hz, CH$_2$*C*H$_3$ rotamer B), 16.4 (d, *J* = 6.0 Hz, CH$_2$*C*H$_3$ rotamer A), 16.5 (d, *J* = 5.5 Hz, CH$_2$*C*H$_3$ rotamer B), 48.4 (d, *J* = 2.5 Hz, C-6a rotamer A), 49.0 (d, *J* = 2.5 Hz, C-6a rotamer B), 60.4 (C-3a rotamer A), 61.0 (C-3a rotamer B), 63.7 (d, *J* = 7.5 Hz, *C*H$_2$CH$_3$ rotamer A), 63.8 (d, *J* = 7.5 Hz, *C*H$_2$CH$_3$ rotamer B), 64.9 (d, *J* = 7.5 Hz, *C*H$_2$CH$_3$ rotamer B), 65.0 (d, *J* = 7.5 Hz, *C*H$_2$CH$_3$ rotamer A), 86.1 (d, *J* = 158.0 Hz, C-1 rotamer A or B), 86.9 (d, *J* = 153.0 Hz, C-1 rotamer A or B), 123.0 (CHAr rotamer A), 123.2 (CHAr rotamer B), 126.4 (C-*ipso* rotamer A), 126.5 (C-*ipso* rotamer B), 127.9 (d, *J* = 2.0 Hz, 2CHAr rotamer A), 128.1 (d, *J* = 1.5 Hz, 2CHAr rotamer B), 128.6 (d, *J* = 5.5 Hz, 2CHAr rotamer B), 128.8 (d, *J* = 4.5 Hz, CHAr rotamer A or B), 128.8 (CHAr rotamer A or B), 128.9 (d, *J* = 5.5 Hz, 2CHAr rotamer A), 132.9 (d, *J* = 4.5 Hz, C-*ipso* rotamer A), 133.6 (d, *J* = 4.0 Hz, C-*ipso* rotamer B), 138.4 (CHAr rotamer B), 138.6 (CHAr rotamer A), 149.2 (C-*ipso* rotamer A), 149.5 (C-*ipso* rotamer B), 150.3 (CHAr rotamer A), 150.5 (CHAr rotamer B), 161.6 (d, *J* = 11.5 Hz, C-3 rotamer A), 162.0 (d, *J* = 12.5 Hz, C-3 rotamer B), 169.7 (d, *J* = 5.0 Hz, CO rotamer A), 169.8 (d, *J* = 5.5 Hz, CO rotamer B), 170.5 (d, *J* = 11.5 Hz, CO rotamer A), 170.6 (d, *J* = 14.5 Hz, CO rotamer B). HRMS C$_{21}$H$_{22}$ClN$_3$O$_5$P [M+H]$^+$ 462.0980; found, 462.0980. Anal. Cald. For C$_{21}$H$_{21}$ClN$_3$O$_5$P: C, 54.61%; H, 4.58%; N, 9.10%; found: C, 55.01%; H, 4.67%; N, 8.86%.

Theoretical calculations

The study of the [3+2] cycloaddition reaction (Scheme 1) was performed for model systems that include the reactants (dimehtyl α-phenylisocyanomethylphosphonate and *N*-methylmaleimide) and a silver cation bound to acetonitrile as the catalytic moiety. Geometry optimizations were carried out using the B3LYP functional[63,64] and the 6-31+G(d) basis set[65] for all atoms but silver,

which was treated with the LANL2DZ basis[66] in conjunction with the effective core potential for inner electrons. The nature of the stationary points (reactant, transition state, and products) was confirmed by inspection of the vibrational frequencies. Intrinsic reaction coordinate calculations[67] were carried out to check the connection between the transition states and the minimum energy structures. To further check the relative stabilities of transition states, geometry optimizations were also performed using the MN15L functional.[68] Finally, solvation calculations were performed with the SMD version[69] of the IEFPCM model to take into account the contribution due to solvation in acetonitrile. All calculations were performed with Gaussian16.[70]

Binding studies

Preparation of cellular membranes. Male Swiss mice (final age 8-10 weeks) and Sprague-Dawley rats weighting 250-300 g (Harlan Interfauna Iberica, Spain) were killed, and the brain cortex dissected and stored at -70ºC until assays were performed. Kidneys were also obtained from male Sprague–Dawley rats. All animal experimental protocols were performed in agreement with European Union regulations (O.J. of E.C. L 358/1 18/12/1986).

Human brain samples were obtained at autopsy in the Basque Institute of Legal Medicine, Bilbao, Spain. Samples from the prefrontal cortex (Brodmann's area 9) were dissected at the time of autopsy and immediately stored at -70 ºC until assay. The study was developed in compliance with policies of research and ethical review boards for postmortem brain studies.

To obtain cellular membranes (P2 fraction) the different samples were homogenized using an ultraturrax in 30 volumes of homogenization buffer (0.25M sucrose, 1mM $MgCl_2$, 5mM Tris–HCl, pH 7.4). The crude homogenate was centrifuged for 5 min at 1000 g (4 ºC) and the supernatant was centrifuged again for 10 min at 40,000g (4 ºC). The resultant pellet was washed twice in 20 volumes of homogenization buffer and recentrifuged in similar conditions. Protein content was measured according to the method of Bradford using BSA as standard.

Competition Binding Assays. The pharmacological activity of the compounds was evaluated through competition binding studies against the I_2-IR selective radioligand [3H]2-BFI (2-[(2-benzofuranyl)-2-imidazoline), the α_2-adrenergic receptor selective radioligand [3H]RX821002 (2-methoxyidazoxan) or the I_1-IR selective radioligand [3H]Clonidine. Specific binding was measured in 0.25 mL aliquots (50 mM Tris-HCl, pH 7.5) containing 100 µg of membranes, which were incubated in 96-well plates either with [3H]2-BFI (2 nM) for 45 min at 25 ºC, [3H]RX821002 (1 nM) for 30 min at 25 ºC or [3H]Clonidine (5 nM) for 45 min at 22ºC, in the absence or presence of the competing compounds (10^{-12}–10^{-3} M, 10 concentrations). [3H]Clonidine binding was performed in the presence of 10µM adrenaline to preclude binding to α_2-AR.

Incubations were terminated by separating free ligand from bound ligand by rapid filtration under vacuum (1450 Filter Mate Harvester, PerkinElmer) through GF/C glass fiber filters. The filters were then rinsed three times with 300 µL of binding buffer, air-dried (120 min), and counted for radioactivity by liquid scintillation spectrometry using a MicroBeta TriLux counter (PerkinElmer). Specific binding was determined and plotted as a function of the compound concentration. Nonspecific binding was determined in the presence of idazoxan (10^{-5} M), a compound with well established affinity for I_2-IR and α_2-adrenergic receptors, in [3H]2-BFI and

[^{3}H]RX821002 assays, or rilmenidine (10^{-5} M) in [^{3}H]Clonidine experiments. Analyses of competition experiments to obtain the inhibition constant (Ki) were performed by nonlinear regression using the GraphPad Prism program. Ki values were normalized to pKi values. I$_2$-IR/α_2 selectivity index was calculated as the antilogarithm of the difference between pKi values for I$_2$-IR and pKi values for α_2-AR. For [^{3}H]Clonidine experiments IC$_{50}$ values were calculated (the concentration of tested ligand that displaces 50% of specifically bound [^{3}H]clonidine).

I$_1$-Binding site assay

Kidneys were obtained from male Sprague–Dawley rats (250–280 g) and cellular membranes (P2 fractions) prepared according to established methods. [^{3}H]RX821002 (2-methoxyidazoxan) binds to α_2 adrenoceptor subtypes and a non-adrenoceptor imidazoline binding site in rat kidney.[70]

Competition binding assays were performed as previously reported with minor modifications.[25] [^{3}H]Clonidine (5 nM, Perkin–Elmer) was bound in the presence of 10 μM adrenaline to preclude binding to α_2-adrenoceptors. The specific component was defined by 1 mM rilmenidine. Membrane aliquots (220 μL, 0.1–0.12 mg protein) were incubated with 10 concentrations of the test compounds over the range 10^{-12}–10^{-3} M.

Incubations were carried out in 96 well plates (final volume 250 μL/well) in 50 mM Tris–HCl buffer (pH 7.4) supplemented with 1 mM MgCl$_2$ at 22 ºC for 45 min with agitation (400 rpm). Bound radioligand and free radioactivity were separated by rapid filtration through pre-soaked (0.5% polyethyleneimine) glass-fibre filters (Whatman GFB). Trapped radioligand was determined by liquid scintillation counting and the data were analysed with GraphPad Prism

version 5.0 for Windows (GraphPad Software, San Diego, CA, USA) to yield IC_{50} values (the

concentration of tested ligand that displaces 50% of specifically bound [^{3}H]clonidine).

3D-QSAR study

Data set preparation. The data set composed of previously synthesized and in vitro tested

bicyclic α-iminophosphonates with different affinities on I_2-IR and $α_2$-AR receptors was used for

the creation of the 3D-QSAR models (Table 1). Additionally, to compare and validate our results

we have added four standard in both data sets, Tracizoline, Idazoxan, BU99008 and LSL60101.

Examined compounds cover wide range of experimental activity (pKi I_2: 3.11-10.28; pKi $α_2$:

3.59-10.27) and structural diversity which ensure good quality and applicability of the created

3D-QSAR models. Selection of dominant forms of studied ligands at physiological pH 7.4 was

obtained by the Marvin Sketch 5.5.1.0 program.[71] Subsequently, they were initially pre-

optimized with semiempirical/PM3 (Parameterized Model revision 3) method[72,73] and then by ab

initio Hartree-Fock/3-21G method[74] using Gaussian 09 software[75] included in Chem3D Ultra

program.[76] Obtained ligands' conformations were used for calculation of specific molecular

descriptors (Grid Independent Descriptors- GRIND) and 3D-QSAR model building.

3D-QSAR study. 3D-QSAR models were created using Pentacle program[77] which calculates

GRID independent descriptors (GRIND and GRIND2) from molecular interaction fields (MIFs).

Four different probes were used to calculate MIFs: O probe (hydrogen bond acceptor groups),

N1 probe (hydrogen bond donor groups), DRY probe (hydrophobic interactions) and TIP probe

(the shape of molecule). A grid spacing was set to 0.5. ALMOND algorithm was used for the

extraction of the most relevant regions, which represent favourable interaction positions between ligand and probe. Consistently Large Auto and Cross Correlation (CLACC) algorithm was used to calculate GRIND descriptors using the correlation between same and different nodes. The smoothing window was set to 0.8Å. Partial Least Square (PLS) regression was applied for 3D-QSAR model building. Initial number of descriptors was reduced using Fractional Factorial Design (FFD) to obtain most significant GRIND variables. The results of node-node energies between the same or a different probe were then presented as correlograms.[78,79]

In vivo studies in mice

Studies and procedures involving mouse brain dissection and extractions followed the ARRIVE[80] and standard ethical guidelines (European Communities Council Directive 2010/63/EU and Guidelines for the Care and Use of Mammals in Neuroscience and Behavioral Research, National Research Council 2003) and were approved by the respective Local Bioethical Committees (Universitat de les Illes Balears-CAIB and University of Barcelona-GenCat). All efforts were made to minimize the number of animals used and their suffering.

Hypothermia

For this study a total of 35 adult CD-1 mice and 9 adult Sprague-Dawley rats bred and housed in standard cages under defined environmental conditions (22 ºC, 70% humidity, and 12 h light/dark cycle, lights on at 8:00 AM, with free access to a standard diet and tap water) in the animal facility at the University of the Balearic Islands were used. Animals were habituated to the experimenter by being handled and weighted for two days prior to any experimental procedures. For the acute treatment, mice or rats received a single dose of **9d** (20 mg/kg, i.p., n=12 for mice, and 20 or 35 mg/kg, i.p., n=3-3 for rats) or vehicle (1mL/kg of DMSO, i.p., n=13

for mice and n=3 for rats), while for the repeated treatment mice were daily treated with **9d** (20 mg/kg, i.p., n=5) or vehicle (i.p., n=5) for 5 consecutive days. The possible hypothermic effect exerted by **9d** was evaluated by measuring changes in rectal temperature before any drug treatment (basal value) and 1 h (for mice) or 1, 2 and 3 h (for rats) after drug injection by a rectal probe connected to a digital thermometer (Compact LCD display thermometer, SA880-1M, RS, Corby, UK). Animals were sacrificed right after the last rectal temperature measurement and the hippocampus was freshly dissected and kept at -80°C for future biochemical analysis.

Western blot analysis for FADD protein

Hippocampal sample proteins (40 μg) were separated by sodium dodecyl sulphate polyacrylamide electrophoresis (SDS-PAGE) on 10 % polyacrylamide minigels (Bio-Rad) and transferred onto nitrocellulose membranes by standard Western blot procedures as described previously.[25] The membranes were incubated overnight with anti-FADD (H- 181) Ab, #sc-5559 (Santa Cruz Biotechnology, Santa Cruz, CA) and then stripped and reprobed for β-actin (clone AC-15) Ab, #A1978 (Sigma). Following secondary antibody (anti-rabbit or anti- mouse) incubation and ECL detection system (Amersham, Buckinghamshire, UK), proteins were visualized on autoradiographic films (Amersham ECL Hyperfilm). Upon densitometric scanning (GS-800 Imaging Densitometer, Bio-Rad) of immunoreactive bands (integrated optical density, IOD) the amount of FADD protein in brain samples of mice from different treatment groups was compared with that of vehicle-treated controls (100%) in the same gel. Quantification of β-actin contents served as a loading control (no differences between treatment groups, data not shown). Each brain sample (and target protein) was quantified in 2-4 gels and the mean value was used as a final estimate.

5xFAD *In vivo* experimental design

Female 5xFAD and WT mice 5-month-old (n = 51) were used to carry out cognitive and molecular analyses. The 5xFAD is a double transgenic APP/PS1 that co-expressed five mutations of AD, and that rapidly develops severe amyloid pathology with high levels of intraneuronal Aβ42 around 2 months of age. The model was generated by the introduction of human APP with the Swedish mutations (K670N/M671L), Florida (I716V), London (Val717Ile) and the introduction of PS1 M146L and L286V. Moreover, 5xFAD presents neuronal loss and cognitive deficits in spatial learning (at approximately four to five months).[81]

The animals were randomly allocated to three experimental groups: WT Control (n = 12) and 5xFAD Control (n = 14), animals administered with vehicle (2-hydroxypropyl)-β-cyclodextrin 1.8%, and 5xFAD treated with **9d** 5 mg/Kg/day (n=25). Administered through drinking water, up to euthanasia, diluted in 1.8% (2-hydroxypropyl)-β-cyclodextrin. Weight and water consumption were controlled each week, and the **9d** concentration was adjusted accordingly to reach the precise dose. Animals had free access to food and water and were kept under standard temperature conditions (22 ± 2 ºC) and 12 hours: 12 hours light-dark cycles (300 lux/0 lux).

After 4 weeks of treatment period animals were under cognitive test to study the effect of treatment in learning and memory, including short- and long-term memory (NORT). Mice were euthanized 3 days after the behavioural test completion by cervical dislocation. Brains were immediately removed from the skull, and the hippocampus was then isolated and frozen on powdered dry ice. They were maintained at -80 ºC for biochemical experiments

Behavioral testing: NORT

In brief, mice were placed in a black L-shape maze consists of 90º, two-arms, 25-cm-long, 20-cm-high, 5-cm-wide. The mice were habituated to the apparatus 10 min on 3 subsequent days, habituation phase. Afterwards, on day 4, training session took place, and two identical objects (A) were placed in the maze, and the mice were allowed to explore freely for 10 min. 2 hours after training sessions one of the objects was replaced by a novel object (B) to assess short term-memory. Again, the amount of time spends exploring each object was scored. During this second trial, objects A and B were placed in the maze, and the times that the animal took to explore the new object (TN) and the old object (TO) were recorded. A Discrimination index (DI) was calculated, defined as (TN-TO)/(TN+TO). 24 hours after the acquisition trial, the mice were tested again to assess long-term memory, with a new object substituting object B, and a new DI calculated. Exploration of an object by a mouse was defined as pointing the nose towards the object at a distance ≤ 2 cm and/or touching it with the nose. Turning or sitting around the object was not considered exploration. To avoid object preference biases, objects A and B were counterbalanced so that one half of the animals in each experimental group were first exposed to object A and then to object B, whereas the other half first saw object B and then object A. All sessions were videotaped, and the time spend with each object were manually recorded. The maze, the surface, and the objects were cleaned with 70% ethanol between the animals' trials to eliminate olfactory cues.

Determination of oxidative stress

Hydrogen peroxide from 40 brain samples of mice of each group was measured as an indicator of OS, and it was quantified using the Hydrogen Peroxide Assay Kit (Sigma-Aldrich, St. Louis, MI) according to the manufacturer's instructions.

RNA extraction and gene expression determination

Total RNA isolation was carried out using TRIzol® reagent according to manufacturer's instructions. The yield, purity, and quality of RNA were determined spectrophotometrically with a NanoDrop™ ND-1000 (Thermo Scientific) apparatus and an Agilent 2100B Bioanalyzer (Agilent Technologies). RNAs with 260/280 ratios and RIN higher than 1.9 and 7.5, respectively, were selected. Reverse Transcription-Polymerase Chain Reaction (RT-PCR) was performed as follows: 2 μg of messenger RNA (mRNA) was reverse-transcribed using the High Capacity cDNA Reverse Transcription Kit (Applied Biosystems). Real-time quantitative PCR (qPCR) from 48 mice of both strains (n = 4-6 per group) was used to quantify mRNA expression of OS and inflammatory genes.

SYBR® Green real-time PCR was performed on a Step One Plus Detection System (Applied-Biosystems) employing SYBR® Green PCR Master Mix (Applied-Biosystems). Each reaction mixture contained 6.75 μL of complementary DNA (cDNA) (which concentration was 2 μg), 0.75 μL of each primer (which concentration was 100 nM), and 6.75 μL of SYBR® Green PCR Master Mix (2X).

TaqMan-based real-time PCR (Applied Biosystems) was also performed in a Step One Plus Detection System (Applied-Biosystems). Each 20 μL of TaqMan reaction contained 9 μL of cDNA (25 ng), 1 μL 20X probe of TaqMan Gene Expression Assays and 10 μL of 2X TaqMan Universal PCR Master Mix.

Data were analyzed utilizing the comparative Cycle threshold (Ct) method (ΔΔCt), where the housekeeping gene level was used to normalize differences in sample loading and preparation[49]. Normalization of expression levels was performed with *β-actin* for SYBR® Green-based real-

time PCR and TATA-binding protein (*Tbp*) for TaqMan-based real-time PCR. Primers

sequences and TaqMan probes used in this study are presented in Table S10. Each sample was

analyzed in duplicate, and the results represent the n-fold difference of the transcript levels

among different groups.

ASSOCIATED CONTENT

Supporting Information.

The following files are available free of charge on the ACS Publications website at DOI:.

Experimental procedures of 10a-10c and 11, theoretical calculations, 3D-QSAR study,

in vitro BBB, DMPK assays, receptor characterization panel, in vivo data, tables of [1]H

and ^{13}C spectra, X-ray crystallography data.

AUTHOR INFORMATION

Corresponding Author

*Phone: +34 934024542. E-mail: cescolano@ub.edu

ORCID: 0000-0002-9117-8239

Notes

C. E., M. P., C. G.-F., S. A., L.-F. C., and G.-S. J. A. are inventors of the patent application on on I_2 imidazoline receptor ligands WO2019/121853 (reference 29). None of the other authors has any disclosures to declare.

Author Contributions

S. A. and S. R.-A. contributed equally to this work. C. G.-F., J. A. G.-S., M. J. G.-F., M. P. and C. E. designed the study. S. A., S. R.-A. and A. B. synthesized, purified and characterized the I_2-IR ligands. C. G.-F., F. V. and M. P. carried out the behavior and cognition studies and cellular parameters determination. I. B.-M., C. M. and L. F. C. performed the binding experiments. B. P. performed the PAMPA-BBB permeation experiments. E. M. conducted the X-ray crystallographic analysis. F. J. L. was in charge of the theoretical studies. P. P.-L. performed the physicochemical studies. S. L., D. D. and L. N. carried out the cytotoxicity studies. J. B. and M. I. L. determined the ADMET parameters. E. H.-H., J. A. G.-S. and M. J. G.-S. performed the hypothermic studies and analysis of FADD protein content. M. R., T. D., K. N. carried out the 3D-QSAR study. C. G.-F., F. J. L, P. P.-L., J. A. G.-S., M. J. G.-S., L. F. C., K. N., M. P. and C. E contributed

to write the manuscript. All the authors have read and approved the final version of the

manuscript.

ABBREVIATIONS

α_2-AR α_2 adrenegic receptor; 2-BFI, 2-[(2-benzofuranyl)-2-imidazoline]; B3LYP, 3-parameter hybrid Becke exchange/Lee-Yang-Parr correlation; BU224, 2-(4,5-dihydroimidazol-2-yl)quinoline; CCK_A, cholecystokinin type A receptor; CCK_B, cholecystokinin type B receptor; Cxcl10, C-X-C motif chemokine 10; DI, discrimination index; 5xFAD mouse model of amyloid deposition expresses five familial AD (FAD) mutations; FADD Fas-associated protein with death domain; GRIND Grid-independent descriptors; HeLa, human cervix carcinoma; 4-HNE, 4-hydroxy-2-nonenal; Hmox1, heme oxygenase (decycling) 1; H_2O_2,

89

hydrogen peroxide; IR, imidazoline receptors; I_1-IR, imidazoline I_1 receptors; I_2-IR, imidazoline I_2 receptors; I_3-IR, imidazoline I_3 receptors; LANLD2DZ LANL2DZ stands for Los Alamos National Laboratory 2-double-z (density functional theory); MDKC, Mandin-Dary canine kidney; MT4 human T-lymphocite; MRC-5, human embryonic lung fibroblast; NORT, Novel object recognition test; iNOS, inducible nitric oxide synthase; OS, Oxidative stress; PhosMic, diethyl isocyanomethylphosphonate; P_e, permeability; pKi, antilog of Ki; pKi_L, low pKi binding site; pKi_H, high pKi binding site; 3D-QSAR 3 dimensions quantitative structure-activity relationships; QM, quantum mechanical; [^{3}H]RX821002, 2-methoxyidazoxan; SAMP8, Senescence accelerated mouse-prone 8; SEM, standard error of the mean; *Tnf-α*, tumor necrosis factor α; TPSA; topological polar surface area; Vero, African green monkey kidney; WT, WT mice.

REFERENCES

(1) Bousquet, P.; Feldman, J.; Schwartz, J. Central cardiovascular effects of alpha adrenergic drugs: differences between catecholamines and imidazolines. *J. Pharmacol. Exp. Ther*. **1984**, *230*, 232-236.

(2) Bousquet, P.; Hudson, A.; García-Sevilla, J. A.; Li, J.-X. Imidazoline receptor system: the past, the present, and the future. *Pharmacol. Rev.* **2020**, *72*, 50-79.

(3) Lowry, J. A.; Brown, J. T. Significance of the imidazoline receptors in toxicology. *Clin. Toxicol.* **2014**, *52*, 454-469.

(4) Regunathan, S.; Reis, D. J. Imidazoline receptors and their endogenous ligands. *Ann. Rev. Pharmacol. Toxicol.* **1996**, *36*, 511-544.

(5) Fenton, C.; Keating, G. M.; Lyseng-Williamson, K. A. Moxonidine: a review of its use in essential hypertension. *Drugs* **2006**, *66*, 477-496.

(6) Reid, J. L. Rilmenidine: a clinical overview. *Am. J. Hypertens.* **2000**, *13*, 106S-111S.

(7) Chang, S. L.; Brown, C. A.; Scarpello, K. E.; Morgan, N. G. The imidazoline site involved in control of insulin secretion: characteristics that distinguish it from I_1- and I_2-sites. *Br. J. Pharmacol.* **1994**, *112*, 1065-1070.

(8) Li, J. X. Imidazoline I_2 receptors: an update. *Pharmacol. Ther.* **2017**, *178*, 48-56.

(9) Li, J. X.; Zhang, Y. Imidazoline I_2 receptors: target for new analgesics? *Eur. J. Pharmacol.* **2011**, *658*, 49-56.

(10) Regunathan, S.; Feinstein, D. L.; Reis, D. J. Anti-proliferative and anti-inflammatory actions of imidazoline agents. Are imidazoline receptors involved? *Ann. N. Y. Acad. Sci.* **1999**, *881*, 410-419.

(11) Smith, K. L.; Jessop, D. S.; Finn, D. P. Modulation of stress by imidazoline binding sites: implications for psychiatric disorders. *Stress* **2009**, *12*, 97-114.

(12) Martín-Gómez, J. I.; Ruíz, J.; Callado, L. F.; Garibi, J. M.; Aguinaco, L.; Barturen, F.; Meana, J. J. Increased density of I$_2$-imidazoline receptors in human gliobastomas. *Neuroreport* **1996**, *7*, 1393-1396.

(13) Callado, L. F.; Martín-Gómez, J. I.; Ruiz, J.; Garibi, J. M.; Meana, J. J. Imidazoline I$_2$ receptors density increases with the malignancy of human gliomas. *J. Neurol. Neurosurg. Psychiatry* **2004**, *75*, 785-787.

(14) Reynolds, G. P.; Boulton, R. M.; Pearson, S. J.; Hudson, A. L.; Nutt, D. J. Imidazoline binding sites in Huntington's and Parkinson's disease putamen. *Eur. J. Pharmacol.* **1996**, *301*, R19-R21.

(15) Gargalidis-Moudanos, C.; Pizzinat, N.; Javoy-Agid, F. ; Remaury, A.; Parini, A. I$_2$-imidazoline binding sites and monoamine oxidase activity in human postmortem brain from patients with Parkinson's disease. *Neurochem. Int.* **1997**, *30*, 31-36.

(16) Meana, J. J.; Barturen, F.; Martín, I.; García-Sevilla, J. A. Evidence of increased non-adrenoreceptor [^{3}H]idazoxan binding sites in the frontal cortex of depressed suicide victims. *Biol. Psychiatry* **1993**, *34*, 498-501.

(17) García- Sevilla, J.; Escribá, P. V.; Sastre, M.; Walzer, C.; Busquets, X.; Jaquet, G.; Reis, D. J.; Guimón, J. Immunodetection and quantitation of imidazoline receptor proteins in platelets of patients with major depression and in brains of suicide victims. *Arch. Gen. Psychiatry* **1996**, *53*, 803-810.

(18) Ruíz, J.; Martín I.; Callado, L. F.; Meana, J. J.; Barturen, F.; García-Sevilla, J. A. Non-adrenoreceptor [^{3}H]idazoxan binding sites (I$_2$-imidazoline sites) are increased in postmortem brain from patients with Alzheimer's disease. *Neurosci. Lett.* **1993**, *160*, 109-112.

(19) García-Sevilla, J. A.; Escribá, P. V.; Walzer, C.; Bouras, C.; Guimón, J. Imidazoline receptor proteins in brains of patients with Alzheimer's disease. *Neurosci. Lett.* **1998**, *247*, 95-98.

(20) Comi, E.; Lanza, M.; Ferrari, F.; Mauri, V.; Caselli, G.; Rovati, L. C. Efficacy of CR4056, a first-in-class imidazoline-2 analgesic drug, in comparison with naproxen in two rat models of osteoarthritis. *J. Pain Res*. **2017**, *10*, 1033-1043.

(21) Rovati, L.C.; Brambilla, N.; Blicharski, T.; Connell, J.; Vitalini, C.; Bonazzi, A.; Giacovelli, G.; Girolami, F.; D'Amato, M. Efficacy and safety of the firts-in-classs imidazoline-2 receptor ligand CR4056 in pain from knee osteoarthritis and desease phenotypes: a randomized, double-blind, placebo-controlled phase 2 trial. *Osteoarthritis and Cartilage*. **2019**, doi.org/10.1016/j.joca.2019.09.002.

(22) Tyacke, R. J.; Myers, J. F. M.; Venkataraman, A. V.; Mick, I.; Turton, S.; Passchier, J.; Husband, S. M.; Rabiner, E. A.; Gunn, R. N.; Murphy, P. S.; Parker, C. A.; Nutt, D. J. Evaluation of ^{11}C-BU99008, a PET ligand for the imidazoline$_2$ binding site in human brain. *J. Nucl. Med.* **2018**, *59*, 1597- 1602.

(23) Wilson, H.; Dervenoulas, G.; Pagano, G.; Tyacke, R. J.; Polychronis, S.; Myers, J.; Gunn, R. N.; Rabiner, E. A.; Nutt, D.; Politis, M. Imidazoline 2 binding sites reflecting astroglia pathology in Parkinson's disease: an *in vivo* ^{11}C-BU99008 PET study. *Brain* **2019**, *0*, 1-13.

(24) Dardonville, C.; Rozas, I. Imidazoline binding sites and their ligands: an overview of the different chemical structures. *Med. Res. Rev.* **2004,** *24*, 639-661.

(25) Abás, S.; Erdozain, A. M.; Keller, B.; Rodríguez-Arévalo, S.; Callado, L. F.; García-Sevilla, J. A.; Escolano, C. Neuroprotective effects of a structurally new family of high affinity imidazoline I$_2$ receptors ligands. *ACS Chem. Neurosci.* **2017**, *8*, 737-742.

(26) Abás, S.; Estarellas, C.; Luque, F. J.; Escolano, C. Easy access to (2-imidazolin-4-yl)phosphonates by a microwave assisted multicomponent reaction. *Tetrahedron* **2015**, *71*, 2872-2881.

(27) Griñán-Ferré, C.; Vasilopoulou, F. Abás, S. ; Rodríguez-Arévalo, S.; Bagán, A.; Sureda, F. X.; Pérez, B.; Callado, L. F.; García-Sevilla, J. A.; García-Fuster, M. J.; Escolano, C.; Pallàs, M. Behavioral and cognitive improvement induced by novel imidazoline I_2 receptor ligands in female SAMP8 mice. *Neurotherapeutics* **2019**, *16*, 416-431.

(28) Arróniz, C.; Molina, J.; Abás, S.; Molins, E.; Campanera, J. M.; Luque, F. J.; Escolano, C. First diastereoselective [3+2] cycloaddition reaction of diethyl isocyanomethylphosphonate and maleimides. *Org. Biomol. Chem*. **2013**, *11*, 1640-1649.

(29) Escolano, C.; Pallás, M.; Griñán-Ferré, C.; Abás, S.; Callado, L.-F.; García-Sevilla, J. A. Synthetic I_2 Imidazoline Receptor Ligands for Prevention or Treatment of Human Brain Disorders. WO 2019/121853 A1, June 27, 2019.

(30) Grijalba, B.; Callado, L. F., Meana, J. J.; García-Sevilla, J. A.; Pazos, A. α_2-Adrenoceptor subtypes in the human brain: a phamacological delineation of [3H]RX-821002 binding to membranes and tissue sections. *Eur. J. Pharmacol.* **1996**, *310*, 83-93.

(31) Callado, L. F.; Maeztu, A. I.; Ballesteros, J.; Gutiérrez, M.; Meana, J. J. Differencial [3H]idazoxan and [3H]2-(2-benzofuranyl)-2-imidazoline (2-BFI) binding to imidazoline I_2 receptors in human postmortem frontal cortex. *Eur. J. Pharmacol.* **2001**, *423*, 109-114.

(32) BU99008 was prepared according to the literature procedure: Tyacke, R. J.; Fisher, A.; Robinson, E. S. J.; Grundt, P.; Turner, E. M.; Husbands, S. M.; Hudson, A. L.; Parker, C. A.; Nutt, D. J. Evaluation and initial in vitro and in vivo characterization of the potential positron

emission tomography ligand, BU99008 (2-(4,5-dihydro-1*H*-imidazol-2-yl)-1-methyl-1*H*-indole),

for the imidazoline$_2$ binding site. *Synapse* **2012**, *66*, 542-551.

(33) CR4056 was prepared according to the literature procedure: Giordani, A.; Mandelli, S.;

Verpilio, I.; Zanzola, S.; Tarchino, F.; Caselli, G.; Piepoli, T.; Mazzari, S.; Makovec, F.; Rovati,

L. C. 6-1H-Imidazo-quinazoline and Quinolines Derivatives, New Potent Analgesics and Anti-

inflammatory Agents. US 8,193,353 B2, June 5, 2012.

(34) Lione, L. A.; Nutt, D. J.; Hudson, A. L. [^{3}H]-2-(2-benzofuranyl)-2-imidazoline: a new

selective high affinity radioligand for the study of rabbit brain imidazoline I$_2$ receptors. *Eur. J.*

Pharmacol. **1996**, *304*, 221-229.

(35) Alemany, R.; Olmos, G.; García-Sevilla, J. A. Labelling I$_{2B}$-imidazoline receptors by

[^{3}H]-2-(2-benzofuranyl)-2-imidazoline (2-BFI) in rat brain and liver: characterization, regulation

and relation to monoamine oxidase enzymes. *Naunyn-Schmiedeberg`s Arch. Pharmacol*. **1997**,

356, 39-47.

(36) Lione, L. A.; Nutt, D. J.; Hudson, A. L. Characterisation and localisation of [^{3}H]-2-(2-

benzofuranyl)-2-imidazoline binding in rat brain: a selective ligand for imidazoline I$_2$ receptors.

Eur. J. Pharmacol. **1998**, *353*, 123-135.

(37) Quaglia, W.; Bousquet, P.; Pigini, M.; Carotti, A.; Carrieri, A.; Dontenwill, M.; Gentili,

F.; Giannella, M.; Maranca, F.; Piergentili A.; Brasili, L. 2-(2-Phenylcyclopropyl)imidazolines:

reversed enantioselective interaction at I$_1$ and I$_2$ imidazoline receptors. *J. Med. Chem*. **1999**, *42*,

2737-2740.

(38) Alemany, R.; Olmos, G.; Escribá, P. V.; Menargues, A.; Obach, R.; García-Sevilla, J. A.

LSL60101, a selective ligand for imidazoline I$_2$ receptors, on glial fibrillary acidic protein

concentration. *Eur. J. Pharmacol.* **1995**, *280*, 205-210.

(39) Ferrari, F.; Fiorentino, S.; Mennuni, L.; Garofalo, P.; Letari, O.; Mandelli, S.; Giordani, A.; Lanza, M.; Caselli, G. Analgesic efficacy of CR4056, a novel imidazoline-2 receptor ligand, in rat models of inflammatory and neuropathic pain. *J. Pain Res.* **2011**, *4*, 111-115.

(40) Pentacle,Version1.0.6, MolecularDiscoveryLtd., Perugia, Italy; 2009

(41) Ghosh, J.; Lawless, M. S.; Waldman, M.; Gombar, V.; Fraczkiewicz, R.; Modeling ADMET. *Methods Mol. Biol.* **2016**, *1425*, 63–83.

(42) ADMET Predictor, v. 9.5, Simulations Plus Inc., Lancaster, CA, USA, https://www.simulations-plus.com

(43) Daina, A.; Michielin, O.; Zoete, V. Swiss ADME: a free web tool to evaluate pharmacokinetics, drug-likeness and medicinal chemistry friendliness of small mol. *Sci. Rep.* **2017**, *7*, 42717.

(44) Biopharmaceutics classification system-based biowaivers, International council for harmonisation of technical requirements for pharmaceutical for human use. https://www.ich.org/fileadmin/Public_Web_Site/ICH_Products/Guidelines/Multidisciplinary/M9 /M9EWG_DraftGuideline_Step2_2018_0606.pdf

(45) International council on harmonisation of technical requeriments for registration of pharmaceuticals for human use. ICH harmonized tripartite guideline. "Stability testing of new drug substance and products". Q1A (R2) (2003).

(46) For information on the Eurofins Lead Profiling Screen, see: http://www.eurofins.com

(47) Cawston, E. E.; Miller, L. J. Therapeutic potential for novel drugs targeting the type 1 cholecystokinin receptor, *Br. J. Pharmacol.* **2010**, *159*, 1009-1021.

(48) Keller, B.; García-Sevilla, J. A. Inhibitory effects of imidazoline receptor ligands on basal and kainic acid-induced neurotoxic signalling in mice. *J. Phychopharmacol*. **2016**, *30*, 875-886.

(49) Thorn, D. A.; An, X. F.; Zhang, Y.; Pigini, M.; Li, J. X. Characterization of the hypothermic effects of imidazoline I_2 receptor agonists in rats. *Br. J. Pharmacol*. **2012**, *166*, 1936-1945.

(50) Craven, J. A.; Conway, E. L. Effects of alpha 2-adrenoceptor antagonists and imidazoline 2-receptor ligands on neuronal damage in global ischaemia in the rat. *Clin. Exp. Pharmacol. Physiol*. **1997**, *24*, 204-207.

(51) Marion, D. W.; Penrod, L. E.; Kelsey, S. F.; Obrist, W. D.; Kochanek, P. M.; Palmer, A. M.; Wisniewski, S. R.; DeKosky, S. T. Treatment of traumatic brain injury with moderate hypothermia. *N. Engl. J. Med*. **1997**, *336*, 540-546.

(52) Maier, C. M.; Ahern, K. V.; Cheng, M. L.; Lee, J. E.; Yenari, M. A.; Steinberg, G. K. Optimal depth and duration of mild hypothermia in focal model of transient cerebral ischemia: effects on neurologic outcome, infarct size, apopotosis, and inflammation. *Stroke* **1998**, *29*, 2171-2180.

(53) Hernández-Hernández, E.; Miralles, A.; Esteban, S.; García-Fuster, M. J. Repeated treatment with the α2-adrenoceptor agonist UK-14304 improves cognitive performance in middle-age rats: Role of hippocampal Fas-associated death domain *Neurobiol. Aging* **2018**, *71*, 115-126.

(54) Hernández-Hernández, E.; Miralles, A.; Esteban, S.; Garcia-Fuster, M. J. Repeated treatment with the α2-adrenoceptor agonist UK-14304 improves cognitive performance in

middle-age rats: role of hippocampal Fas-associated death domain. *J. Psychopharmacol.* **2018**, *32*, 248-255.

(55) Bilkei-Gorzo, A. Genetic mouse models of brain ageing and Alzheimer's disease. *Pharmacol. Ther.* **2014**, *142*, 224-257.

(56) Antunes, M.; Biala, G. The novel object recognition memory: neurobiology, test procedure, and its modifications. *Cogn. Process.* **2012**, *13*, 93-110.

(57) Heneka, M. T.; McManus, R. M.; Latz, E. Inflammasome signalling in brain function and neurodegenerative disease. *Nat. Rev. Neurosci.* **2018**, *19*, 610–621.

(58) Gao, H.-M.; Zhou, H.; Hong, J. S. Oxidative stress, neuroinflammation, and neurodegeneration. In: Peterson P. K.; Toborek, M. (Eds.) Neuroinflammation and neurodegeneration, **2014**. Springer, New York, N.Y. pp. 81-104

(59) Ekert J. O.; Gould, R. L.; Reynolds, G.; Howard, R. J. TNF alpha inhibitors in Alzheimer's disease: a systematic review. *Int. J. Geriatr. Psychiatry* **2018**, *33*, 688–694.

(60) Iadecola, C.; Zhang, F.; Casey, R.; Nagayama, M.; Ross, M. E. Delayed reduction of ischemic brain injury and neurological deficits in mice lacking the inducible nitric oxide synthase gene. *J. Neurosci.* **1997**, *17*, 9157-9164.

(61) Schipper, H.M.; Song, W.; Tavitian, A.; Cressatti, M. The sinister face of heme oxygenase-1 in brain aging and disease. *Prog. Neurobiol.* **2019**, *172*, 40-70.

(62) Griñán-Ferré, C.; Sarroca, S.; Ivanova, A.; Puigoriol-Illamola, D.; Aguado, F.; Camins, A.; Sanfeliu, C.; Pallàs, M. Epigenetic mechanisms underlying cognitive impairment and Alzheimer disease hallmarks in 5xFAD mice. *Aging* **2016**, *8*, 664-684.

(63) Becke, A. D. Density-functional thermochemistry. III. The role of exact exchange. *J. Chem. Phys.* **1993**, *98*, 5648.

(64) Lee, C.; Yang, W.; Parr, R. G. Development of the Colle-Salvetti correlation-energy formula into a functional of the electron density. *Phys. Rev. B: Condens. Matter* **1988**, *37*, 785.

(65) Clark, T.; Chandrasekhar, J.; Spitznagel, G. W.; Schleyer, P. v. R. Efficient diffuse function-augmented basis sets for anion calculations. III. The 3-21+G basis set for first-row elements, Li–F. *J. Comput. Chem.* **1983**, *4*, 294–301

(66) Wadt, W. R.; Hay, P. J. Ab initio effective core potentials for molecular calculations. Potentials for K to Au including the outermost core orbitals. *J. Chem. Phys.* **1985**, *82*, 284.

(67) Gonzalez, C.; Schlegel, H. B. An improved algorithm for reaction path following. *J. Chem. Phys.* **1989**, *90*, 2154

(68) Yu, H. S.; He, X.; Truhlar, D. G. MN-15: A new local exchanged-correlation functional for Kohn-Sham density functional theory broad accuracy for atoms, molecules, and solids. *J. Chem. Theory Comput.* **2016**, *12*, 1280–1293.

(69) Marenich, A. V.; Cramer, C. J.; Truhlar, D. G. Universal solvation model based on solute electron density and on a continuum model of the solvent defined by the bulk dielectric constant and atomic surface tensions. *J. Phys. Chem. B* **2009**, *113*, 6378-6396.

(70) *Gaussian 16*, Revision B.01, Gaussian, Inc.: Wallingford CT, 2016.

(71) Callado, L. F.; Gabilonedo, A. M.; Meana, J. J. [^{3}H] RX821002 (2-methoxyidazoxan) binds to α_2-adrenoceptor subtypes and a non-adrenoceptor imidazoline binding site in rat kidney. *Eur. J. Pharmacol.* **1996**, *316*, 359-368.

(72) MarvinSketch 5.5.1.0. ChemAxon, Budapest, Hungary, 2011; software available at https://www.chemaxon.com

(73) Stewart, J. J. P. Optimization of parameters for semiempirical methods I. Method, *J. Comput. Chem.* **1989**, *10*, 209–220.

(74) Stewart, J. J. P. Optimization of parameters for semiempirical methods II.Method, *J. Comput. Chem.* **1989**, *10*, 221–264.

(75) Hehre, W. J.; Radom, L.; Schleyer, PvR.; Pople, J. A. Ab initio molecular orbital theory, Vol 1, Wiley, New York, 1986.

(76) Frisch, M. J.; Trucks, G. W.; Schlegel, H. B.; Scuseria, G. E.; Robb, M.A.; Cheeseman, J. R.; Scalmani, G.; Barone, V.; Mennucci, B.; Petersson, G. A.; Nakatsuii, H.; Caricato, M.; Li, X.; Hratchian, H. P.; Izmaylov, A. F.; Bloino, J.; Zheng, G.; Sonnenberg, J. L.; Hada, M.; Ehara, M.; Toyota, K.; Fukuda, R.; Hasegawa, J.; Ishida, M.; Nakajima, T.; Honda, Y.; Kitao, O.; Nakai, H.; Vreyen, T.; Montgomery, J. A.; Peralta, Jr. J. E.; Ogliaro, F.; Bearpark, M.; Heyd, J. J.; Brothers, E.; Kudin, K. N.; Staroverov, V. N.; Kobayashi, R.; Normand, J.; Raghavachari, K.; Rendell, A.; Burant, J. C.; Ivengar, S. S.; Tomasi, J.; Cossi, M.; Rega, N.; Millan, J. M.; Klene, M.; Knox, J. E.; Cross, J. B.; Bakken, V.; Adamo, C.; Jaramillo, J.; Gomperts, R.; Stratmann, R. E.; Yazyev, O.; Austin, A. J.; Cammi, R.; Pomelli, C.; Ochterski, J. W.; Martin, R. L.; Morokuma, K.; Zakrzewski, V. G.; Voth, G. A.; Salvador, P.; Dannenberg, J. J.; Dapprich, S.; Daniels, A. D.; Farkas, Ó.; Foresman, J. B.; Ortiz, J. V.; Ciolowski, J.; Fox, D. J. Gaussian 09, Revison D.01, Gaussian Inc., Wallingford CT, 2009.

(77) CambridgeSoft Corporation. 2013. ChemBio3D Ultra, Version 13.0. Cambridge, MA, USA.

(78) Durán, Á.; Zamora, I.; Pastor, M. Suitability of GRIND-Based principal properties for the description of molecular similarity and ligand-based virtual screening. *J. Chem. Inf. Model.* **2009**, *49*, 2129–2138.

(79) Durán, Á.; Pastor, M. An advanced tool for computing and handling grid-independent descriptors. User Manual Version 1.06; 2011.

(80) Ojha, P. K.; Roy, K. Comparative QSARs for antimalarial endochins: Importance of descriptor-thinning and noise reduction prior to feature selection. *Chemom. Intell. Lab. Syst.* **2011**, *109*, 146–161.

(81) Kilkenny, C.; Borwnw W. J.; Cuthill, I. C.; Emerson, M.; Altman, D. G. Improving biocesce research reporting: the ARRIVE guidelines for reporting animal research. *PloS Biol.* **2010**, *8*, 6.

(82) Oakley, H.; Cole, S. L.; Logan, S.; Maus, E.; Shao, P.; Craft, J.; Guillozet-Bongaarts, A.; Ohno, M.; Disterohoft, J.; Van Eldik, L.; Berry, R.; Vassar, R. Intraneuronal beta-amyloid aggregates, neurodegeneration, and neuron loss in transgenic mice with five familial Alzheimer's desease mutations: potential factors in amyloid plaque formation. *J. Neurosci.* **2006**, *26*, 10129–10140.

Table of Contents Graphic